APPENDICES

to the final report for NCHRP Project 01-45,

"Models for Estimating the Effects of Pavement Condition on Vehicle Operating Costs"

APPENDIX A

FUEL CONSUMPTION MODELS

A1 - IDENTIFICATION AND EVALUATION OF FUEL CONSUMPTION MODELS

This appendix summarizes the detailed equations and relationships of current fuel consumption models. These models were also evaluated regarding their applicability to the paved surfaces and traffic and environmental conditions encountered in the United States that are capable of addressing the full range of vehicle types.

EXISTING VOC MODELS

The VOC models can be grouped into empirical- and mechanistic-based models. The only available U.S. VOC models are those of the Texas Research and Development Foundation (TRDF) developed by Zaniewski et al; an updated version of this model is in the MicroBENCOST VOC module (McFarland et al., 1993). The most recent VOC models have been developed outside the U.S., and are mechanistic-empirical in nature. The relevant models are:

- The World Bank's HDM 3 and 4 VOC models;
- Australian NIMPAC VOC models (adopted in HDM 3 with some modifications) and ARFCOM model of fuel consumption (adopted in HDM 4 with some modifications);
- Saskatchewan VOC models;
- Swedish VETO models.

As mentioned earlier, the VOC are a function of the following six categories of costs:

1. Fuel consumption costs
2. Oil consumption costs
3. Tire consumption costs
4. Repair and maintenance costs
5. Capital costs (depreciation and interest)
6. License and insurance costs

Based on the literature review, only fuel consumption, tire wear and repair and maintenance costs are affected by pavement conditions. Therefore, the focus of this research was

only on estimating these costs. The models are either empirical or mechanistic-empirical models. This section briefly reviews some of the major fuel consumption models (identified by the research team) that have been developed.

Empirical Models

Early work conducted in the US established charts and tables for calculating fuel consumption cost based on vehicle class only (Winfrey, 1969). Later Zaniewski et al. (1982) updated the fuel consumption tables based on empirical models derived from experimental field trials. Although this is the most comprehensive study conducted in the US to date, it did not treat all aspects of the problem. While fuel consumption tests were carried out for idling, acceleration, deceleration, and constant speed driving, the effect of pavement conditions on VOCs was only considered in the constant speed case. Constant speed mode was used for most of the experimental effort in these field trials, which also tested the effect of speed, grade, surface type, and pavement condition. No tests were carried out for larger truck combinations, and relations were assumed for a 3-S2 unit. Also the fuel consumption values were based on only one test vehicle in each class, except for the medium size car, where two identical vehicles were used so that the variance between the two identical cars could be used in the statistical analysis. However, the tests on the effect of pavement conditions showed no significant difference between the two identical cars, which means it was not necessary to do these tests after all (Zaniewski et al., 1982). According to Zaniewski's tables and charts, pavement conditions had a minor effect on fuel consumption. They found that grade, curvature, and speed were the major factors that affect fuel consumption.

The US Department of Transportation (USDOT) recently conducted a study to investigate highway effects on vehicle performance (Klaubert, 2001). The study developed the following fuel consumption model based on regression analysis:

$$FC = \frac{1}{FE} \qquad (A.1)$$

$$FE = a\left(\frac{T}{2} + b\right)^{c} \qquad (A.2)$$

where:

FC = Fuel consumption in L/km

FE = Fuel economy (km/L)

T = Engine torque (N-m)

a, b, c = regression coefficients, depending on gear number

Mechanistic-Empirical Models

Mechanistic models predict that the fuel consumption of a vehicle is proportional to the forces acting on the vehicle. Thus, by quantifying the magnitude of the forces opposing motion one can establish the fuel consumption. Mechanistic models are an improvement over empirical models since they can allow for changes in the vehicle characteristics and are inherently more flexible when trying to apply the models to different conditions. Some of the most recent mechanistic fuel consumption models are given below. The research team noted that most of the models are derived from earlier ones. The following models are discussed chronologically.

The South African fuel consumption model considers that the fuel consumption is proportional to the total energy requirements that are governed by the total engine power and an engine efficiency factor (Bester, 1981). Equation (A.3) shows the form of this model.

$$FC = 1000\beta\frac{P_{tot}}{v} \qquad \text{(A.3)}$$

where:

FC = Fuel consumption in mL/km

β = Fuel efficiency factor in ml/kW/s or mL/KJ

P_{tot} = Total power requirement in kW

v = Vehicle velocity in m/s

The South African model assumes that the fuel efficiency of the vehicle is independent from the driving mode. However, a number of studies that were conducted in the early 1980's in Australia to model fuel consumption found that the fuel efficiency increases in the acceleration case (Biggs, 1987). An improved mechanistic model was then developed to predict fuel consumption using the following relationship.

$$IFC = \alpha + \beta P_{tr} + \frac{\beta_2 M a^2 v}{1000} \quad \text{(A.4)}$$

where:

α = Steady state fuel consumption in mL/s

β = Steady state fuel efficiency parameter in mL/(KJm/s)

β_2 = Acceleration fuel efficiency parameter in mL/(KJm/s^2)

M = Vehicle mass in kg

v = Vehicle velocity in m/s

Some studies in the later 1980's in Australia found that the fuel efficiency is not only a function of tractive power but also a function of the engine power. The following mechanistic model (ARRB ARFCOM model) was developed to predict the fuel consumption as a function of the input (engine) and output power. The general form of the model is described by the following equations (Biggs, 1988):

$$IFC = \max(\alpha, \beta * (Pout - Peng)) \quad \text{(A.5)}$$

$$\beta = \beta_b (1 + ehp * P_{out} / P_{\max}) \quad \text{(A.6)}$$

where:

P_{out} = The total output power of the engine required to provide tractive force and run the accessories (KW)

P_{eng} = The power required to run the engine (KW)

P_{max} = The rated power or the maximum power (KW)

β_b = Base fuel efficiency parameter in mL/(KJm/s)

ehp = Proportionate decrease in efficiency at high output power

The model predicts the engine and accessories power as a function of the engine speed. These relationships are from a regression analysis and are given below as Equations (A.7) and (A.8).

$$Pacs = EALC * \frac{RPM}{TRPM} + ECFLC * P_{\max} \left(\frac{RPM}{TRPM} \right)^{2.5} \quad \text{(A.7)}$$

$$Peng = ceng + beng * \left(\frac{RPM}{1000} \right)^{2} \quad \text{(A.8)}$$

where:

EALC = The accessory load constant (KW)

ECFLC = The cooling fan constant

P_{max} = The rated power or the maximum power (KW)

RPM = Engine speed

TRPM = Load governed maximum engine speed

ceng = Speed independent engine drag parameter

beng = Speed dependent engine drag parameter

However, Biggs (1988) noted that the determination of the parameter values for the engine drag equation was quite problematic with low coefficients of determination and high standard errors.

Also, Biggs estimates the engine speed as a function of the vehicle speed in order to compute the engine power. There are two different equations in the engine speed model: One for a vehicle in top gear; the other for a vehicle in less than top gear. However, these equations lead to a discontinuous relationship between vehicle speed and engine speed when the vehicle shifts into top gear. Such discontinuities lead to inconsistent fuel consumption predictions and should therefore be avoided (Biggs, 1988).

Recently, the World Bank updated the mechanistic fuel consumption model in the HDM-4 module (Bennett et al, 2003). The model adopted is based on the ARRB ARFCOM mechanistic model (Australian model) described above, but with a change to the prediction of engine speed, accessories power, and engine drag. The general form of the model is expressed conceptually by Equation (A.9).

$$IFC = f\left(Ptr, Paccs + Peng\right) = \max\left(\alpha, \xi * Ptot * \left(1 + dFuel\right)\right) \quad \text{(A.9)}$$

where:

IFC = Instantaneous Fuel consumption in mL/s

P_{tr} = Power required to overcome traction forces (kW)

P_{accs} = Power required for engine accessories (e.g. fan belt, alternator etc.) (kW)

P_{eng} = Power required to overcome internal engine friction (kW)

α = Fuel consumption at Idling (mL/s)

ξ = Engine efficiency (mL/KW/s)

$$= \xi_b \left(1 + ehp \frac{\left(P_{tot} - P_{eng} \right)}{P_{\max}} \right)$$

ξ_b = Engine efficiency depends on the technology type (gasoline versus diesel)

P_{max} = Rated engine power

ehp = engine horsepower

$dFuel$ = Excess fuel conception due to congestion

The engine efficiency decreases at high levels of output power, resulting in an increase in the fuel efficiency factor ξ. The total power required is divided into tractive power, engine drag, and vehicle accessories, respectively. The total requirement can be calculated by two alternative methods depending on whether the tractive power is positive or negative as shown in Table A-1. The tractive power is a function of the aerodynamic, gradient, curvature, rolling resistance and inertial forces. The aerodynamic forces are expressed as a function of the air density and the aerodynamic vehicle characteristics and are given in Table A-2. The gradient forces are a function of vehicle mass, gradient, and gravity. The curvature forces are computed using the slip energy method. The rolling resistance forces are a function of vehicle characteristics, pavement conditions, and climate. The inertial forces are a function of the vehicle mass, speed, and acceleration.

Table A-1 Current HDM 4 Fuel Consumption Model

Name	Description	Unit
Total power (P_{tot})	$P_{tot} = \frac{P_{tr}}{edt} + P_{accs} + P_{eng}$ for $P_{tr} \geq 0$, uphill/level $P_{tot} = edtP_{tr} + P_{accs} + P_{eng}$ for $P_{tr} < 0$, downhill	kW
edt	Drive-train efficiency factor	
Engine and accessories power ($P_{engaccs} = P_{eng} + P_{accs}$)	$Pengaccs = KPea * P\max * \left(Paccs\_a1 + (Paccs\_a0 - Paccs\_a1) * \frac{RPM - RMPIdle}{RPM100 - RPMIdle}\right)$	kW
KPea	Calibration factor	
Pmax	Rated engine power	kW
Paccs_a1	$Paccs\_a1 = \frac{-b + \sqrt{b^2 - 4 * a * c}}{2 * a}$ $\begin{cases} a = \xi_b * ehp * kPea^2 * P\max * \frac{100 - PctPeng}{100} \\ b = \xi_b * kPea * P\max \\ c = -\alpha \end{cases}$	
ξ_b	Engine efficiency depends on the technology type (gasoline versus diesel)	mL/kW/s
ehp	Engine horsepower	hp
α	Fuel consumption at Idling	mL/s
Paccs_a0	Ratio of engine and accessories drag to rated engine power when traveling at 100 km/h	
PctPeng	Percentage of the engine and accessories power used by the engine (Default = 80%)	%
Engine speed (RPM)	$RPM = a0 + a1 * SP + a2 * SP^2 + a3 * SP^3$ $SP = \max(20, v)$	Rev/min
υ	Vehicle speed	m/s
a0 to a3	Model parameter (Table A.3)	
RPM100	Engine speed at 100Km/h	Rev/min
RPMIdle	Idle engine speed	Rev/min
Traction power (P_{tr})	$P_{tr} = \frac{v(Fa + Fg + Fc + Fr + Fi)}{1000}$	kW
Fa	Aerodynamic forces	N
Fg	Gradient forces	N
Fc	Curvature forces	N
Fr	Rolling resistance forces	N
Fi	Inertial forces	N

Table A-2 Current HDM 4 Traction Forces Model

Name	Description	Unit
Aerodynamic forces (*Fa*)	$Fa = 0.5 * \rho * CDmult * CD * AF * \upsilon^2$	N
CD	Drag Coefficient	
CDmult	CD multiplier	
AF	Frontal Area	m^2
ρ	Mass density of the air	Kg/m^3
υ	Vehicle speed	m/s
Gradient forces (*Fg*)	$Fg = M * GR * g$	N
M	Vehicle weight	Kg
GR	Gradient	radians
g	The gravity	M/s^2
Curvature forces (*Fc*)	$Fc = \max\left(0, \frac{\left(\frac{M*\upsilon^2}{R} - M*g*e\right)^2}{Nw*Cs} * 10^{-3}\right)$	N
R	curvature radius	m
Superelevation *(e)*	$e = \max(0, 0.45 - 0.68 * Ln(R))$	m/m
Nw	Number of wheels	
Tire stiffness *(Cs)*	$Cs = KCS * \left[a0 + a1 * \frac{M}{Nw} + a2 * \left(\frac{M}{Nw}\right)^2\right]$	
KCS	Calibration factor	
a0 to a2	Model parameter (Table A-4)	
Rolling resistance (F_r)	$Fr = CR2 * FCLIM * (b11 * Nw + CR1 * (b12 * M + b13 * \upsilon^2))$	N
CR1	Rolling resistance tire factor	
Rolling resistance parameters *(b11, b12, b13)*	$b11 = 37 * Dw$ $b12 = \begin{cases} 0.067 / Dw & old\ \ tires \\ 0.064 / Dw & latest\ \ tires \end{cases}$ $b12 = 0.012 * Nw / Dw^2$	
Rolling resistance surface factor *(CR2)*	$= Kcr2[a0 + a1 * Tdsp + a2 * IRI + a3 * DEF]$	
Kcr2	Calibration factor	
a0 to a3	Model coefficient (Table A-5)	
Tdsp	Texture depth using sand patch method	mm
IRI	International roughness index	m/km
DEF	Benkelman Beam rebound deflection	mm
Climatic factor (*FCLIM)*	$FCLIM = 1 + 0.003 * PCTDS + 0.002 * PCTDW$	
Inertial forces (F_i)	$Fi = M * \left(a0 + a1 * \arctan\left(\frac{a2}{\upsilon^3}\right)\right) * a$	
a0 to a2	Model parameter (Table A-6)	

Table A-3 Engine Speed Model Parameters for the Current HDM 4 model (Bennett and Grennwood, 2003)

Vehicle Type	Engine speed			
	a0	**a1**	**a2**	**a3**
Motorcycle	-162	298.86	-4.6723	-0.0026
Small car	1910	-12.311	0.2228	-0.0003
Medium car	1910	-12.311	0.2228	-0.0003
Large car	1910	-12.311	0.2228	-0.0003
Light delivery car	1910	-12.311	0.2228	-0.0003
light goods vehicle	2035	-20.036	0.356	-0.0009
four wheel drive	2035	-20.036	0.356	-0.0009
light truck	2035	-20.036	0.356	-0.0009
medium truck	1926	-32.352	0.7403	-0.0027
heavy truck	1905	-12.988	0.2494	-0.0004
articulated truck	1900	-10.178	0.1521	0.00004
mini bus	1910	-12.311	0.2228	-0.0003
light bus	2035	-20.036	0.356	-0.0009
medium bus	1926	-32.352	0.7403	-0.0027
heavy bus	1926	-32.352	0.7403	-0.0027
Coach	1926	-32.352	0.7403	-0.0027

Table A-4 Cs Model Parameters for the Current HDM 4 model (Bennett and Grennwood, 2003)

coefficient	<=2500kg		>2500Kg	
	Bias	radial	bias	radial
a0	30	43	8.8	0
a1	0	0	0.088	0.0913
a2	0	0	-0.0000225	-0.0000114
Kcs	1	1	1	1

Table A-5 Parameters for CR2 Model in the Current HDM 4 Model (Bennett and Grennwood, 2003)

Surface class	surface type	<=2500kg				>2500Kg			
		a0	a1	a2	a3	a0	a1	a2	a3
Bituminous	AM or ST	0.5	0.02	0.1	0	0.57	0.04	0.04	1.34
Concrete	JC or GR	0.5	0.02	0.1	0	0.57	0.04	0.04	0
unsealed	GR	1	0	0.075	0	1	0	0.075	0
unsealed	-	0.8	0	0.1	0	0.8	0	0.1	0
block	CB, BR or SS	2	0	0	0	2	0	0	0
unsealed	SA	7.5	0	0	0	7.5	0	0	0

Table A-6 Effective Mass Ratio Model Parameters for the Current HDM 4 model (Bennett and Grennwood, 2003)

Vehicle Type	Effect Mass ratio Model Coefficients		
	a0	a1	a2
Motorcycle	1.1	0	0
Small car	1.14	1.01	399
Medium car	1.05	0.213	1260.7
Large car	1.05	0.213	1260.7
Light delivery car	1.1	0.891	244.2
light goods vehicle	1.1	0.891	244.2
four wheel drive	1.1	0.891	244.2
light truck	1.04	0.83	12.4
medium truck	1.04	0.83	12.4
heavy truck	1.07	1.91	10.1
articulated truck	1.07	1.91	10.1
mini bus	1.1	0.891	244.2
light bus	1.1	0.891	244.2
medium bus	1.04	0.83	12.4
heavy bus	1.04	0.83	12.4
coach	1.04	0.83	12.4

EVALUATION OF THE EXISTING VOC MODELS

This section evaluates the existing models. The most recent fuel consumption model (HDM 4) have been implemented in EXCEL spreadsheets in order to study the sensitivity of the various input variables and to compare their predictions with the results from the U.S. empirical models (Zaniewski et al., 1982). In general, the model evaluation and selection was based on a set of criteria that encompasses two distinctive and equally important aspects: (1) practicality of the model and (2) statistical soundness.

Practicality of the Model

1- Ease of use and availability of appropriate input data: the HDM 4 model is more complicated than an empirical/regression model because it needs more input variables. However, it is more flexible than the empirical ones because of its nature, i.e. mechanistic. The input variables are available from different sources of data. Appendix A2 summarizes the source for the different input data along with a summary distribution.

2- The ability of the model to incorporate pavement surface conditions as currently being measured: The input variables related to pavement surface conditions are not as currently being measured. In fact, the rolling resistance model uses:

- Benkelman beam deflection, and not the FWD deflection to take into account pavement response. These two measurements can be correlated (for example, see Ullidtz, 1989); and
- Sand patch method to measure surface texture depth (Tsdp). Currently, DOTs uses laser -based pavement surface texture measurement devices, which measure the Mean Profile Depth (MPD) of the pavement. The relationship between these two measurements is $Tsdp = 1.02 * MPD + 0.28$.

3- Reasonableness and applicability to U.S. conditions: From literature review, it became apparent that most of the existing models are derived from previous ones; each model aims to correct a problem found in a previous one. Some major points and/or noteworthy corrections follow:

- The South African model assumes that the fuel efficiency of the vehicle is independent from the driving mode. However, Biggs found that the fuel efficiency increases in the acceleration case (Biggs, 1987). An improved mechanistic model was then developed.

- In the ARFCOM model, there are two different equations in the engine speed model: One for a vehicle in top gear; the other for a vehicle in less than top gear. However, these equations lead to a discontinuous relationship between vehicle speed and engine speed when the vehicle shifts into top gear. Such discontinuities lead to inconsistent fuel consumption predictions (Biggs, 1988). In HDM 4, a new regression equation relating vehicle speed to the engine speed was developed.

- Even though the Swedish model is purely mechanistic, it was noted that it gives unreasonably high results compared with the real field data. Thus, Hammarström and Henriksson (1994) calibrated the HDM III to Swedish conditions.

Considering the above point, the research team selected the HDM 4 model for further evaluation and discussion. In order to evaluate the reasonableness and applicability to U.S. conditions, the research team compared the empirical (Zaniewski et al.) models to the newer mechanistic (HDM 4) models. To do so, the research team, first, had to update the Zaniewski tables using the national average fuel consumption data collected from the Bureau of Transportation Databases. Figure A.1 shows the evolution of fuel consumption for passenger cars from 1960 through 2004. The research team followed the same procedure as the one used by Zaniewski to update the Winfrey tables. Second, the research team applied US conditions, i.e., car make and models, tires, and weather conditions and ranges for roughness and texture depths (collected from the LTPP databases and included in Appendix A.2).

Figure A.2 shows the updated Zaniewski model and HDM IV with US conditions. Although the shapes of the curves are similar, there are some differences relative to HDM 4 predictions that should be further evaluated:

- First, at low speeds, unlike the HDM 4 predictions, the Zaniewski tables assume that small cars consume more than large cars, which is counter-intuitive observation.
- Second, unlike the HDM 4 predictions, the Zaniewski tables assume much lower fuel consumption at higher speeds.

The research team recognizes that these differences are the result of the calibration of some model parameters to the condition of other countries.

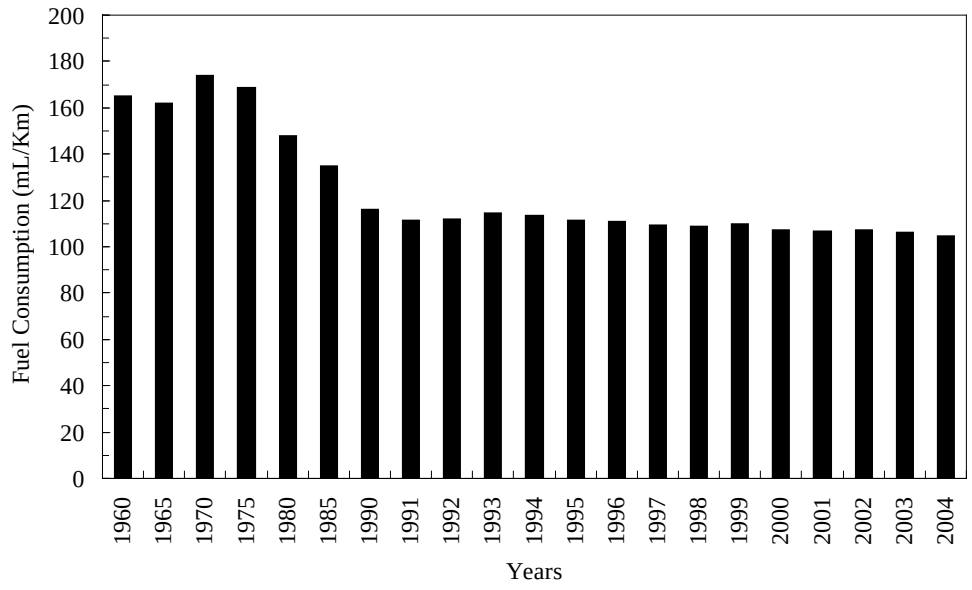

Figure A-1 Annual Fuel Consumption per Vehicle (Passenger Cars)

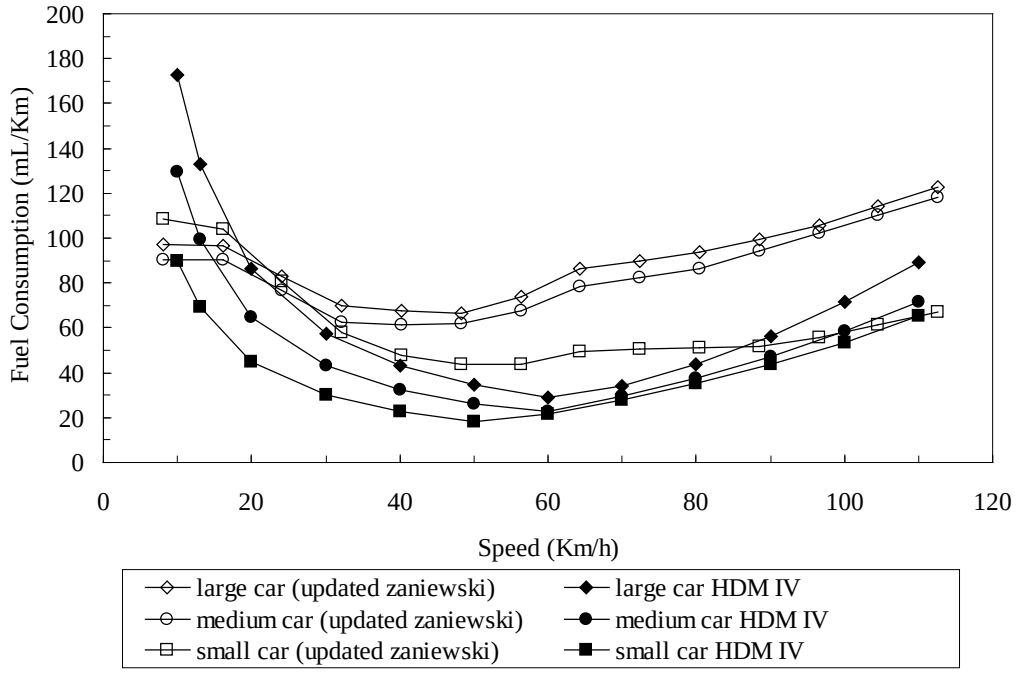

Figure A-2 Comparison between Zaniewski's et al. and HDM 4 Fuel Consumption Prediction (Passenger Cars)

Statistical Soundness of the Models

Most of the empirical models were estimated making use of classical regression assumptions: normality, independence, constant variance. However, it is known that many of the response variables (VOCs) do not follow the classical assumptions. Also, these models and their estimates are generally not transferable outside the economical, technological, fleet operating, and regulatory conditions under which they were developed (Bein, 1993).

Given their nature, the mechanistic models are theoretically formulated so that they encompass the main physical parameters according to basic laws of physics/mechanics. Therefore, the assumptions and the formulation should be valid and reasonably accurate. Also, one can introduce a calibration factor to consider the effect of emerging vehicle technologies on fuel consumption, which makes the model more flexible for future predictions. This improvement will result in models that are theoretically sound and more accurate, which directly translates into more accurate predictions.

A2 - TYPICAL US CONDITIONS: INPUT DATA SOURCES AND DISTRIBUTIONS

The research team identified and classified the data elements required for developing the anticipated models based on their availability level and collection status. The data elements (i.e. input and output data) are classified within 5 categories:

- Pavement condition,
- Vehicle and tire characteristics,
- Environment,
- traffic, and
- VOC data.

For each category, there are 3 levels of availability:

- Level 1: The data are readily available or could be generated from field tests.
- Level 2: The data are not readily available, but they could be estimated or assumed as a constant (e.g., averaging a range of published data values).
- Level 3: The data are not readily available and will not be generated as part of the field tests. In this category, the data will be obtained from other sources if available or will be set to default values as in HDM-4.

In the following sections, the different input parameters, the VOC data and their availability are presented.

Tables A-7 and A-8 present the different inputs for the traction forces and their sources of data. All the input data are readily available (level 1).

The engine and accessories powers are mainly functions of vehicle characteristics. Table A-9 presents input parameters and their sources of data. All the data are of level 1 availability.

Table A-7 Input Parameters for Traction Forces

	Pavement Condition	Environment	Vehicle Characteristics	Tire Characteristics
Aerodynamic		• Altitude • Air temp • Wind speed	• Drag Coefficient • Frontal Area	
Rolling resistance	• Surface type • Texture depth • IRI • Deflection	• % driving – snow • % driving – rain	• Vehicle mass • Vehicle speed • No. of wheels	• Tire type • Wheel diameter.
Curvature	• Curvature radius		• Vehicle mass • Vehicle speed • No. of wheels	• Tire type
Gradient	• Gradient		• Vehicle mass	
Inertial			• Vehicle type • Vehicle mass • Vehicle speed • Vehicle acceleration	

Table A-8 Data Sources for Input Parameters for Traction Forces

	Input parameters	Data Sources	Method	Status
Pavement Condition	• Surface type • Texture depth • IRI, SV • Gradient • Curvature radius • Deflection (FWD)	• Field trials	• Selection matrix • Test measurement • Records	• Selection of test sites completed • Basic summary condition data and records collected • Detailed test measurements to be collected during field trials
Environment	• Altitude • Air temp • Wind speed • % driving – snow • % driving – rain	• Weather station • National Climatic Data Center	• Records	Collected
Vehicle Characteristics	• Vehicle Type, mass • Vehicle Speed, acceleration • Drag Coefficient Frontal Area • No. of wheels	• Vehicle manufacturers	• Selection matrix	Collected
Tire Characteristics	• Tire type • Wheel diameter	• Tire manufacturers	• Selection matrix	Collected

Table A-9 Input Parameters and Data Sources for Engine & Accessories Power

Vehicle Characteristics	Data sources	Status
• Vehicle Type • Vehicle speed	• Selection matrix	Collected
• Rated engine power • Engine efficiency	• Vehicle manufacturer	Collected
• Idle fuel consumption	• Field trials	collected

Figures A-3 through A-9 show typical input data for pavement condition, environment (temperature) and vehicle characteristics in the US. Figures A-3(a) through (d) show the distributions of pavement types in the US. It can be seen that 65% of the roads in the US are paved. Among the paved roads, 57% are flexible, 6% are rigid, 11% are composite and 26% are thin surfaced pavements (source: FHWA). IRI data for all states as of 2006 have been extracted from the FHWA website.

Figures A-4 (a) through (c) show the distributions of IRI of Interstate, US and state highways in selected states. These data support the distribution of pavement sections by pavement type and roughness in the proposed experimental matrix for the field trials presented in chapter 3.

Figure A-5 (a) shows the average monthly air temperatures (2007) for representative states above and below the national average, while Figure A-5 (b) shows the data for Michigan conditions. These data was used to correct for the environmental conditions during the field trials for fuel consumptions.

Vehicle aerodynamic characteristics for all classes in the US have been collected (source: EPA report, 2007). Figures A-6 (a) and (b) show typical ranges of these characteristics for passenger cars. Figures A-6 (c) and (d) show these characteristics for specific car models of popular US and imported brands. These data was used for inputting the specific data for the vehicles used in the field trials. Figure A-7 reports vehicle weight statistics in the U.S. for trucks and passenger cars.

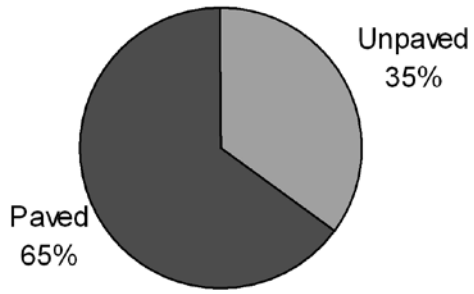

(a) Percent of Mileage by Pavement Category

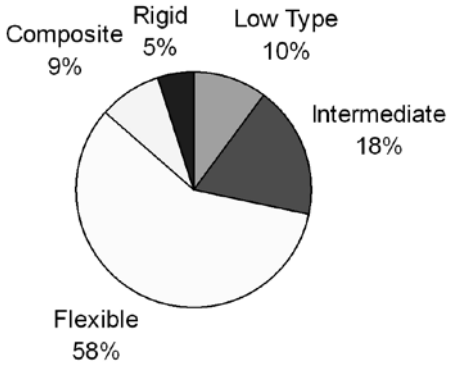

(b) Percent of Mileage by Surface Type (Rural Roads)

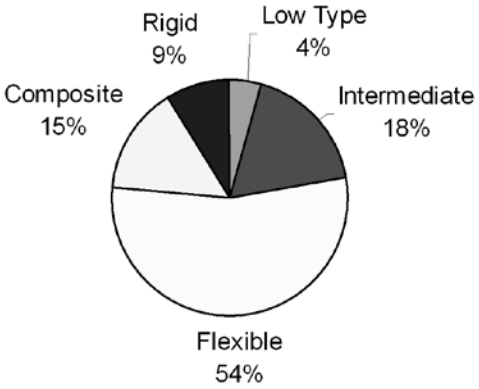

(c) Percent of Mileage by Surface Type (Urban Roads)

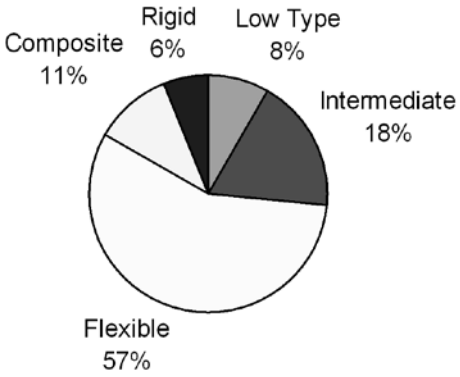

(d) Percent of Mileage by Surface Type (All Roads)

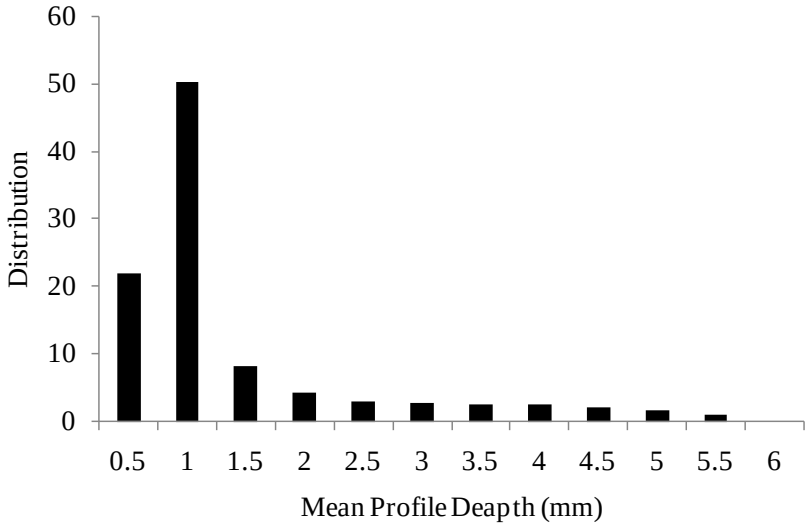

1 mm = 0.04 in

(d) Mean Proficle Depth (All Roads)

Figure A-3 Latest Pavement Type and Mean Profile Depth Frequency Distribution (source: HPMS Database)

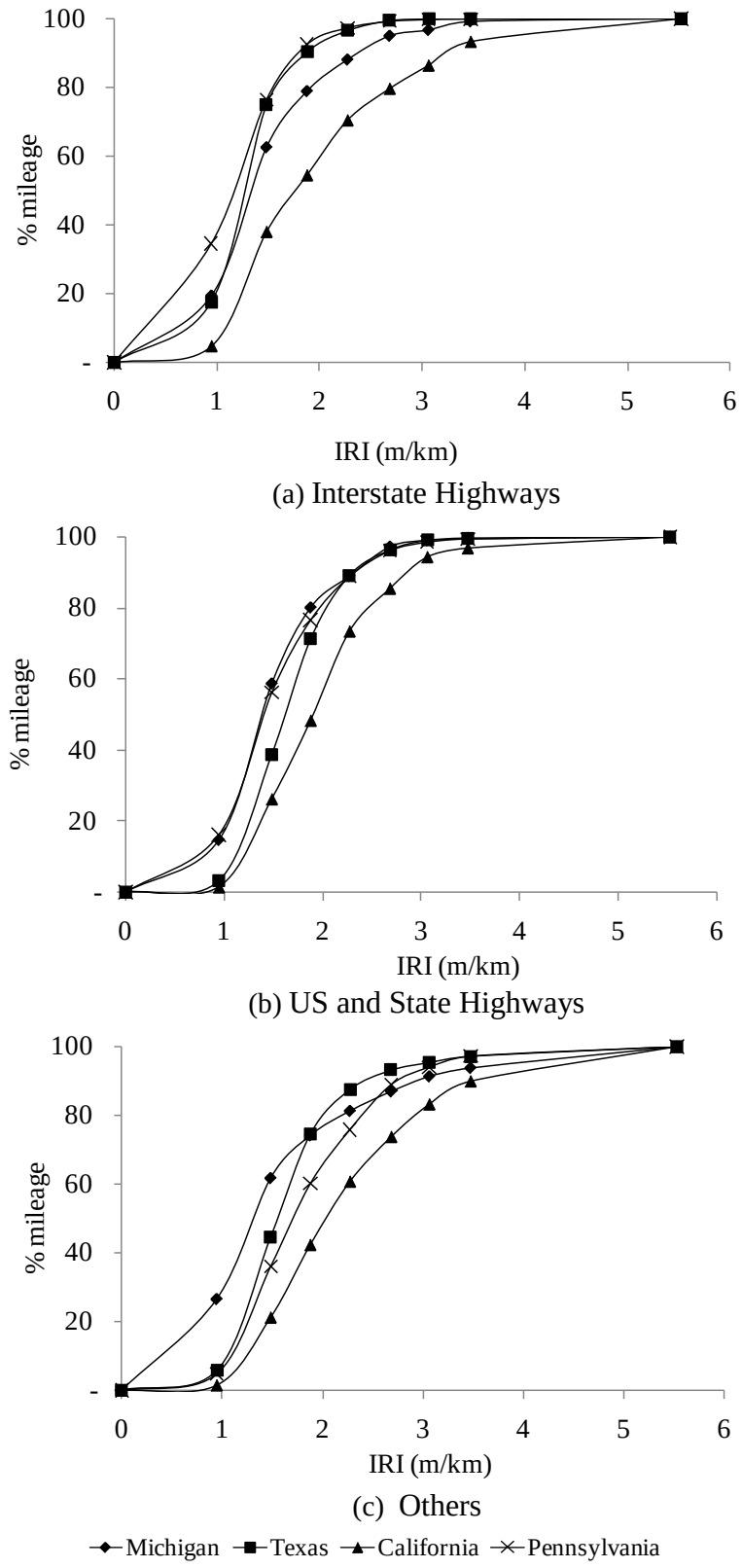

(a) Interstate Highways

(b) US and State Highways

(c) Others

1 m/km = 63.4 in/mile

Figure A-4 Latest Pavement Roughness Frequency Distribution (source: HPMS database)

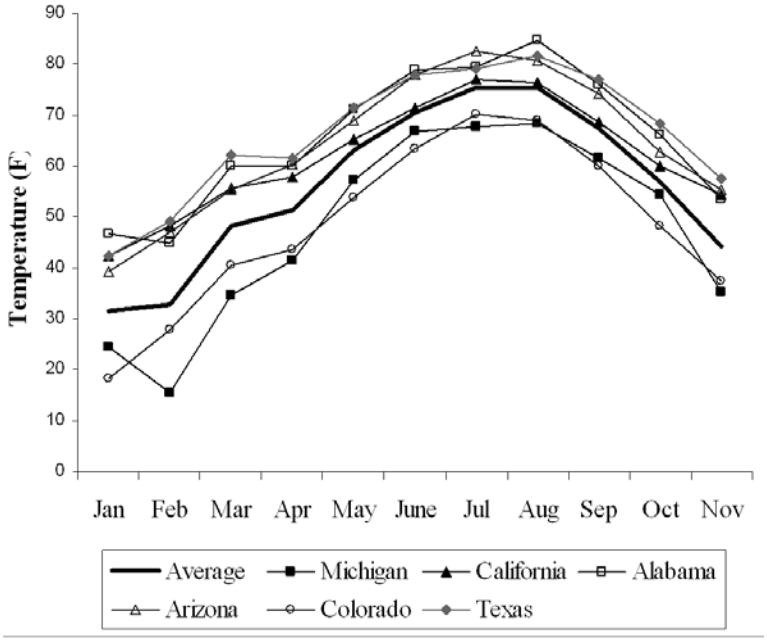

(a) Temperature Distribution in Different States

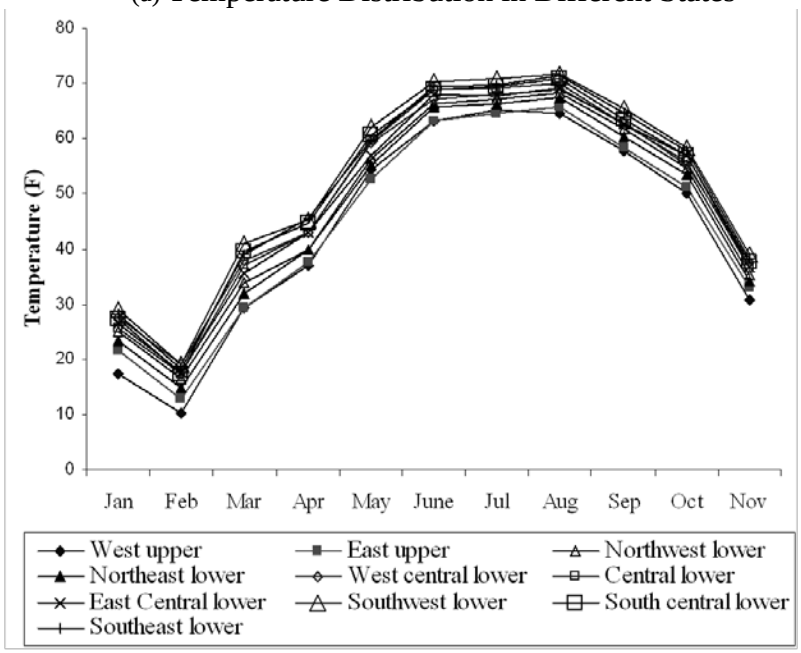

(b) Temperature Distribution in Michigan ($^{\circ}F = \frac{9}{5} * ^{\circ}C + 32$)

Figure A-5 Environment Conditions in the US for 2007 (source: National Climatic Data Center))

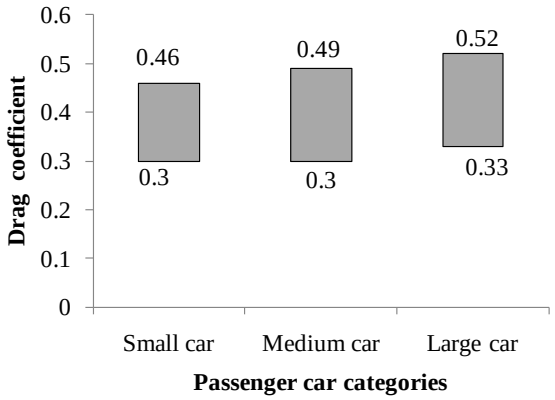

(a) Drag Coefficient Ranges by Vehicle Class

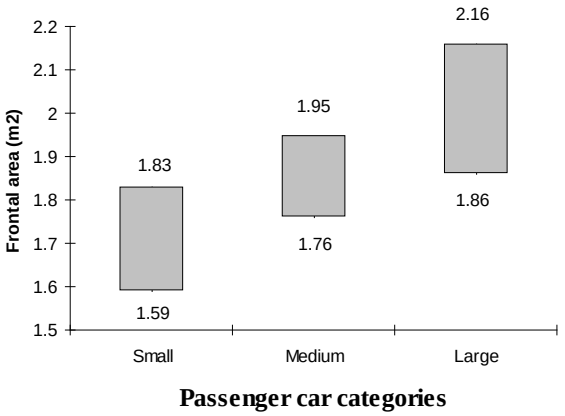

(b) Frontal Area Ranges by Vehicle Class

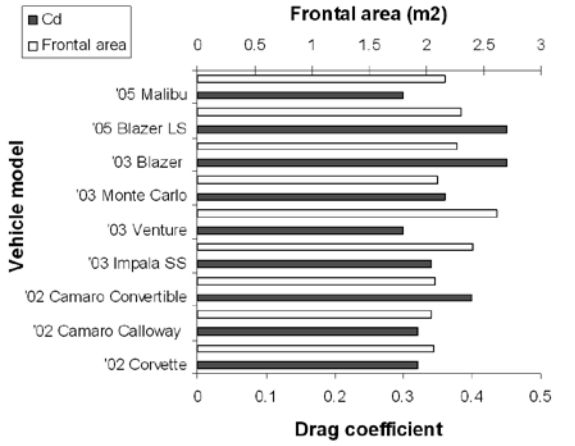

(c) Frontal Area and Drag Coefficient for Chevrolet

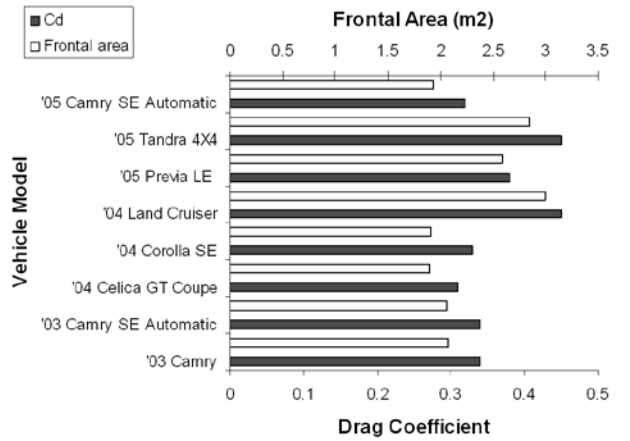

(d) Frontal Area and Drag Coefficient for Toyota

Figure A-6 Latest Aerodynamic Parameters in the US (sources: EPA and CarTest software)

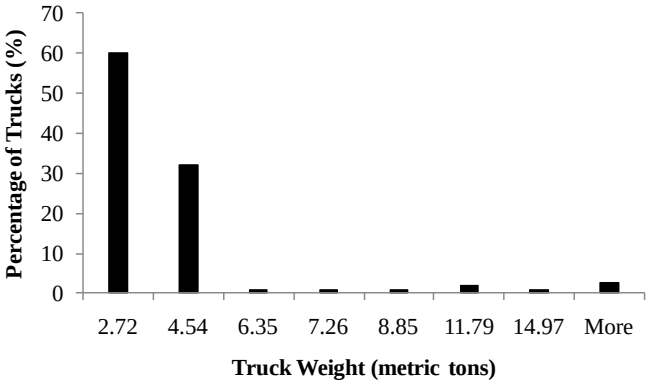

(a) Percentage of Truck by Truck Weight Class in metric tons

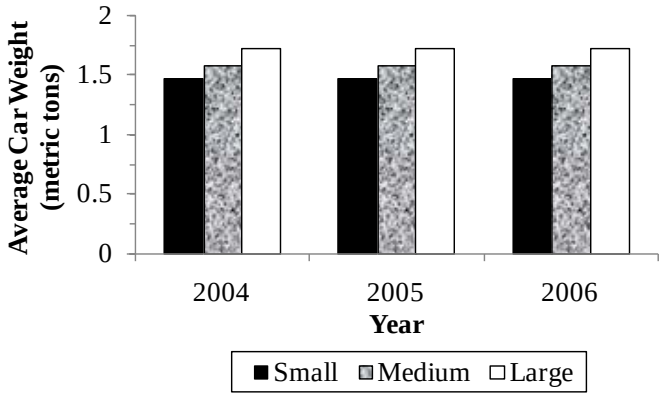

(b) Average Car Weight by Class for 2004-2006 in metric tons

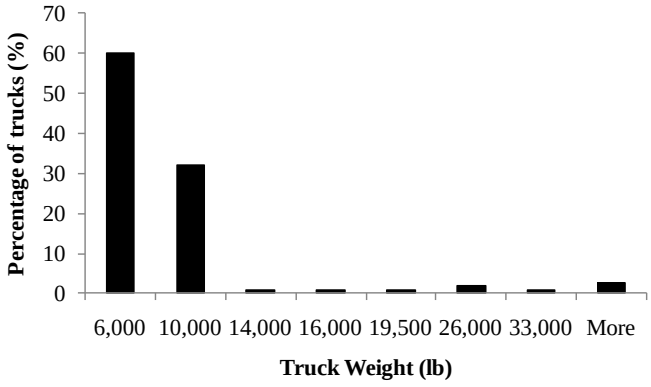

(c) Percentage of Truck by Truck Weight Class in lb

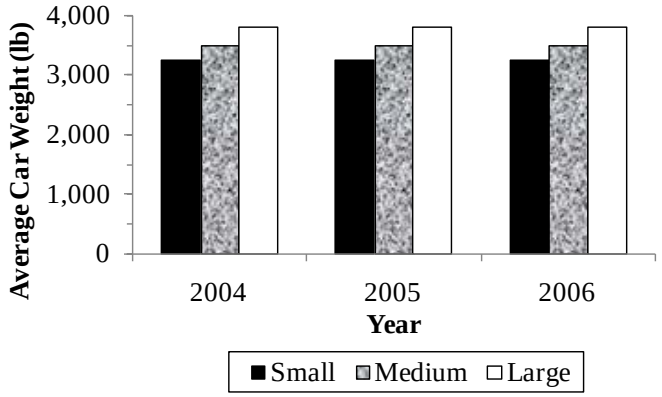

(d) Average Car Weight by Class for 2004-2006 in lb

Figure A-7 Vehicle Weight Statistics in the US Grouped by EPA Vehicle Classification (source: FHWA)

Fuel efficiency data for all vehicles in the US market are readily available from manufacturers and other sources. Figures A.8 and A.9 shows distributions of these engine performance parameters for passenger cars and trucks respectively (source: EPA report, 2007). Specific fuel efficiency values for the vehicles used in the field trials are extracted from the vehicle manufacturer catalogs. The rated engine power for any vehicle can be determined using the relationship shown in Figure A-10 (source: EPA report, 2007).

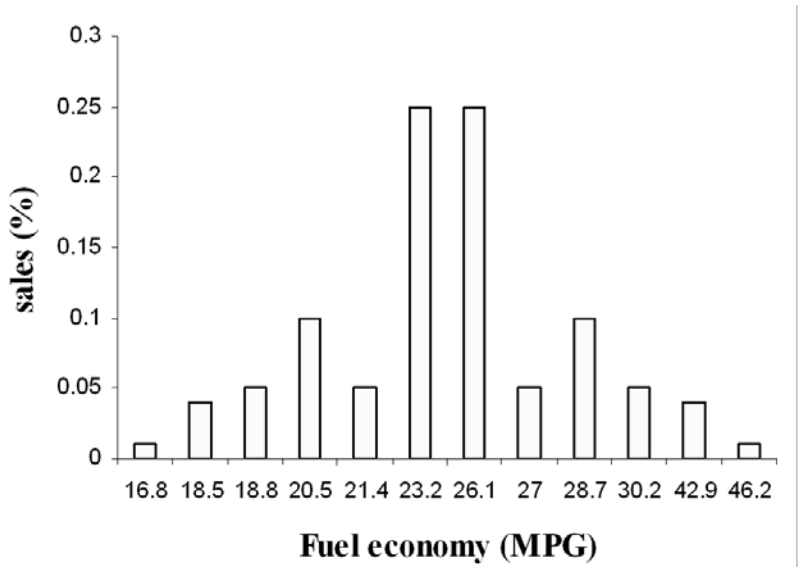

(a) Average Distribution of Fuel Economy for Passenger Car in the US

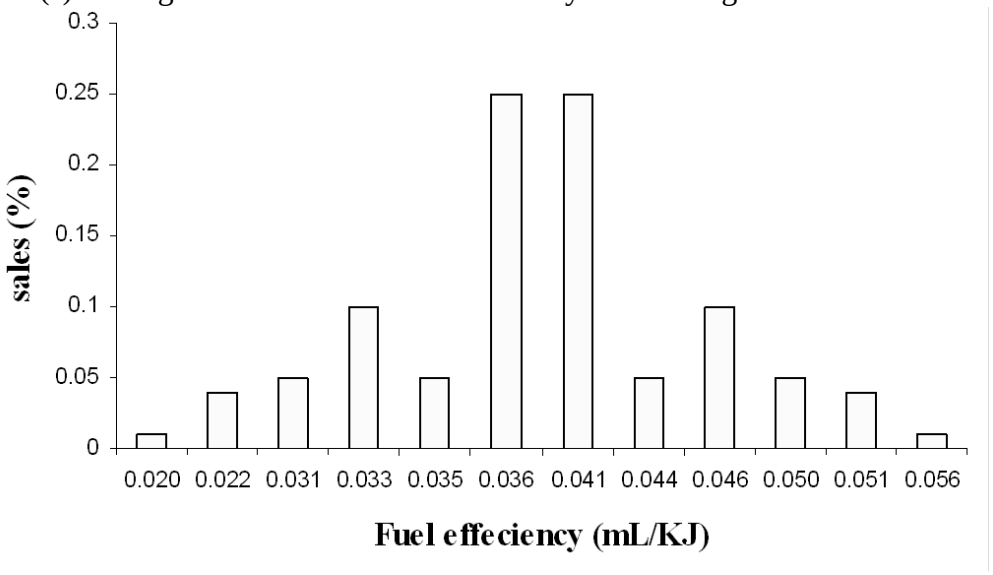

(b) Average Distribution of Fuel Efficiency for Passenger Car in the US

Figure A-8 Latest Fuel Economy and Efficiency Distribution in the US for Passenger (source: Consumer Report, 2007)

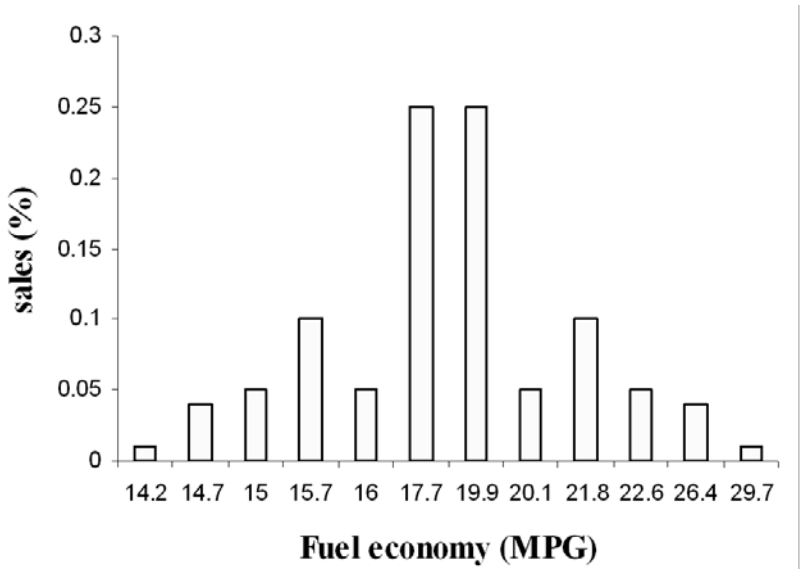

(a) Average Distribution of Fuel Economy for Trucks in the US

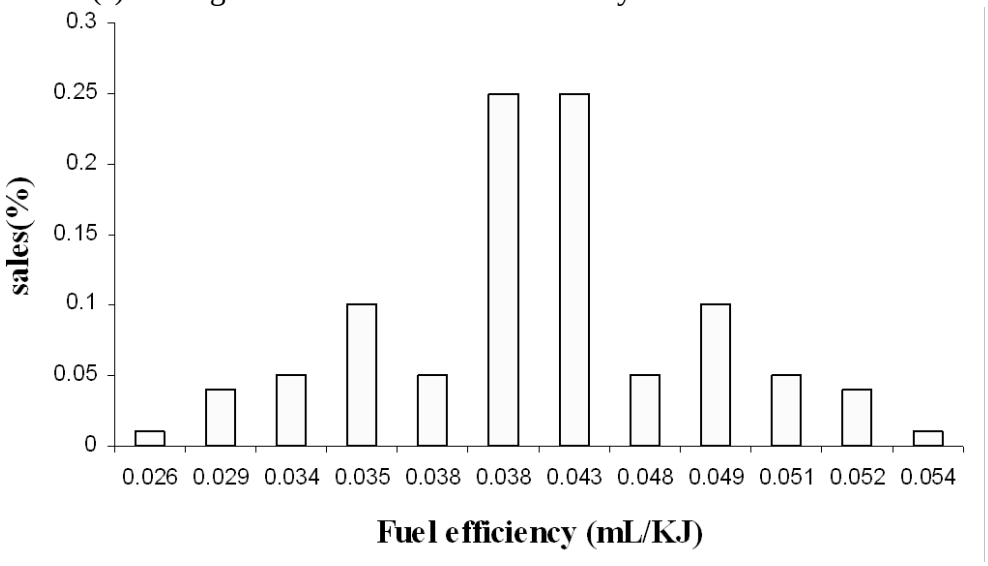

(b) Average Distribution of Fuel Efficiency for Trucks in the US

Figure A-9 Latest Fuel Economy and Efficiency Distribution in the US for Trucks (source: Consumer Report, 2007)

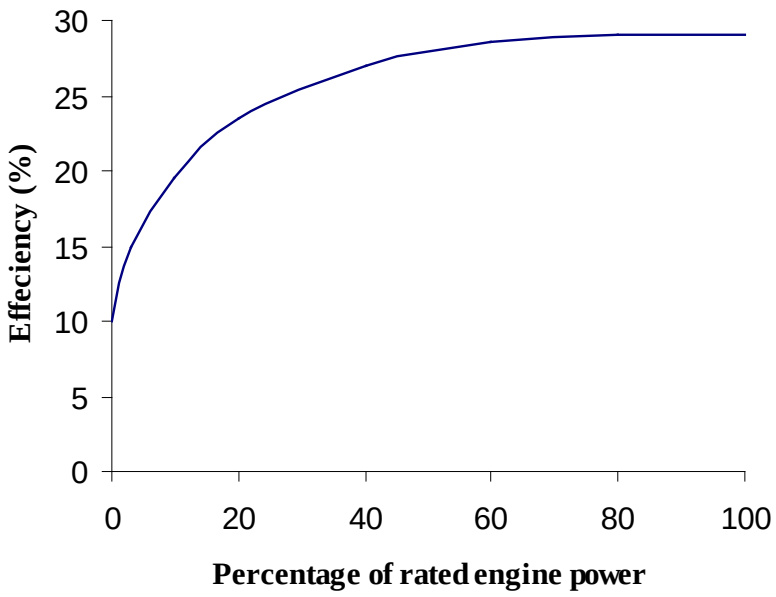

Figure A-10 Relationship between Engine Efficiency and Rated Power (source: EPA Report, 2007)

The data from bureau of census database (VITRIS, 2005) was also collected. The database contains detailed information on trucks in US fleets (Truck use, body type, vehicle size, annual miles of travel, age, vehicle acquisition, truck type, range of operation, and fuel type, etc.). Figure A-11 shows an example of such data taken from this source. Figure A-11a shows annual fuel consumption by vehicle class. It can be seen from the figure that passenger cars, single unit trucks (SUT), heavy trucks and buses consume about 45, 33, 21 and 1 percent of the total fuel consumed, respectively. Figure A-11b presents the percent of vehicle-miles traveled by vehicle class: The data shows similar trends as fuel consumption. Trucks and buses have the highest fuel consumption as compared to cars and SUT (see Figure A-11c). Although trucks showed a smaller percent of the total fuel consumed and mileage traveled, they have the highest annual traveled mileage by vehicle class (see Figure A-11d). Furthermore, time series data for average mileage per gallon by vehicle class indicates that there is no significant change from 1995 to 2002. However, with increasing fuel costs and demands, it is anticipated that this trend (in Figure A-11e) will not remain the same. This simple example indicates that the interaction between various VOC-related factors needs to be considered.

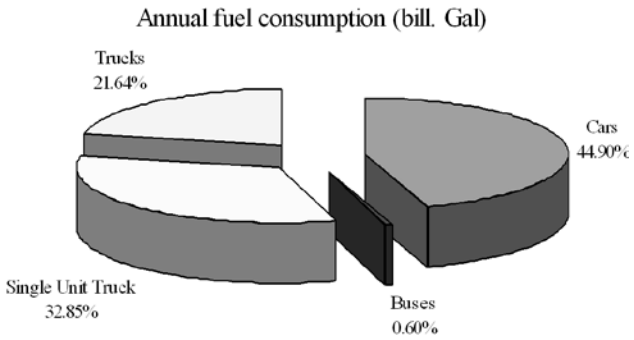

(a) Annual fuel consumption by vehicle class

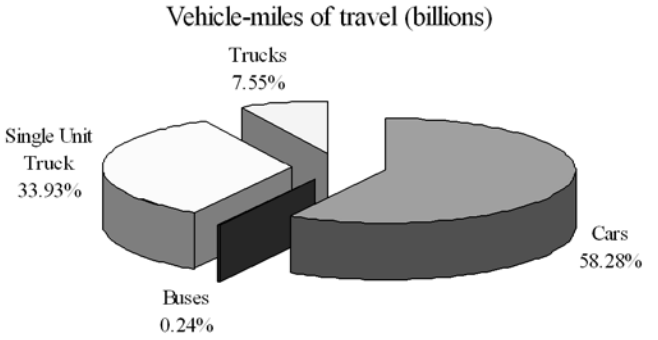

(b) Average vehicle miles by vehicle class

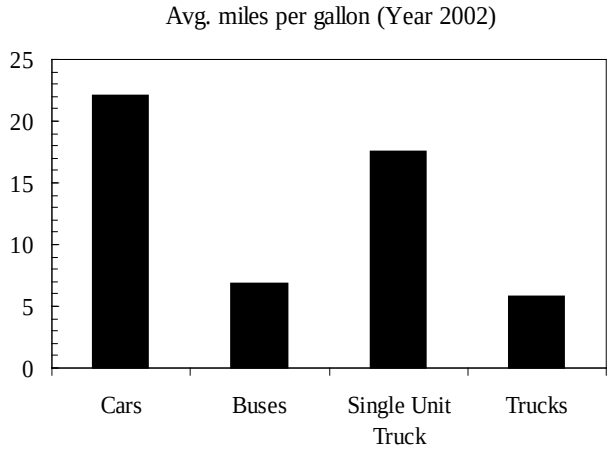

(c) Average miles per gallon by vehicle class

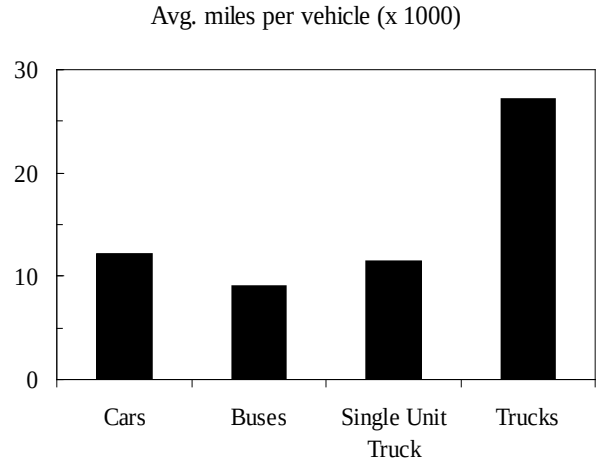

(d) Average annual miles by vehicle class

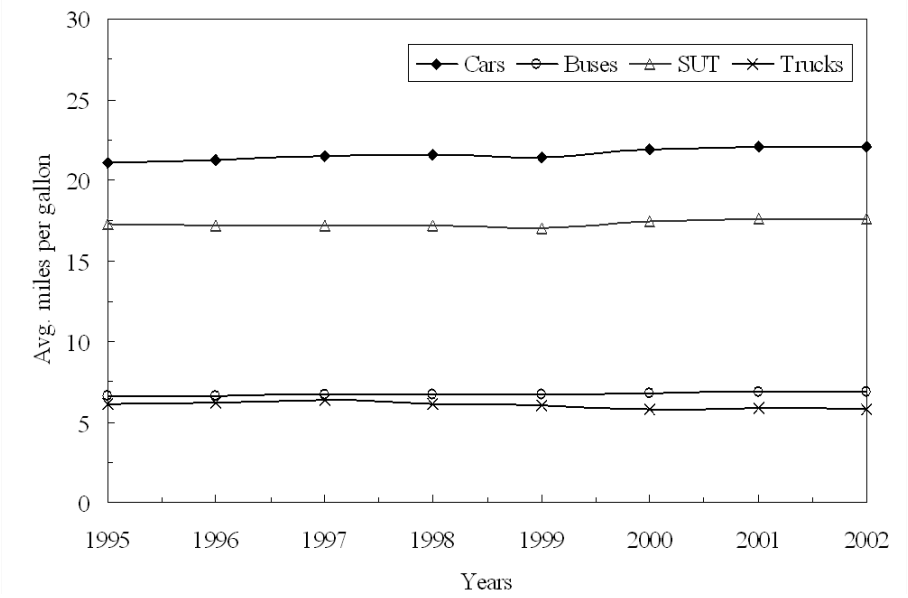

(e) Average miles per gallon by vehicle class, time series

Figure A-11 Vehicle Mileage by Vehicle Class for the US (Source: US Census)

APPENDIX B

TIRE WEAR MODELS

B1 - IDENTIFICATION AND EVALUATION OF TIRE WEAR MODELS

This appendix summarizes the detailed equations and relationships of current tire wear models. These models were also evaluated regarding their applicability to the paved surfaces and traffic and environmental conditions encountered in the United States that are capable of addressing the full range of vehicle types.

EXISTING VOC MODELS

Although tire consumption is a significant component of the total VOC, especially for heavy vehicles, unlike fuel consumption, it has received much less attention. For example, it was found in New Zealand that tire costs constitute about 18% of the VOC for heavy trucks, compared to only 5% for passenger cars (Bennett and Greenwood, 2003). Cost associated with tire wear has been affected by changes in tire design and technology in the tire manufacturing. Radial design and belted construction have increased the mileage life of tires, but increased prices have offset these gains to some extent (Zaniewski et al. 1982). There are two types of models which have been developed for predicting tire consumption: (1) empirical, which can be developed from fleet survey data, and (2) mechanistic, which relate tire consumption to the fundamental equations of motion and are developed from controlled experiments. This section briefly reviews some of the major tire consumption models that have been developed.

Empirical Models

Winfrey developed tables for calculating tire wear cost per mile. The tire wear cost was a function of vertical and horizontal curves, and speed changes (Winfrey, 1969).

In 1973, the U.S. Forest Service funded a project to develop tire wear predictions (based on the slip energy concept) from measurable tire/road interactions for use in a VOC model for the national forest service road system. Zaniewski et al. (1982) developed a new model based on the slip energy concept to calculate tire wear and then present the results in tabular format. The most current models follow a mechanistic modeling approach to develop tread wear models.

The Saskatchewan Department of Highways and Transportation (SHT), Canada, adopted the following tire wear model.

$$TC = \frac{C_t N_t}{L_t K_{tt} K_{tr}} \quad \text{(B.1)}$$

where:

C_t = Cost per tire, $/tire
N_t = Number of tires
K_{tr} = Road roughness coefficient
K_{tt} = Road texture coefficient
L_t = Life of tire (km)

As shown in Equation (B.1), the tire costs are a function of tire type, tire quality, road conditions, and tire maintenance practices. The effect of road surface on tire cost is primarily a function of road surface texture and roughness.

Mechanistic-Empirical Models

In the US, the tire wear model was developed by relating the volume of tread rubber worn to the amount of slip energy expanded at the pavement-tire interface. Equation (B.2) shows the form of the model:

$$V_{WR} = E_{SLIP} / S_{WE} \quad \text{(B.2)}$$

where:

V_{WR} = Volume of worn tread rubber, in^3 (1 in = 25.4 mm)
E_{SLIP} = Slip energy, lb-mi (1 lb-mi = 7,159 N.m)
S_{WE} = Slip energy-volume wear coefficient, (lb-mi)/in^3

In this model two coefficients must be experimentally determined to be representative of specific tire and pavement surface types; these are slip and energy-volume wear coefficients.

The World Bank HDM 3 model adopted the slip energy model to calculate the changes in tread wear as shown below:

$$\Delta TWT = K_0 \times \mu \times NFT \times \lambda \quad \text{(B.3)}$$

where:

ΔTWT = Change in tread wear
K_0 = Calibration factor reflecting pavement properties
μ = Coefficient of friction
NFT = Normal force on the tire (N)
λ = Tire slip

For HDM 4, the model has been extended to include horizontal curvature force and traffic interaction effects, as shown below (Bennett and Greenwood, 2003).

The general form of the tire consumption model is the following:

$$TC = \frac{NW * EQNT}{MODFAC} \quad \text{(B.4)}$$

where:

NW = Number of wheels
EQNT = Number of equivalent new tires consumed per 1000 km
MODFAC = Tire life modification factor

Table B.1 presents the details of this model. Carpenter and Cenek (2000) noted that, when testing the model, the values for C0tc were found to be too low and resulted in an unreasonably high tire life. Therefore, due to the problems with this model, an interim model was adopted for HDM 4. In fact, a constant was added to the EQNT equation in Table B-1, which becomes as follows:

$$EQNT = \left(\frac{1 + RREC * NR}{1 + RTWR * NR}\right) * \frac{TWT}{VOL} + 0.0027 \quad \text{(B.5)}$$

The tire life modification factors were proposed by Harrison and Aziz (1998). They depend on the roughness, tire type and congestion level and are calculated using the equation described in Table B-1.

Table B-1 HDM 4 Tire Consumption Model

Name	Description	Unit
Number of equivalent new tires (***EQNT)***	$EQNT = \frac{1 + RREC * NR}{1 + RTWR * NR} * \frac{TWT}{VOL}$	1/1000 km
RREC	= The ratio of the cost of retreads to new tires	
RTWR	= The life of a retreaded tire relative to a new tire	
VOL	= Tire volume	dm^3
Number of retreading *(NR)*	$NR = \max\left(0, NR0 * e^{(-0.03224 * RImod)} - 1\right)$	
NR0	= The base number of retreads for very smooth, tangent roads (Table B.2)	
RImod	= Model Parameter (Table B.2)	
Total change in tread wear (*TWT)*	$TWT = C_{0tc} + C_{tcte} \times \frac{CFT^2 + LFT^2}{NFT}$ $TWT = C_{0tc} + C_{tcte} \times TE$	dm^3/1000 km
C_{0tc}	= The tread wear rate constant (Table B.2)	dm^3/1000 km
C_{tcte}	= The tread wear coefficient (Table B.2)	dm^3/MNm
The tire energy *(TE)*	$TE = \frac{CFT^2 + LFT^2}{NFT}$	MNm/1000 km
The circumferential force on the tire *(CFT)*	$CFT = \frac{(1 + CTCON * dFUEL) * (Fa + Fr + Fg)}{NW}$	N
CTCON	= The incremental change of tire consumption related to congestion.	
dFUEL	= The incremental change of fuel consumption related to congestion	
Fa	= The aerodynamic forces	N
Fr	= The rolling resistance forces	N
Fg	= The gradient forces	N
The lateral force on the tire *(LFT)*	$LFT = \frac{Fc}{NW}$	N
Fc	= The curvature forces	N
NW	= Number of wheels	
The normal force on the tire *(NFT)*	$NFT = \frac{M * g}{NW}$	N
M	= Vehicle mass	kg
g	= Gravity	m/sec^2
Tire life medication factor *(MODFAC)*	$MODFAC = VEHFAC * TYREFAC * CONFAC$	
VEHFAC	= A vehicle specific modification factor (Table B.2)	
TYREFAC	= A tire type modification factor (see Table B.3)	
Congestion modification factor *(CONFAC)*	$CONGFAC = \begin{cases} 0.7 & VCR < 0.85 \\ 1.0 & VCR \geq 0.85 \end{cases}$	

Table B-2 Tread Wear Rate Constants (Bennett and Greenwood, 2003)

Vehicle type	C_{0tc} (dm^3/1000 km)	C_{tcte} (dm^3/MNm)	RImod	NR0	VEHFAC
Motorcycle	0.00639	0.0005	IRI	1.3	2
Small car	0.02616	0.00204	IRI	1.3	2
Medium car	0.02616	0.00204	IRI	1.3	2
Large car	0.02616	0.00204	IRI	1.3	2
Light delivery car	0.024	0.00187	IRI	1.3	2
Light goods vehicle	0.024	0.00187	IRI	1.3	2
Four wheel drive	0.024	0.00187	IRI	1.3	2
Light truck	0.024	0.00187	IRI	1.3	2
Medium truck	0.02585	0.00201	min(7,IRI)	1.3	1
Heavy truck	0.03529	0.00275	7	1.3	1
Articulated truck	0.03988	0.00311	min(7,IRI)	1.3	1
Mini bus	0.024	0.00187	IRI	1.3	2
Light bus	0.02173	0.00169	IRI	1.3	2
Medium bus	0.02663	0.00207	7	1.3	1
Heavy bus	0.03088	0.00241	min(7,IRI)	1.3	1
Coach	0.03088	0.00241	min(7,IRI)	1.3	1

Table B-3 Tire Type Modification Factor (Harrison and Aziz (1998))

Tire Type	Paved Roads	Unpaved Roads	
		IRI<=6 m/Km	IRI>6 m/Km
Bias	1	1	1
Radial	1.25	1.2	1

EVALUATION OF THE EXISTING VOC MODELS

This section evaluates the existing models. The most recent tire wear model (HDM 4) has been implemented in EXCEL spreadsheets in order to study the sensitivity of the various input variables and to compare their predictions with the results from the U.S. empirical models (Zaniewski et al.).

Practicality of the Model

1- Ease of use and availability of appropriate input data: The HDM 4 model is more

complicated than the empirical/regression models because it needs more input variables. However, it is more flexible than the empirical ones given its nature, i.e., mechanistic. The input variables are available from different sources of data, e.g., tire manufacturers. Appendices A2 and B2 summarize the source for the different input data along with a summary distribution.

2- The ability of the model to incorporate pavement surface conditions as currently being measured: The input variables related to pavement surface conditions (e.g., roughness) are not necessarily compatible with what is currently being measured/used in the U.S. In fact, the rolling resistance model uses:

- Benkelman beam deflection, and not the FWD deflection to take into account pavement response. These two measurements can be correlated (for example, see Ullidtz, 1989); and
- Sand patch method to measure surface texture depth (Tsdp). Currently, DOTs uses laser -based pavement surface texture measurement devices, which measure the Mean Profile Depth (MPD) of the pavement. The relationship between these two measurements is $Tsdp = 1.02 * MPD + 0.28$.

3- Reasonableness and applicability to US conditions: Similarly to fuel consumption, the research team applied US conditions to the HDM 4 model and compared it to the Zaniewski model. Figure B-1 shows many similarities between the two models. In fact, the curves have the same shape. The results from both models are in agreement, i.e., large cars consume more tread than medium cars which consume more than small cars.

Figure B-2 shows the interaction between roughness and tire consumption. Roughness appears to have a major effect on tire consumption which is in agreement with the literature review. Even though Figures B-1 and B-2 show the results for only passenger cars, similar results were found for heavy vehicles. However, because of large differences in scale, results for passenger cars and heavy vehicles could not be displayed on the same graph. Figure B-3 shows the effect of roughness on truck tire consumption.

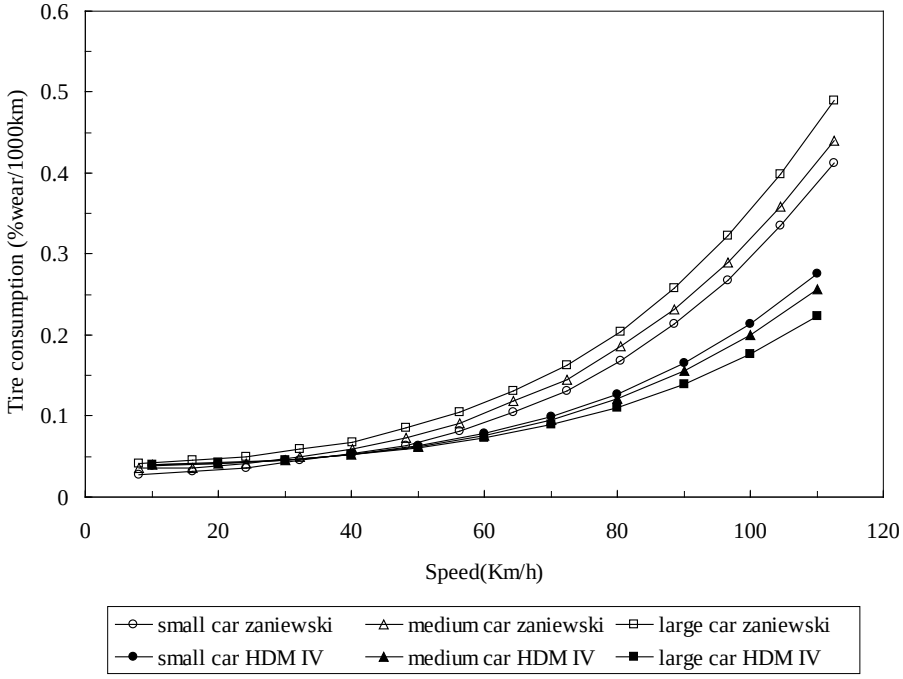

Figure B-1 Comparison between Zaniewski and HDM 4 Models (Tire Wear)

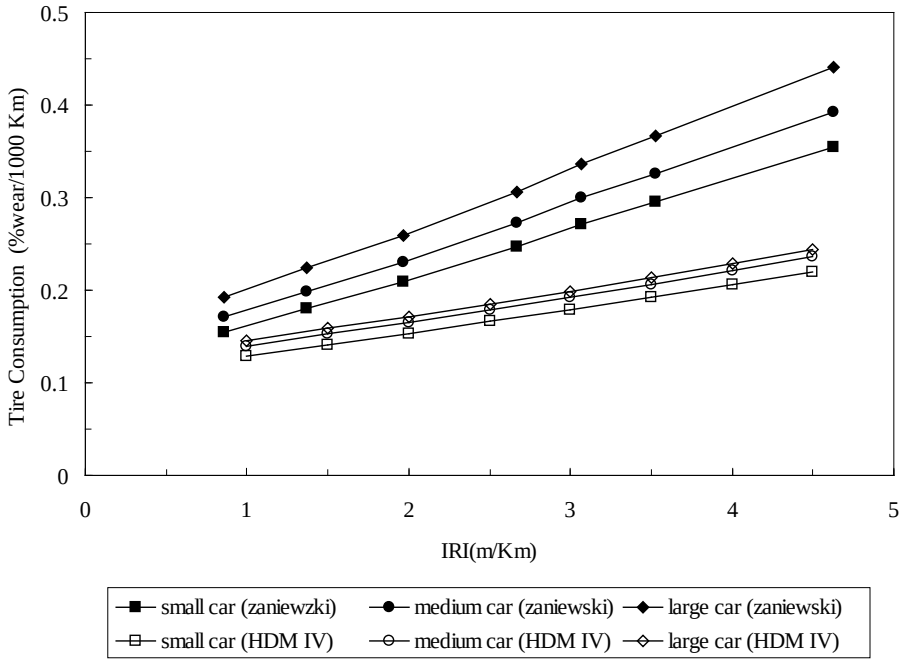

Figure B-2 Effect of Roughness on Tire Consumption for Passenger Cars (HDM 4)

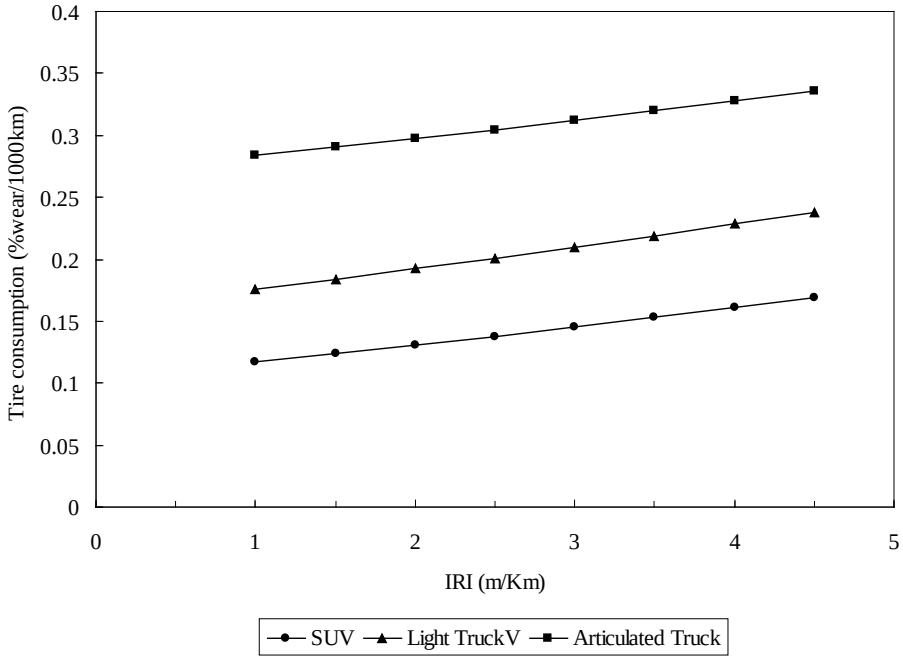

Figure B-3 Effect of Roughness on Tire Consumption for Trucks (HDM 4)

Statistical Soundness of the Models

While empirical models and their estimates are generally not transferable outside the economical, technological, fleet operating, and regulatory conditions under which they were developed (Bein, 1993), the assumptions and the formulation of mechanistic models are valid and reasonably accurate. Therefore, mechanistic models are theoretically sound and more accurate, which directly translates into more accurate predictions.

B2 - TYPICAL US CONDITIONS: INPUT DATA SOURCES AND DISTRIBUTIONS FOR TIRE WEAR DATA

Tables B-4 and B-5 present the different inputs for the traction forces in the HDM 4 and their sources of data. All the input data are readily available (same as fuel consumption). Possible exceptions are the tire wear rate coefficients, C_{tcte} and C_{otc}. The values for C_{otc} used in HDM 4 were arrived at by using estimated tire lives. The tread wears were calculated using typical pavement conditions and tire lives proposed by Cenek and Carpenter (HDM 4, 2000). A further review of the literature revealed more information on these rates. Reported tire wear rate results include (Kennedy et al, 2002):

- Environment Agency (1998) summarized passenger car tire wear rate information in the United Kingdom. Using a life of tire weight loss of 1.5 kg over 50,000 km estimated wear per km corresponds to 30 mg/km/tire or (0.03 dm^3/1000 km). This corresponds to a wear rate of 120 mg/VKT under average driving conditions. (VKT = Vehicle Kilometers Traveled)
- Muschak (1990) estimated that motor vehicles lost 120 mg/VKT in Germany.
- New Zealand Ministry of Transportation (1996) estimated that 1,850 g of rubber was lost from a tire during the time that it took to be replaced. This amount to 53 mg/km (0.053 dm^3/1000 km) per tire if a lifetime of 35,000 km is assumed.
- Legret & Pagotto (1999) identified an average wear rate for a single tire as 17 mg/km (0.017 dm^3/1000 km). This was based upon the following information: 50,000 km wear, dimensions 0.54 m in diameter, 0.12 m wide, 6 mm thickness, density of 1 g/cm3, 30% void due to tread depth, total material loss 857 g. The authors assumed that the amount for heavy vehicles (>3.5 tons is twice this quantity).
- Le Maitre et al. (1998) reported tire wear rates for passenger vehicles from tire/driver surveys of wear rates. They reported wear rates for passenger cars under a range of route/driving conditions. For example:

  Highway use: 0.5 g/100 km or 5 mg/km (0.0005 dm^3/1000 km).

  Urban use: 2.8 g/100 km or 28 mg/km (0.028 dm^3/1000 km).

  Medium use: 3.3 g/100 km or 33 mg/km (0.033 dm^3/1000 km).

  Severe use: 7.8 g/100 km or 78 mg/km (0.078 dm^3/1000 km).

Table B-4 Input Parameters for Tire Consumption Model

	Pavement Condition	Environment/ Traffic	Vehicle Characteristics	Tire Characteristics
Equivalent new tire Number of retreadings	• IRI • Texture • Curvature • Gradient			• Tire volume • Ratio of cost of retreads to new tires • Life of retreated tire relative to new tire
Tire life modification factor	• Pavement type	• Volume to capacity ratio	• Vehicle type	• Tire type
Traction forces	Same as Fuel Consumption			

Table B-5 Data Sources for Input Parameters of the Tire Consumption Model

	Input parameters	Data Sources	Method	Status
Pavement Condition	• Surface type • IRI • Texture • Curvature • Gradient	• Field trials, NCAT • HPMS	• Selection matrix • Test measurement • Records	• Selection of test sites completed • Basic summary condition data and records collected • Detailed test measurements to be collected during field trials
Environment/ Traffic	• Same as Fuel consumption / • Volume to capacity ratio	• SHA	• Records	Collected
Vehicle Characteristics	• Vehicle Type	• Known	• Selection matrix	Collected
Tire Characteristics	• Tire type • Tire volume • Ratio of cost of retreads to new tires = 50% • Life of retreated tire relative to new tire = 75%	• Tire manufacturers • Information Bureau of Retreading	• Selection matrix	Collected

- Kennedy et al (2002) reported the following wear rates for New Zealand based on industry-supplied measures for material loss and a minimum service life of 35,000 km for passenger cars (PC), light trucks and heavy trucks. Industry- indicators over the tire service life were:

  Passenger car tire: 0.031 g/km (0.031 dm^3/1000 km)
  Light truck tire: 0.051 g/km (0.051 dm^3/1000 km)
  Heavy truck tire: 0.21 g/km (0.21 dm^3/1000 km)

Table B-6 provides a summary of the wear rate information based on average life of tire wear rates described above (Kennedy et al., 2002).

Table B-6 Summary of Average Vehicle Tire Wear Rates Under Average Driving Conditions (Kennedy et al, 2002)

Reference	Passenger Car (dm^3/1000 km)	Light Truck (dm^3/1000 km)	Heavy Truck (dm^3/1000 km)
Cadle & Williams (1978)	0.03		
Rogge et al. (1993)	0.006-0.09		
New Zealand Ministry of Transport (1996)	0.037-0.053		
New Zealand Environmental Agency (1998)	0.0355		
Le Maitre et al. (1998)	0.033 (medium use)		
Legret & Pagotto (1999)	0.017		~0.034
Cenek et al. (1993) and Carpenter and cenek (1999)	0.02 (low severity)		
New Zealand industry estimate (Kennedy et al, 2002)	0.022-0.031	0.026-0.035	0.046-0.062

Cenek (1993) measured a value for C_{tcte} of 0.00041 dm^3/MNm for the Nissan Pulsar. He reported that an earlier study by Hodges & Koch (1979) had measured values for C_{tcte} for a car in the range 0.0003 to 0.0009 dm^3/MNm for radial car tires on different road surfaces. The values for C_{tcte} used in HDM 4 were arrived at by assuming that these lower and upper values of C_{tcte} to be representative of truck tires and motorcycle tires respectively. The values for the other vehicle classes are:

- For motorcycles C_{tcte} = 0.0009 dm^3/MNm
- For all cars, delivery vehicles and 4 wheel drives : C_{tcte} = 0.0005 dm^3/MNm
- For all trucks and buses: C_{tcte} = 0.0003 dm^3/MNm

The truck tire consumption data as well as pavement surface roughness and texture depth data were collected from NCAT. These data was used to estimate the tire wear rate and validate the HDM-4 tire consumption model for trucks. Figure B-4 shows the tire replacement data for steer and drive-trailer axles for the NCAT test track.

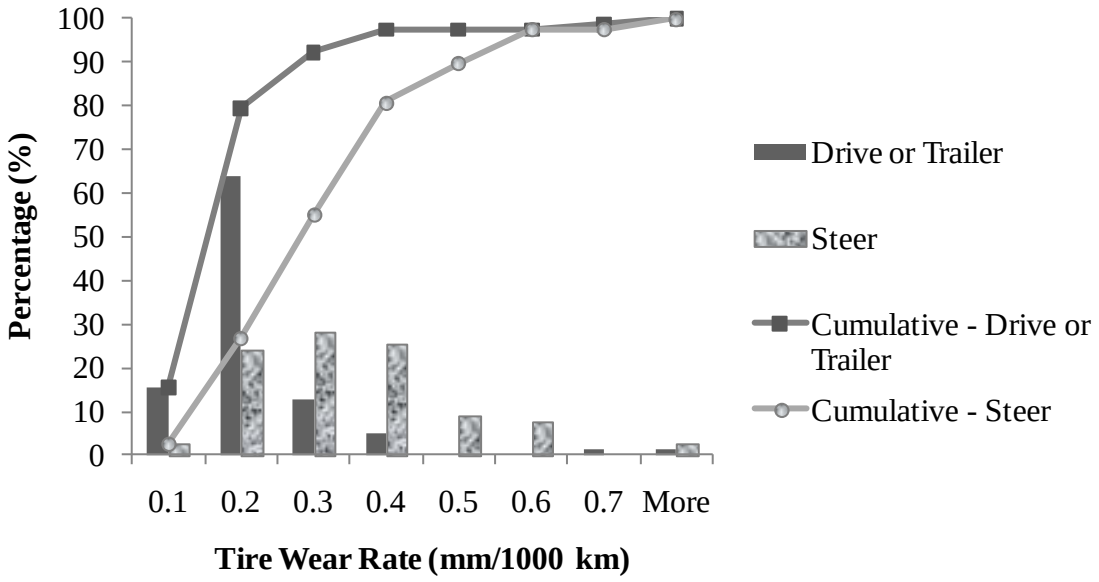

Figure B-4 Tire Consumption Data from the NCAT Test (source: NCAT)

Field trials were conducted to collected tire wear data for passenger cars. Assuming that a measurable tire wear using the laser scanner (tread depth apparatus accuracy is 4 microns) is about 0.1 mm and using the tire life information (Table 4.2), the minimum length for road sections at which the vehicle is driven at constant speed is 1040 km for passenger cars. Figure B-5 shows the results for the M99 sections. It was observed that the variability in tire wear between trials was significant. It is believed that, since 0.1 mm is a very small number, it is very sensitive to measurement error.

Figures B-6 through B-10 show the “before” and “after” tread depth data for each field trial. The comparison of the “before” and “after” tread depth data within each trial showed that:

- For the left front tire (both positions) and the right rear tire first position: The overall trend is similar for all field trials except for Trial 3. The trend of the “before” data for Trial 3 was different than the trend of the “after” data for Trial 2. It is believed that an error in the laser positioning caused this difference. Therefore, the data collected during the third trial could not be used.

- For the right rear tire second position: The overall trend is similar for all field trials except for Trial 2. The level of error was too high and an increase in tread depth was observed. Therefore, the data collected during Trial 2 could not be used.

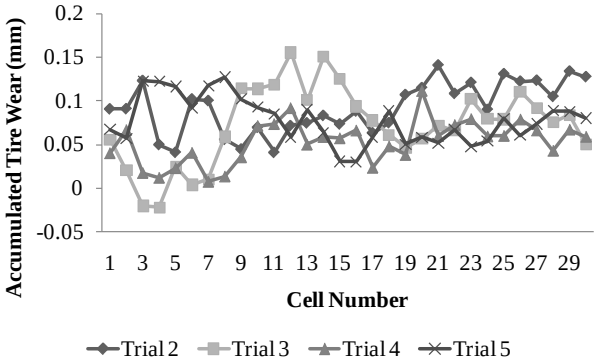

(a) Left Front Tire --- First Position

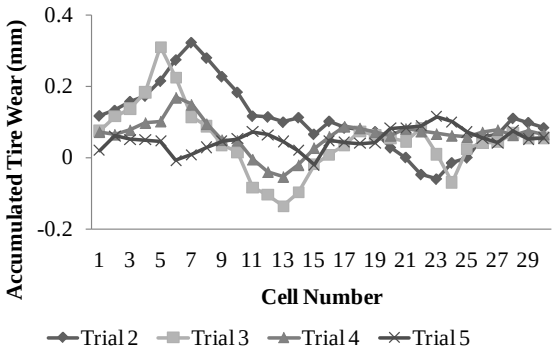

(b) Left Front Tire --- Second Position

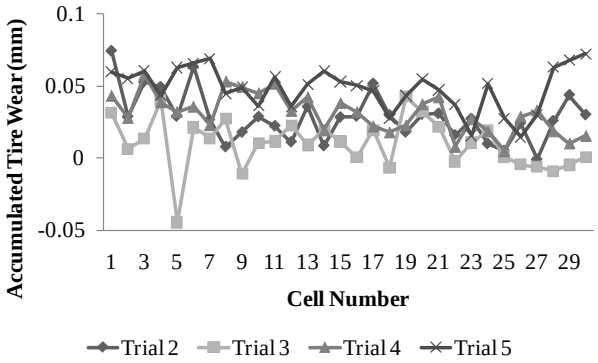

(c) Right Rear Tire --- First Position

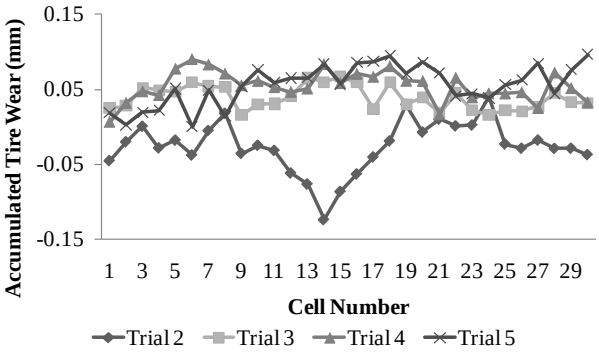

(d) Right Rear Tire --- Second Position

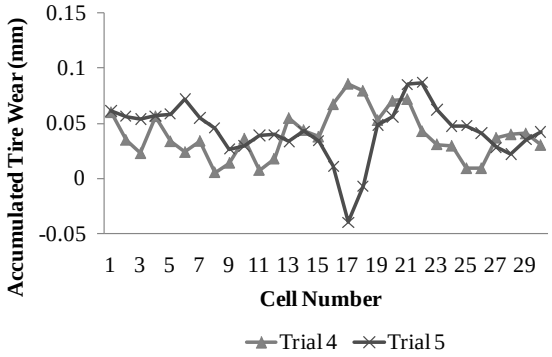

(e) Left Rear Tire --- First Position

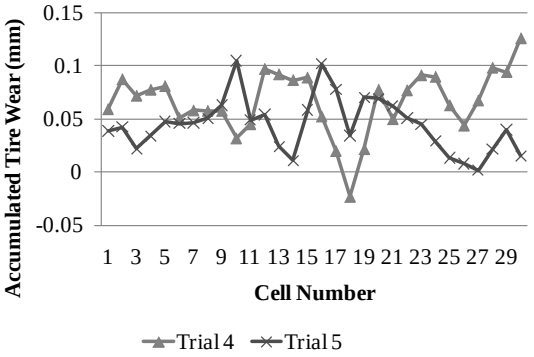

(f) Left Rear Tire --- Second Position

Figure B-5 Tire Wear Data Collected for Each Field Trial for the M99 (1040 km)

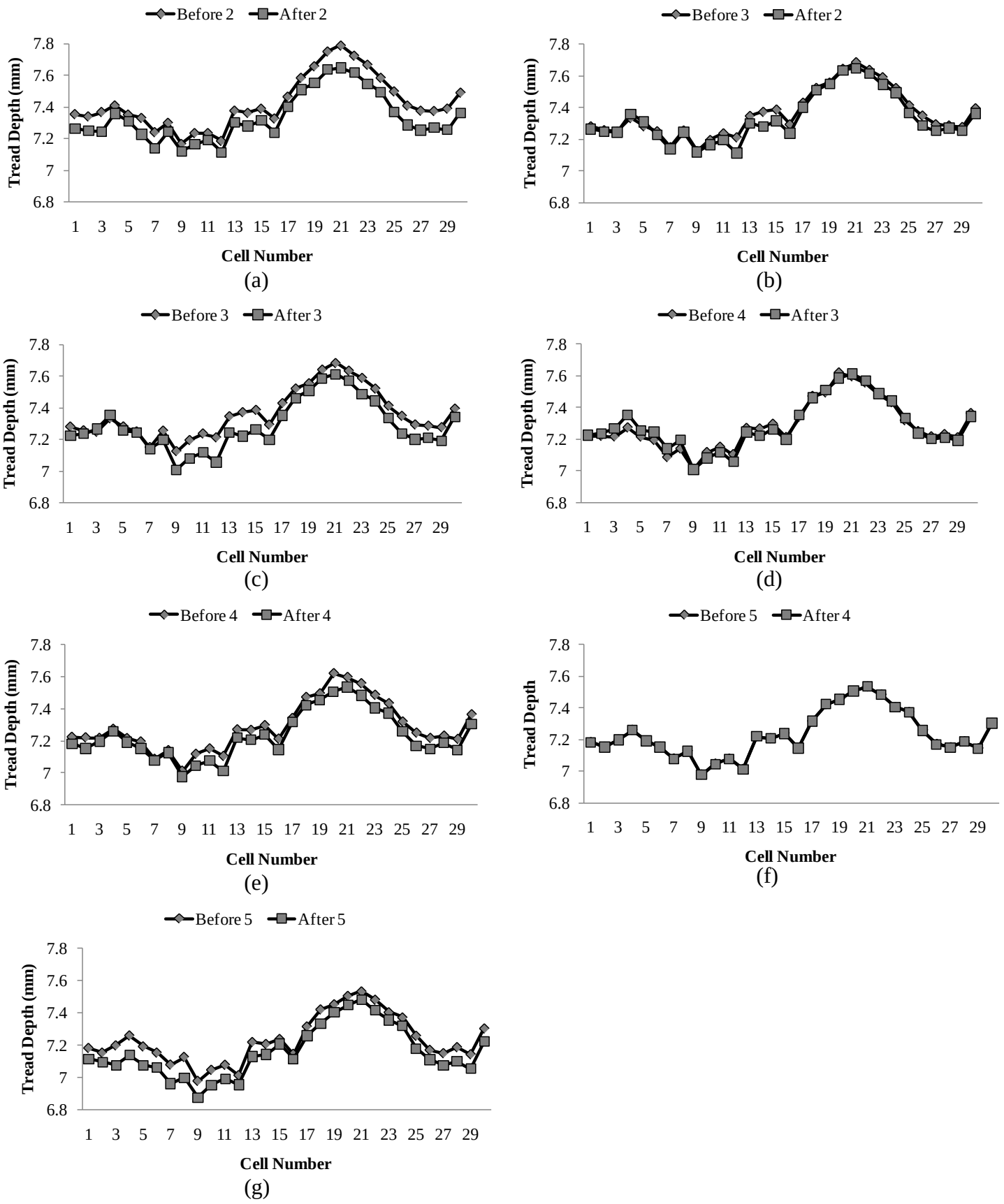

Figure B-6 Tire Comparison between “before” and “after” tread depth data for each field test – Left front position 1

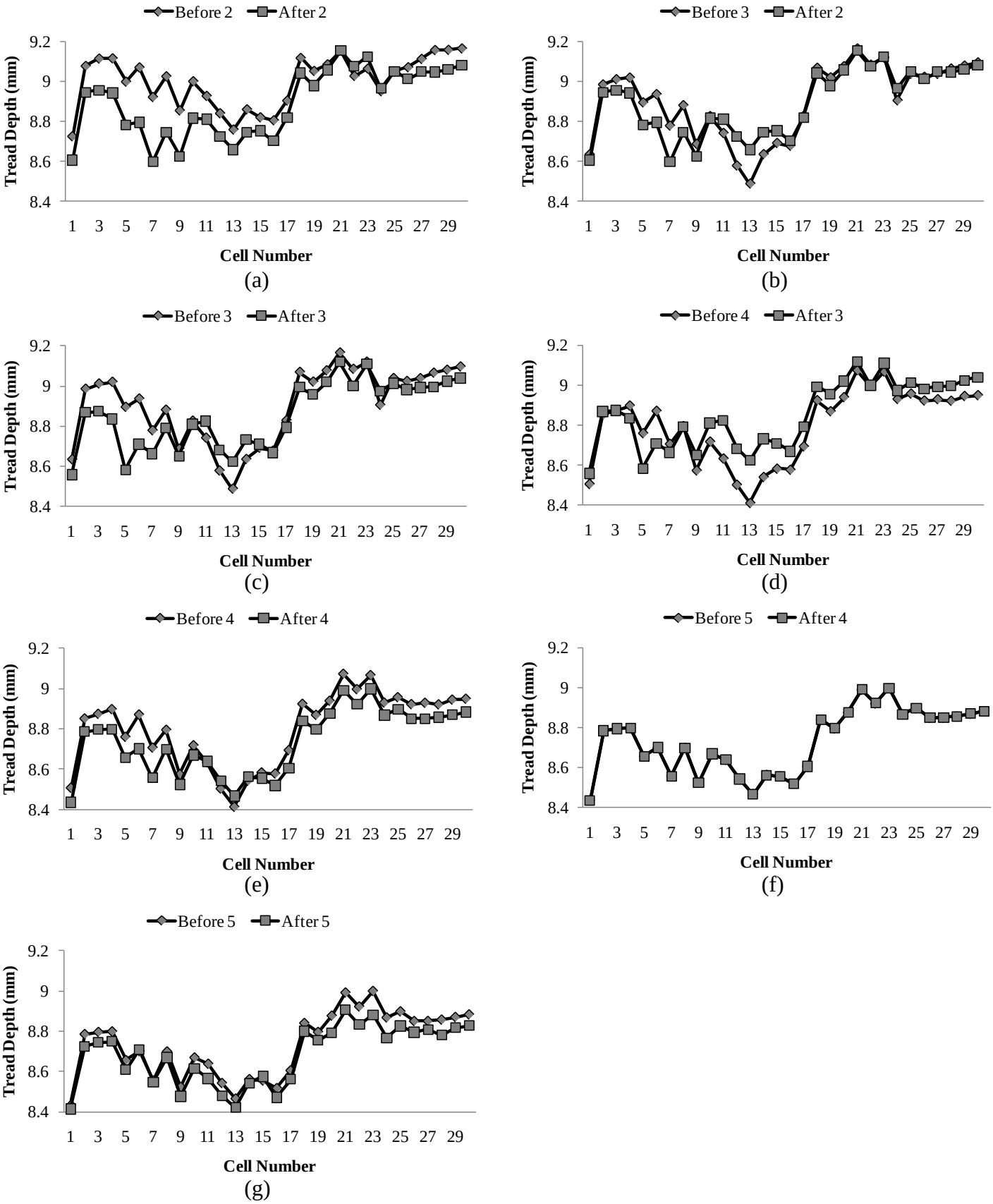

Figure B-7 Comparison between "before" and "after" tread depth data for each field test – Left front position 2

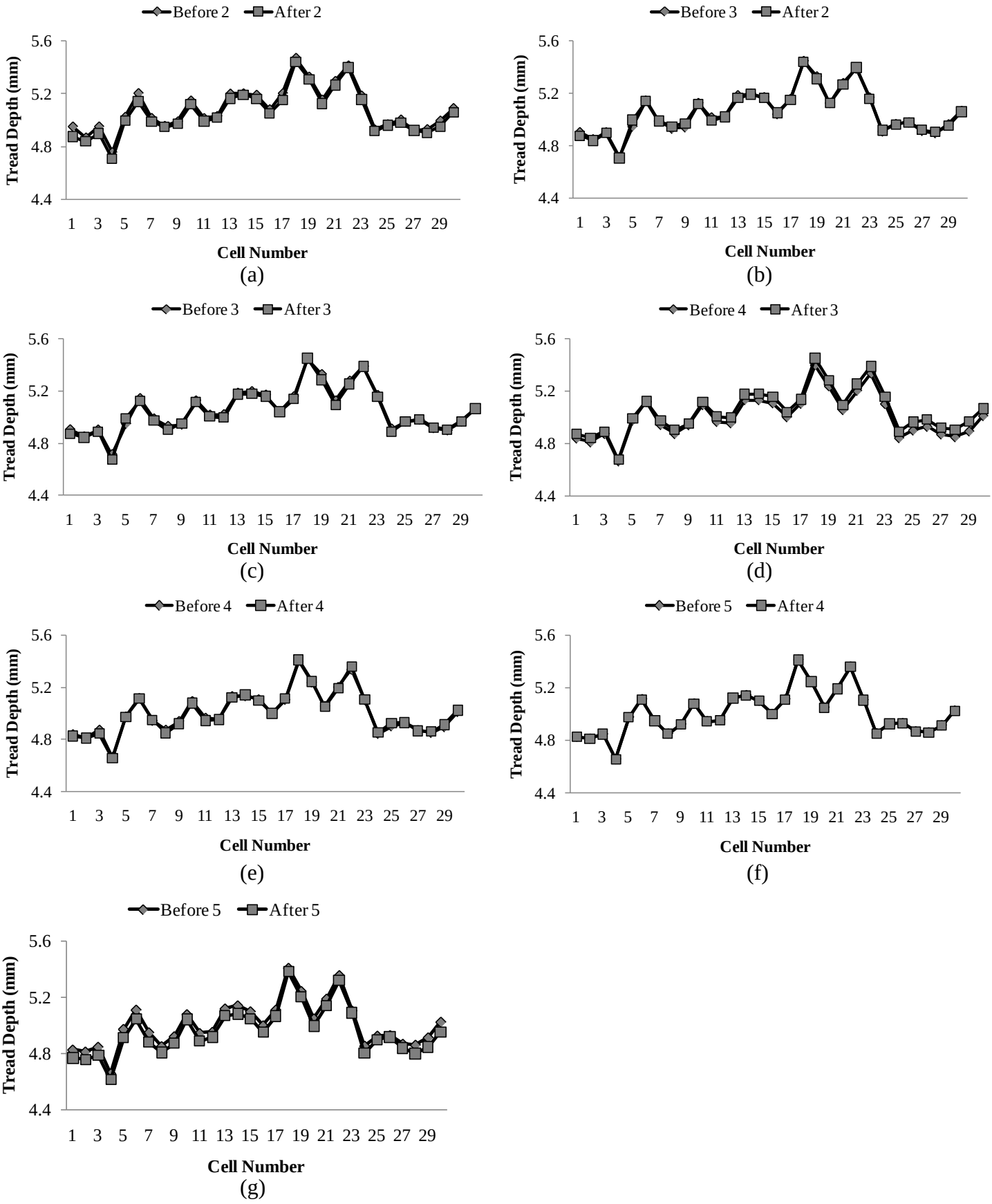

Figure B-8 Comparison between “before” and “after” tread depth data for each field test – Right Rear position 1

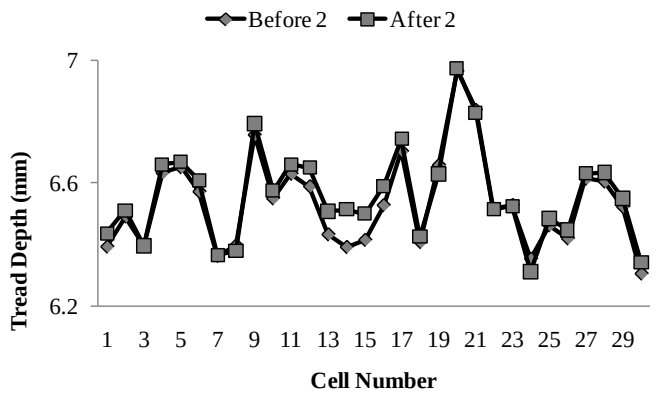

(a)

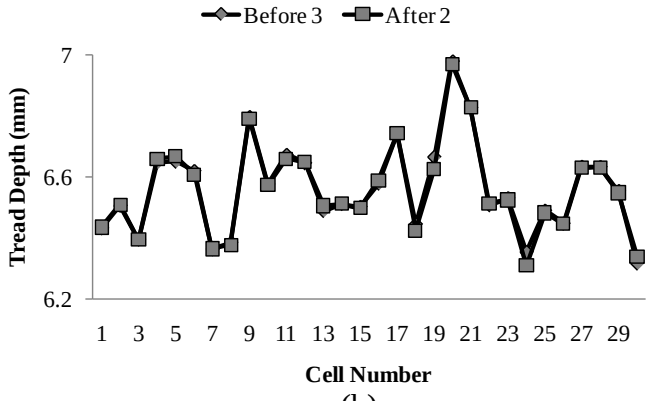

(b)

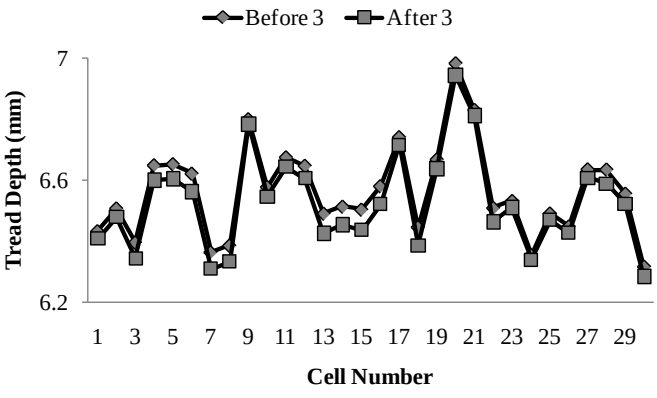

(c)

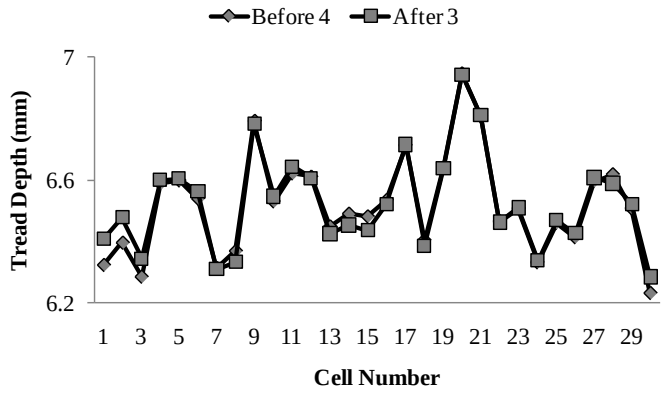

(d)

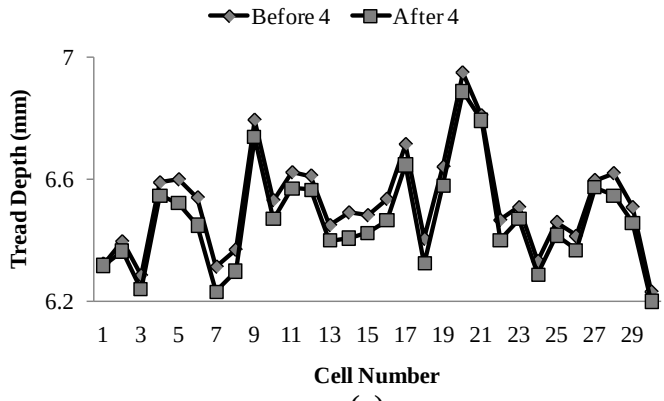

(e)

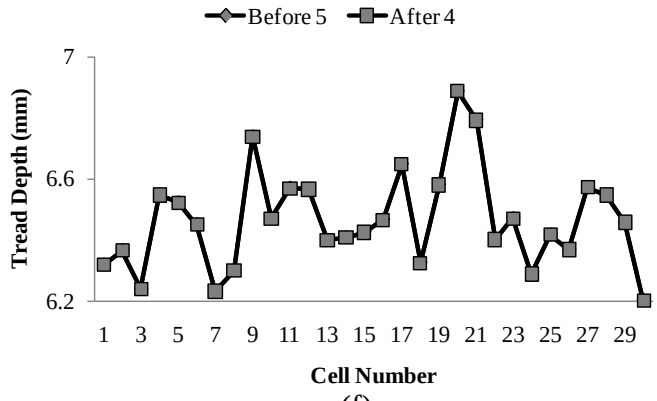

(f)

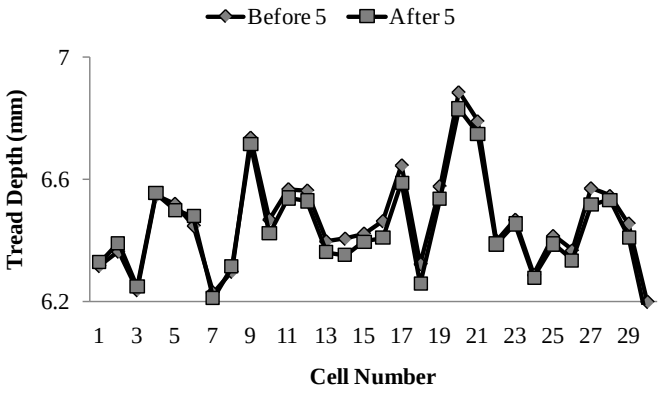

(g)

Figure B-9 Comparison between “before” and “after” tread depth data for each field test – Right Rear position 2

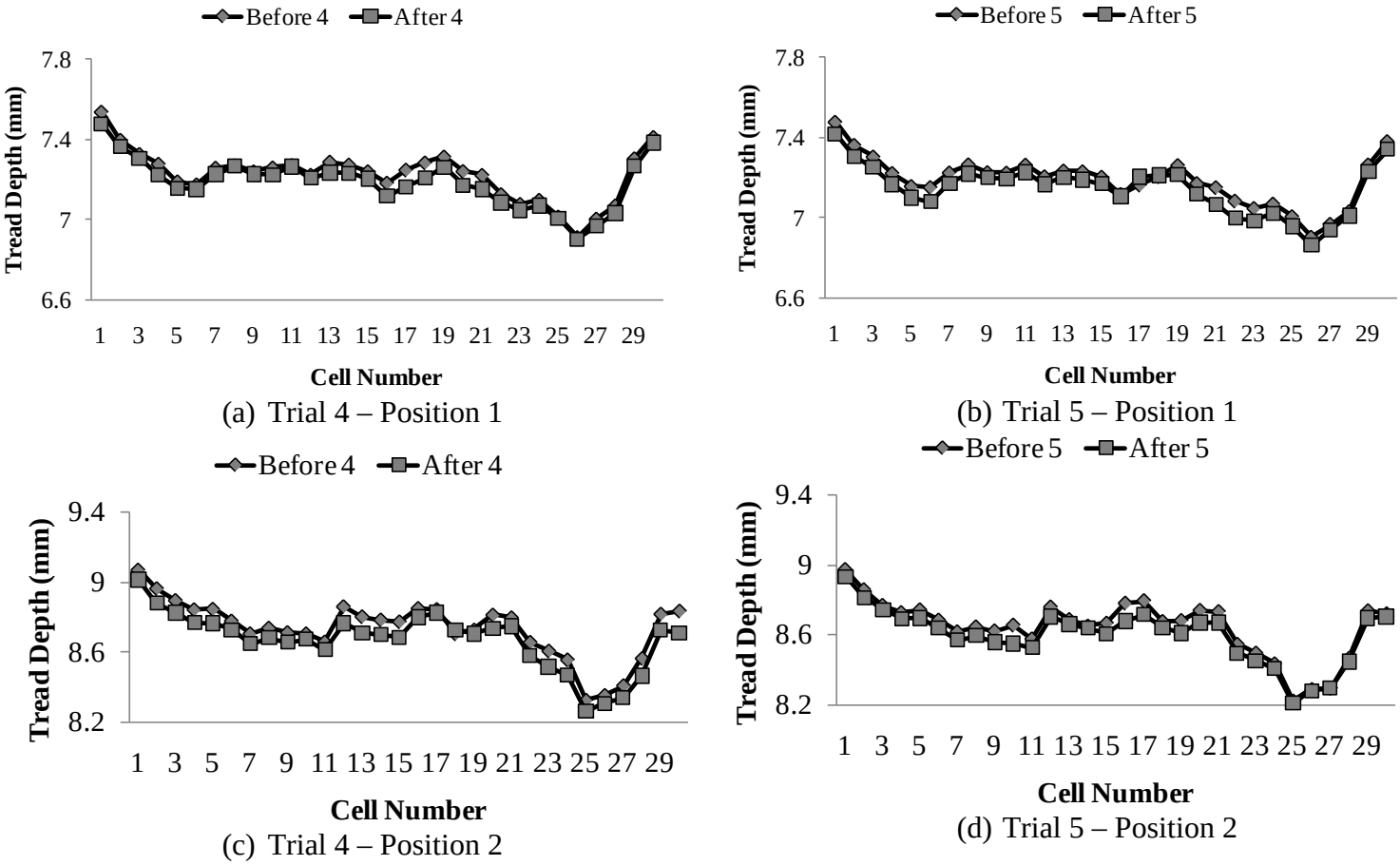

(a) Trial 4 – Position 1

(b) Trial 5 – Position 1

(c) Trial 4 – Position 2

(d) Trial 5 – Position 2

Figure B-10 Comparison between "before" and "after" tread depth data for each field test – Left Rear

A sensitivity analysis was performed to field-test whether the estimated minimum distance is sufficient to establish a statistically measurable tire wear. The cumulative tire wear was first computed for 1040, 2080, 3120 and 4000 km (650, 1300, 1950 and 2500 miles). Then, it was normalized to the same mileage (1000 km), see Figure B-11. Finally, the coefficient of correlation was computed using: the 4000 km data as the baseline for left front tire (positions 1 and 2) and right rear tire (position 1); 3120 km data for right rear tire (position 2); and 2080 km data for the left rear tire (positions 1 and 2). Figure B-12 shows these results. Assuming that a reasonable level of the coefficient of correlation (ρ) is 0.7, it is concluded that the vehicle should be driven for at least 3120 km to obtain a measurable tire wear. According to the Uniform Tire Quality Grading Standards (UTQGS) in 49 CFR 575.104, the vehicle should be driven for at least 2560 km (1600 miles) for measuring tire wear. Therefore, the results shown in Figure B-12 confirm this recommendation. Nonetheless, it was decided to extend the field test to 4000 km, and use the data from 4000 km runs where ever possible.

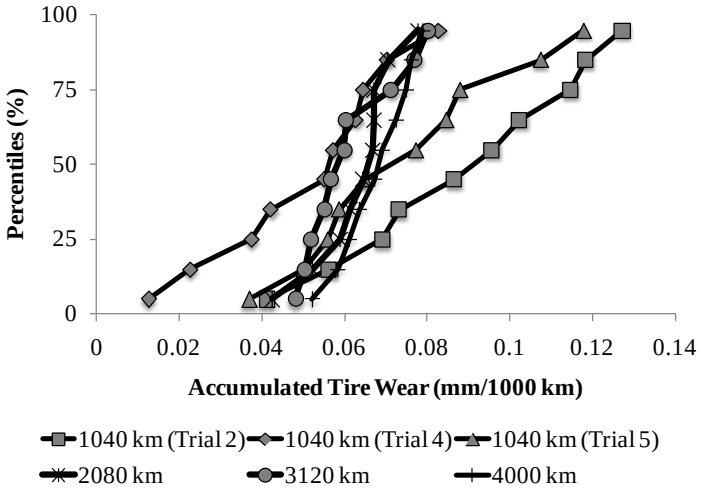

(a) Left Front tire --- First Position

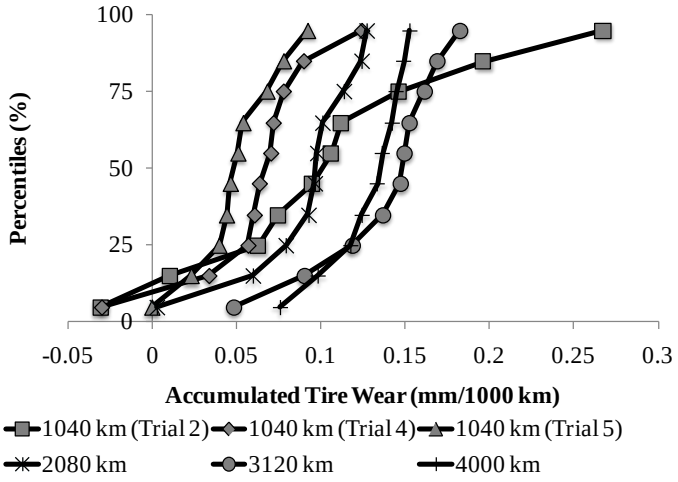

(b) Left Front tire --- Second Position

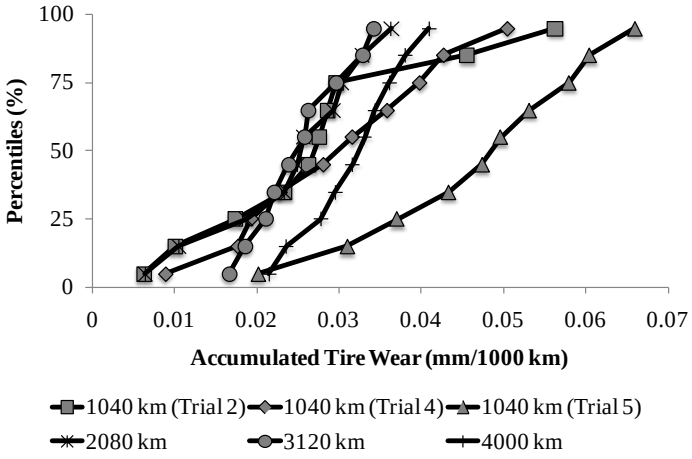

(c) Right Rear tire --- First Position

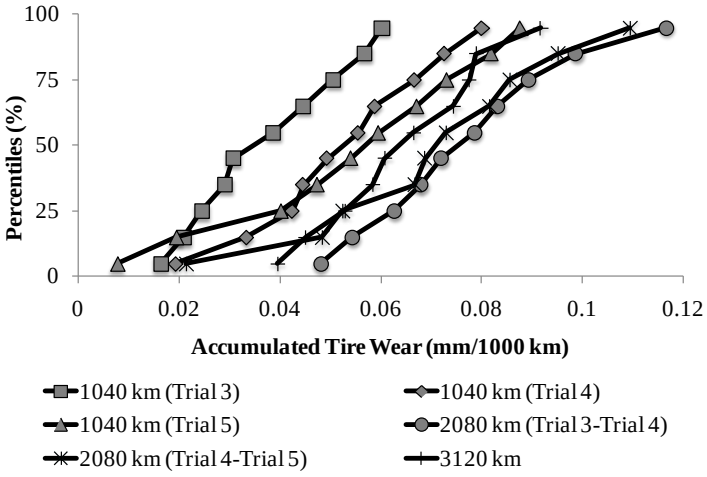

(d) Right Rear tire --- Second Position

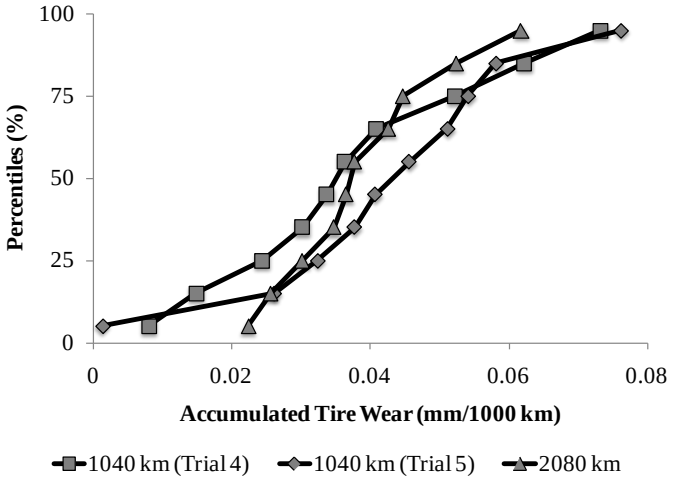

(e) Left Rear tire --- First Position

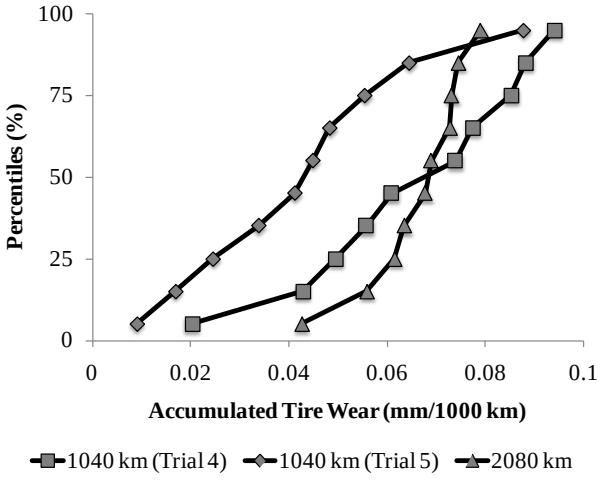

(f) Left Rear tire --- Second Position

Figure B-11 Normalized tire wear percentiles for each possible mileage – M99

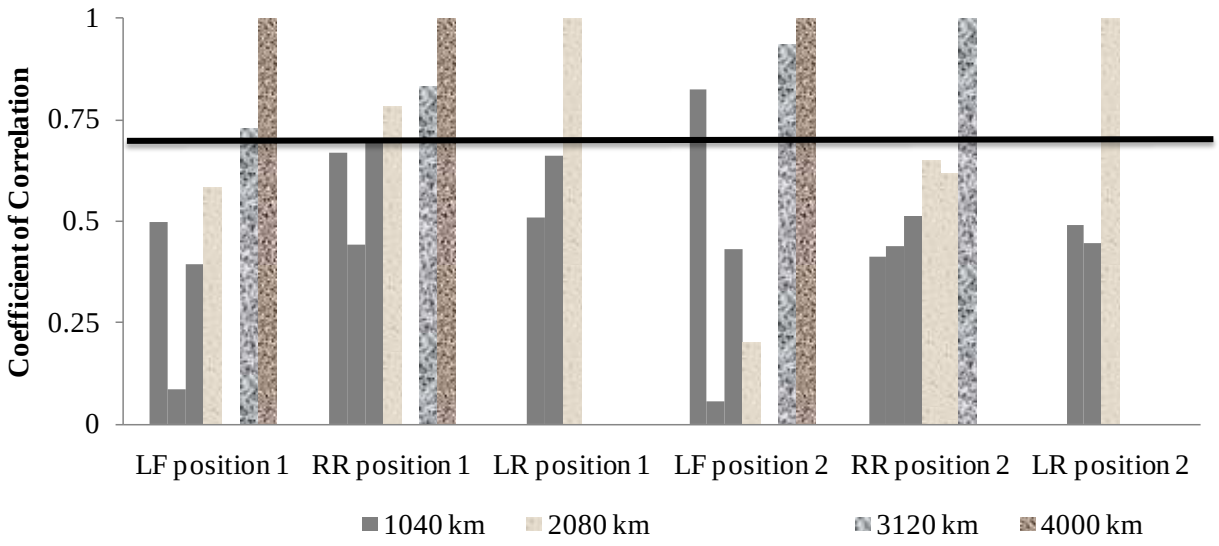

Figure B-12 Coefficients of Correlation between Tire Wear Data for 1040, 2080, 3120 and 4000 km (650, 1300, 1950 and 2500 miles)

In cases where the 4000 km wear data is not available, it was deemed acceptable to use the data from 3120 km runs. The accumulated tire wear is computed as the change in tread depth from "before" trial 2 to "after" trial 5 (4000 km) for LF both positions and RR tires position 1. For RR tires position 2, the change in tread depth was computed using the "before" data of Trial 3 and the "after" data of Trial 5 (3120 km). Since the tire wear for the LR tires could only be measured after 2080 km (using the "before" data of Trial 4 and "after" data of Trial 5), the M99 data for the LR tires were not used. The results are shown in Figure B-13. Figure B-14 shows the tire wear data collected during the I69 field test. The measurement was performed before the test start and after 4000 km.

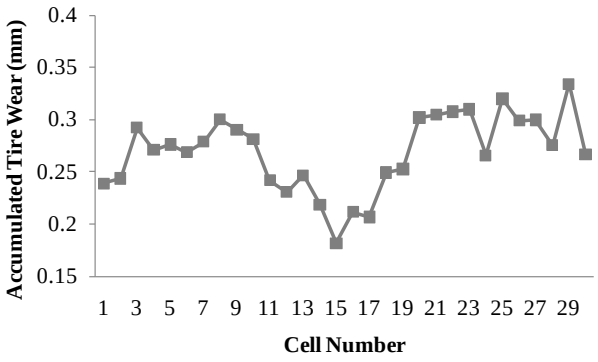

(a) Left Front Tire --- First Position

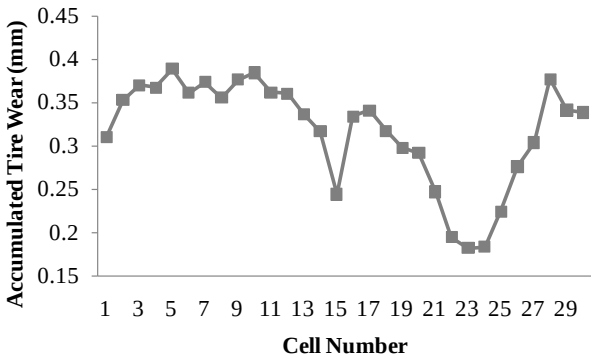

(b) Left Front Tire --- Second Position

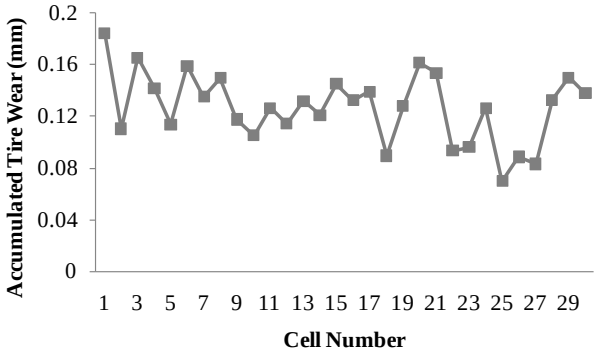

(c) Right Rear Tire --- First Position

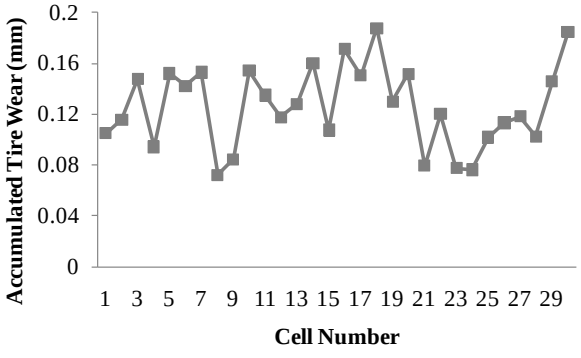

(d) Right Rear Tire --- Second Position

Figure B-13 Accumulated Tire Wear Data Collected During Field Tests for M99 (2080 km)

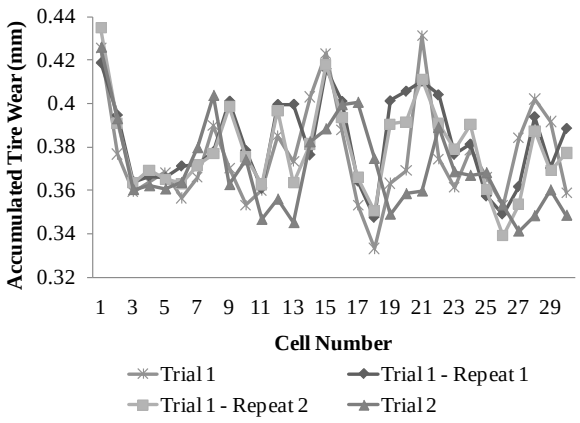

(a) Left Front Tire --- First Position

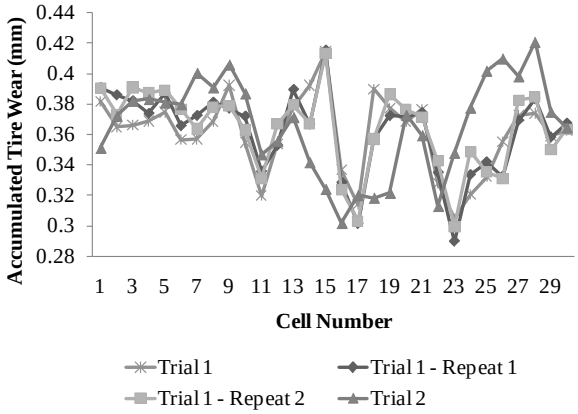

(b) Left Front Tire --- Second Position

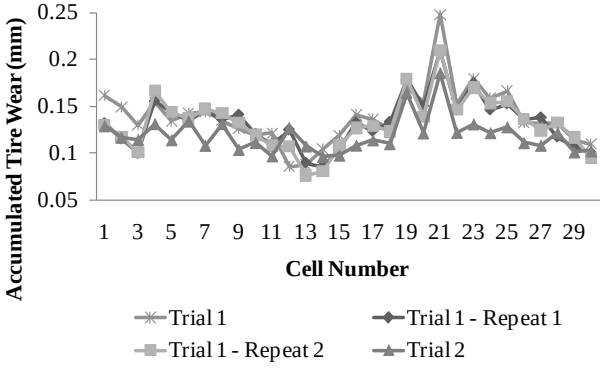

(c) Right Rear Tire --- First Position

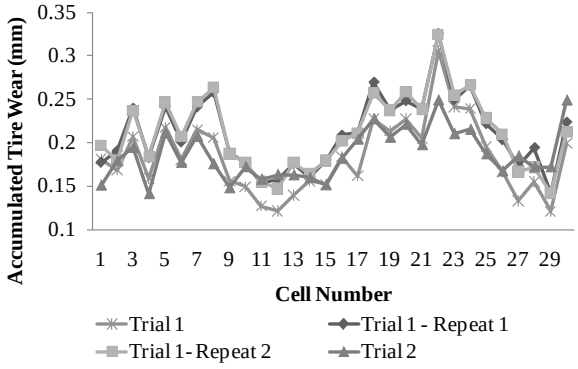

(d) Right Rear Tire --- Second Position

Figure B-14 Accumulated Tire Wear Data Collected During Field Tests for I69 (4000 km)

APPENDIX C

REPAIR AND MAINTENANCE MODELS

C1 - IDENTIFICATION AND EVALUATION OF REPAIR AND MAINTENANCE MODELS

This appendix summarizes the detailed equations and relationships of current repair and maintenance models. These models were also evaluated regarding their applicability to the paved surfaces and traffic and environmental conditions encountered in the United States that are capable of addressing the full range of vehicle types.

EXISTING VOC MODELS

Vehicle repair/maintenance costs are mainly comprised of two components: Parts consumption and labor hours. The current models can be grouped into empirical- and mechanistic-based models. The only available U.S. models are also those of the Texas Research and Development Foundation (TRDF) developed by Zaniewski et al (1982). The most recent models have been developed outside the U.S. The relevant models are:

- The World Bank's HDM 3 and 4 models;
- Saskatchewan models (Canada);
- South African model
- Swedish VETO models.

This section briefly reviews some of the major fuel consumption models (identified by the research team) that have been developed.

Empirical Models

Winfrey (1969) presented maintenance costs based on the results of surveys. These were updated by Claffey (1971) and Zaniewski et al. (1982) using an approach which has been termed the constituent component approach. Papagiannakis (1999) provided the results of a study into heavy truck parts consumption. It was noted that there is a significant increase in the maintenance costs with vehicle age, and at the same time the percentage of the costs due to labor decreases. This indicates, not unexpectedly, an increase in the number of parts replaced as the vehicle ages. The parts consumption was affected by road roughness even at low levels (< 2 IRI m/km). Also, considering the effect of roughness on vehicle maintenance, SHT, Canada adopted

a vehicle maintenance cost model that relates maintenance costs to roughness:

$$MC = M_{cf} K_{mr} \quad \text{(C.1)}$$

where:

MC	= Maintenance cost ($/km)
M_{cf}	= Average maintenance cost ($/km)
K_{mr}	= Road roughness coefficient

HDM 3 allowed users to predict VOC using relationships derived from road user cost studies in Brazil, India, Kenya, and the Caribbean. The Brazil relationships were the 'standard' relationships in HDM 3. Equations C.2 through C.6 show the Brazilian model.

$$PARTS = C0SP \times CKM^{kp} \times \exp(CSPIRI \times IRI) \quad \text{for IRI} \leq \text{IRI0SP} \quad \text{(C.2)}$$

$$PARTS = CKM^{kp} \ (a_0 + a_1 \times IRI) \quad \text{for IRI} > \text{IRI0SP} \quad \text{(C.3)}$$

$$a_0 = C0SP \ \exp(CSPIRI \times IRI0SP)(1 - CSPIRI \times IRI0SP) \quad \text{(C.4)}$$

$$a_1 = C0SP \times CSPIRI \ \exp(CSPIRI \times IRI0SP) \quad \text{(C.5)}$$

$$LH = C0LH \quad PARTS^{CLHPC} \exp(CLHIRI \quad IRI) \quad \text{(C.6)}$$

where:

PARTS	= Standardized parts consumption as a fraction of the replacement vehicle price per 1000 km
CKM	= Vehicle cumulative kilometer and it is calculated as half the lifetime kilometreage
a_0, a_1	= Model parameters
kp	= Model Constant (Table C-1)
IRI	= Roughness in IRI m/km
IRI0SP	= Transitional roughness beyond which the relationship between parts consumption and roughness is linear
C0SP	= Parts model constant
CSPIRI	= Parts model roughness coefficient
LH	= Number of labor hours per 1000 km
C0LH	= Labor model constant
CLHIRI	= Labor model roughness coefficient

The Brazilian model (Equations C.2 through C.6) actually incorporates several vehicle classes including passenger cars, utility vehicles, buses and trucks. For example, the HDM 3 maintenance model suggests parameters for parts and labor for all the above vehicle classes, as shown in Table C-1.

The structure of the parts model as shown above is quite complicated because trucks were found to have a linear response to roughness while passenger cars, utility vehicles, and buses had an exponential response. Therefore, a linear relationship was adopted above a certain roughness level (IRI0SP).

Table C-1 HDM 3 Maintenance Model Parameters (Bennett and Greenwood, 2003)

Vehicle Class	Parts Model Parameters				Labor Model Parameters		
	kp	C0SP ($x10^{-6}$)	CSPIRIP ($x10^{-3}$)	IRI0SP	C0LH	CLHPC	CLHIRI
Passenger Car	0.308	32.49	178.1	9.2	77.14	0.547	0
Utility	0.308	32.49	178.1	9.2	77.14	0.547	0
Large Bus	0.483	1.77	46.28	14.6	293.44	0.517	0.0715
Light and Medium Truck	0.371	1.49	3273.27	0	242.03	0.519	0
Heavy Truck	0.371	8.61	459.03	0	301.46	0.519	0
Articulated Truck	0.371	13.94	203.45	0	652.51	0.519	0

The Council for Scientific and Industrial Research (CSIR) in South Africa developed models for parts and labor consumption (du Plessis, 1989). The research can be grouped into two areas: Speed and roughness effects on parts consumption as well as labor costs. Equations C.7 presents the speed effect on the total cost. Equation C.8 presents the roughness effect on parts consumption. Equations C.9 and C.10 present the South African labor hours' relationships. The South African model includes two separate equations for buses and trucks when modeling labor costs:

$$PCST = a_1 + a_2 \times v + \frac{a_3}{S} + a_4 \times v^2 \quad \text{(C.7)}$$

$$PARTS = \exp(-3.0951 + 0.4514 \ln CKM + 1.2935 \ln(13\, IRI)) \times 10^3 \quad \text{(C.8)}$$

$$LH = 0.763 \exp(0.0715\, IRI)\left(\frac{PARTS}{NVPLT}\right)^{0.517} \quad \text{for buses} \quad \text{(C.9)}$$

$$LH = \max\left(3,\ -0.375 + 0.0715\left(\frac{PARTS}{NVPLT}\right) + 0.182 IRI\right) \quad \text{for trucks} \quad \text{(C.10)}$$

where:

PCST = Maintenance cost in cents/km

v	= Speed (km/h)
a_1 to a_4	= Model constants
PARTS	= Standardized parts consumption as a fraction of the replacement vehicle price per 1000 km
CKM	= Vehicle cumulative kilometer and it is calculated as half the lifetime kilometrage
IRI	= Roughness in IRI m/km
LH	= Labor hours per 1000 km
NVPLT	= the replacement vehicle price less tires

The key problem with this model is that it is sensitive to the assumed average speed. In fact, du Plessis (1989) proved that there is a huge difference in the parts cost when assuming urban versus rural speed.

For HDM 4, the parts model was simplified over that used in HDM 3 (Bennett and Greenwood 2000). Equations C.11 through C.14 show the final model.

$$\text{PARTS} = \left(\text{K0}_{\text{pc}} \left[\text{CKM}^{\text{kp}} \left(\text{a}_0 + \text{a}_1 \text{ RI}\right)\right] + \text{K1}_{\text{pc}}\right)\left(1 + \text{CPCON} \times \text{dFUEL}\right) \quad \text{(C.11)}$$

$$RI = \max\left(IRI, \min\left(IRI0, a_2 + a_3 * IRI^{a_4}\right)\right) \quad \text{(C.12)}$$

$$a_2 = IRI0 - a_5$$

$$a_3 = \frac{a_5}{IRI0^{\frac{IRI0}{a_5}}} \quad \text{(C.13)}$$

$$a_4 = \frac{IRI0}{a_5}$$

$$a_5 = IRI0 - 3$$

$$\text{LH} = \text{K0}_{\text{lh}} \left(\text{a}_6 \times \text{PARTS}^{\text{a}_7}\right) + \text{K1}_{\text{lh}} \quad \text{(C.14)}$$

where:

PARTS	= Standardized parts consumption as a fraction of the replacement vehicle price per 1000 km
$K0_{pc}$	= Rotational calibration factor (default = 1.0)
CKM	= Vehicle cumulative kilometer (Table C-2)
a_0, a_1, kp	= Model Constants (Table C-2)
RI	= Adjusted roughness
IRI	= Roughness in IRI m/km
IRI0	= Limiting roughness for parts consumption in IRI m/km (3 m/km)
a_2 *to* a_5	= Model parameters
$K1_{pc}$	= Translational calibration factor (default = 0.0)
CPCON	= Congestion elasticity factor (default = 0.1)

dFUEL = Additional fuel consumption due to congestion as a decimal
LH = Number of labor hours per 1000 km
$K0_{lh}$ = Rotation calibration factor (default = 1)
$K1_{lh}$ = Translation calibration factor (default = 0)
a_6 , a_7 == Model Constants (Table C-2)

HDM 4 repair and maintenance model suggests parameters for parts and labor for all the above vehicle classes, as shown in Table C-2.

Table C-2 HDM 4 Maintenance Model Parameters

Vehicle Type	Parts consumption model				Labor Model	
	CKM (km)	kp	a_0*1E^{-6}	a_1*1E^{-6}	a_6	a_7
Motorcycle	50,000	0.308	9.23	6.2	1161.42	0.584
Small car	150,000	0.308	36.94	6.2	1161.42	0.584
Medium car	150,000	0.308	36.94	6.2	1161.42	0.584
Large car	150,000	0.308	36.94	6.2	1161.42	0.584
Light delivery car	200,000	0.308	36.94	6.2	611.75	0.445
Light goods vehicle	200,000	0.308	36.94	6.2	611.75	0.445
Four wheel drive	200,000	0.371	7.29	2.96	611.75	0.445
Light truck	200,000	0.371	7.29	2.96	2462.22	0.654
Medium truck	240,000	0.371	11.58	2.96	2462.22	0.654
Heavy truck	602,000	0.371	11.58	2.96	2462.22	0.654
Articulated truck	602,000	0.371	13.58	2.96	2462.22	0.654
Mini bus	120,000	0.308	36.76	6.2	611.75	0.445
Light bus	136,000	0.371	10.14	1.97	637.12	0.473
Medium bus	245,000	0.483	0.57	0.49	637.12	0.473
Heavy bus	420,000	0.483	0.65	0.46	637.12	0.473
Coach	420,000	0.483	0.64	0.46	637.12	0.473

The model suggests eliminating the effects of roughness on parts consumption at low IRI. This is achieved by using Equations C.12 and C.13. However, Papagiannakis (2000) reported that even low magnitude roughness has an effect on parts consumption (see Table C-3 below).

Table C-3 Effect of Operating Conditions on VOC Components (Papagiannakis 2000)

VOC Component	Effect on VOC Component		
	Geometry	Roughness	Capacity
Fuel	✓	•	✓
Tire	-	✓	•
Oil	-	•	-
Parts	-	✓	•
Labor	-	✓	•
Depreciation and Interest	✓	•	✓
Crew	✓	•	✓
Passenger Time	✓	•	✓

Index: - No effect • Minor effect ✓ Major effect

Mechanistic Models

The only purely mechanistic model is the VETO model which was developed by the Swedish Road and Traffic Research Institute (VTI) (Hammarström and Karlsson, 1991). It contains two approaches to the calculation of parts and maintenance labor: one empirical and one mechanistic. The former relies on the HDM Brazil relationships (Equations C..2 to C.6) while the latter employs a "wear index" for vehicle components. The mechanistic model is a detailed simulation of an idealized two-dimensional vehicle traveling over a surface with a specified profile. The model works on the basis that the wear and tear of components depends upon the product of the number of stress cycles they have been subjected to and the stress amplitude raised to the sixth power. The number of cycles is assumed to be constant per unit length of road (independent of roughness) while the stress amplitude for each component is proportional to the RMS value of the dynamic component of the wheel load. The model does not take into account the static load. The model was calibrated by looking at the life expectancy of different components. Only four components were studied and so the model does not yet provide a total cost calculation. Nevertheless, it is interesting to note that the change in vehicle wear with increasing roughness that it calculates is far higher than the change in parts cost predicted by the empirical model. In spite of developing a complex model, Hammarström and Karlsson (Hammarström, 1994) concluded that:

> *"… it would probably be virtually impossible to develop a model which could be used for calculating the relationship between total repair costs and road unevenness, component by component."*

Hammarström and Henrikson (1994) produced coefficients for calibrating HDM 3 to Swedish conditions. The study produced scaling constants (C0SP) and was also able to examine how parts consumption changes with vehicle age (kp). However, it did not provide information on the effect of roughness on parts consumption. Now, the Swedish Road and Traffic Research Institute are trying to update the HDM 4 model to Sweden condition (Hammarstrom, 1994).

EVALUATION OF THE EXISTING VOC MODELS

This section evaluates and recommends the existing models The most recent repair and maintenance model (HDM 4) have been implemented in EXCEL spreadsheets in order to study the sensitivity of the various input variables and to compare their predictions with the results from the U.S. empirical models (Zaniewski et al.). In general, the model evaluation and selection was based on a set of criteria that encompasses two distinctive and equally important aspects: (1) practicality of the model and (2) statistical soundness.

Practicality/ Statistical Soundness of the Model

From the literature review, it became clear that most of the models are derived from previous ones. Each model attempts to address a problem found in a previous one. Some major points and/or corrections that are noteworthy follow:

- As shown in the previous section, the structure of the Brazilian parts consumption model is quite complicated because trucks were found to have a linear response to roughness while passenger cars, utility vehicles and buses had an exponential response. Also, it requires many input variables that are not easy to compute;
- The key problem with the South African model is that it is sensitive to the assumed average speed. In fact, du Plessis (1989) proved that there are huge differences in repair and maintenance cots depending on whether urban or rural speed is assumed.

Because of the above points, the research team selected the HDM 4 model for further evaluation and discussion.

1- <u>Ease of use and availability of appropriate input data:</u> The literature review presented earlier suggests that current repair/maintenance models are empirical in nature because of wide variations in maintenance practices and long term data requirements among other factors.

This is because of the following (Bennett and Greenwood 2000):

- The costs usually arise infrequently over the life of the vehicle;
- The maintenance practices of the owners/operators have a major impact on the costs;
- The maintenance costs for similar vehicles can vary significantly among manufacturers;
- Vehicles operating in harsh conditions may be of more robust construction and therefore have lower maintenance costs than standard vehicles, and;
- Correlating maintenance costs with operating conditions is difficult since vehicles tend to operate over a range of roads; therefore the costs are averaged out.

It should also be noted that the estimation of parameters for the parts model is particularly problematic. There is a general consensus opinion that improvements in vehicle technology and other factors given modern technology lower maintenance costs, and that modern technology vehicles are also less sensitive to roughness. However, there have been relatively few studies done to verify this consensus opinion, particularly with passenger cars. Given its empirical nature, the input variables for the model are available from different sources of data.

2- The ability of the model to incorporate pavement surface conditions as currently being measured: The input variables related to pavement surface conditions (e.g. roughness) are as currently being measured. In fact, the model characterizes roughness by the International Roughness Index.

3- Reasonableness and applicability to U.S. conditions: Repair and maintenance data from vehicle fleets as reported in NCHRP 1-33 were correlated with pavement condition (IRI) and compared with HDM 4 predictions (Figure C-1). It can be seen that:

- The parts consumption according to NCHRP1-33 is lower than the predictions by HDM 4.
- The labor hours according to NCHRP 1-33 are much lower than those predicted by HDM 4.

The predictions from HDM 4 do not appear to be reasonable for US conditions. These observations could be explained by the fact that HDM 4 model was calibrated using data from

developing countries (e.g., Brazil, India). It is well known that the labor hours in those countries are much higher than in the US. Also, the difference between parts consumption in the US and those predicted from HDM 4 could be explained by the inflation in the parts and vehicle prices. For the most part, it is expected that the bulk of any correction/calibration to match US conditions could be achieved using macro-economic model corrections based on overall (average) economic data (e.g., average labor hours for typical vehicles and average parts cost comparisons). Therefore, in this research, the latest comprehensive research conducted in the US, i.e. Zaniewski's tables/charts, was updated to current conditions.

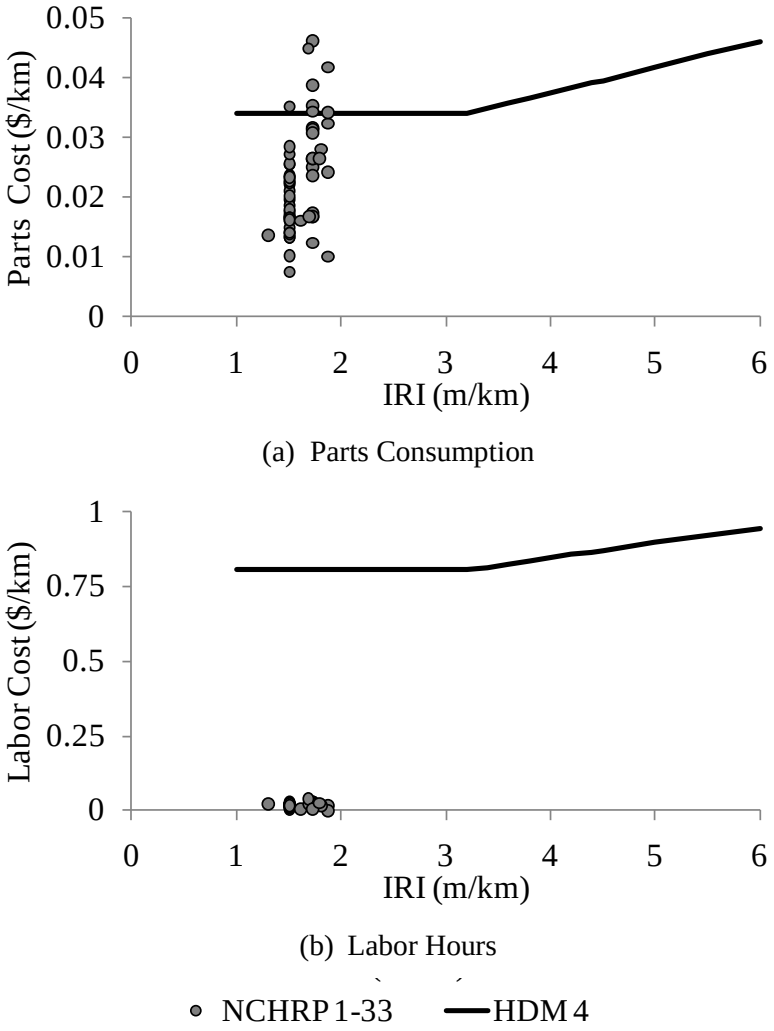

Figure C-1 Comparison between HDM-4 Predictions and Data from Truck Fleets (NCHRP 1-33)

C2 - TYPICAL US CONDITIONS: INPUT DATA SOURCES AND DISTRIBUTIONS FOR REPAIR AND MAINTENANCE

Tables C-4 and C-5 present the different input parameters for repair and maintenance costs and their sources. Pavement condition and traffic data are readily available. Vehicle characteristics data and the output data are not readily available. These data have been collected from different sources which include NCHRP 1-33 (Truck fleets), and Texas and Michigan DOTs.

Table C-4 Input parameters for the repair and maintenance model

	Pavement Condition	Traffic	Vehicle Characteristics
Parts consumption	• IRI	• Congestion	• Vehicle Type • Cumulative mileage • Vehicle acceleration
Labor hours	Same as Parts Consumption		

Table C-5 Data sources for input parameters of the repair and maintenance model

	Input parameters	Data Sources	Method	Status
Pavement Condition	• IRI	• HPMS • NCAT	• Records	Collected
Traffic	• Congestion	• SHA	• Records	Available
Vehicle Characteristics	• Vehicle Type • Cumulative mileage • Vehicle acceleration	• SHA + other fleets • NCAT	• Records	Collected

MICHIGAN DEPARTMENT OF TRANSPORTATION (MDOT) DATA

Pavement condition, vehicle characteristics and repair and maintenance costs data have been collected from Michigan DOTs. Figure C-2 shows a map view of the eight district of Michigan.

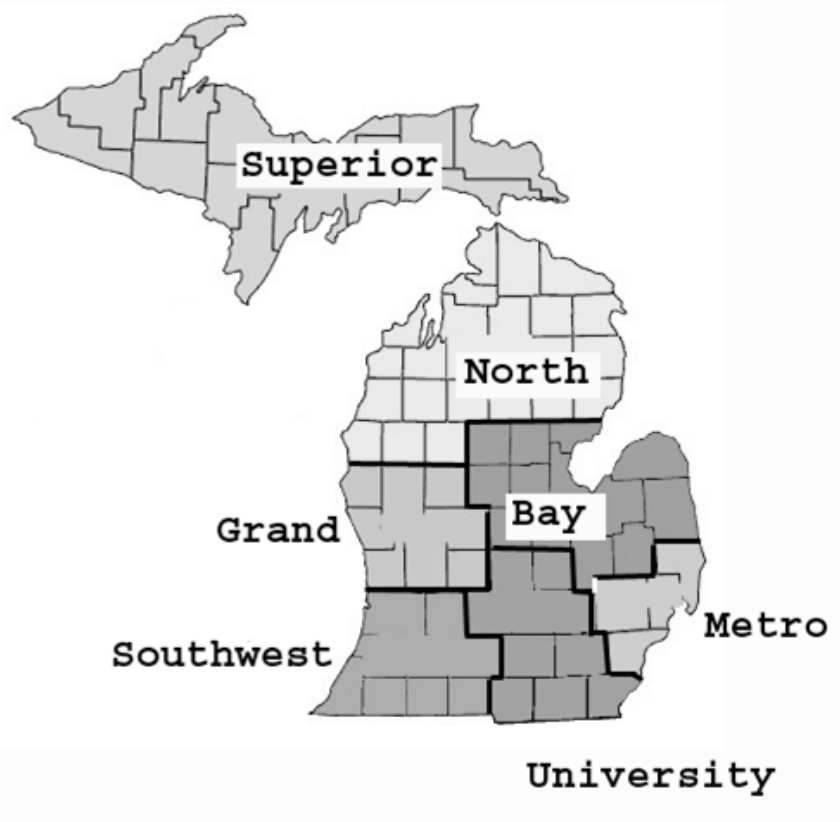

Figure C-2 Michigan Regions

Figure C-3 shows the distribution of roughness in terms of Ride Quality Index (RQI) in the eight regions of Michigan. RQI reflects the user's perception about pavement ride quality. According to Lee et al. (2002), RQI and IRI have a good correlation, with the RQI increasing asymptotically with increasing IRI to a plateau value of about 100 as the IRI-values approach the 4 to 5 m/km range. The IRI-value corresponding to an RQI of 70 is about 2.4 m/km (threshold for rehabilitation in Michigan). Figure C-4 shows the percent of sections with IRI > 2.4 m/km.

Figure C-5 shows the distribution of repairs by region for different vehicle classes. Figure C.6 shows the average labor and parts costs versus roughness for different vehicle classes for Michigan. It should be noted that the graphs were corrected for mileage. A data point in the graphs represents the average labor hours or parts costs for all the vehicles within a district for each vehicle class.

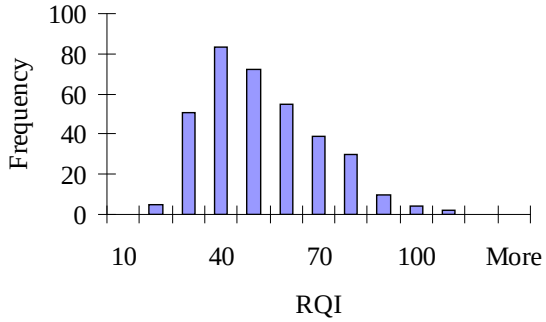

(a) Superior region

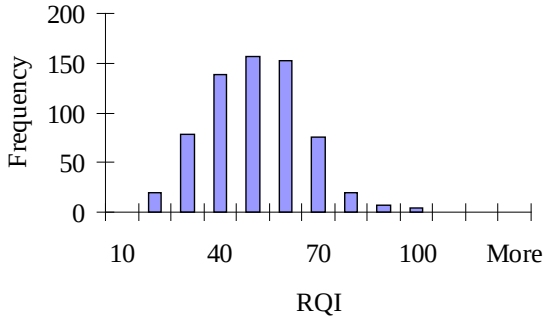

(b) North region

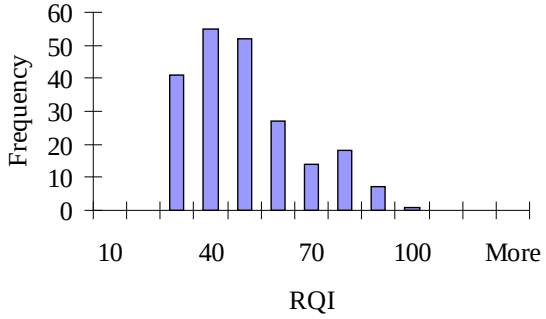

(c) Grand region

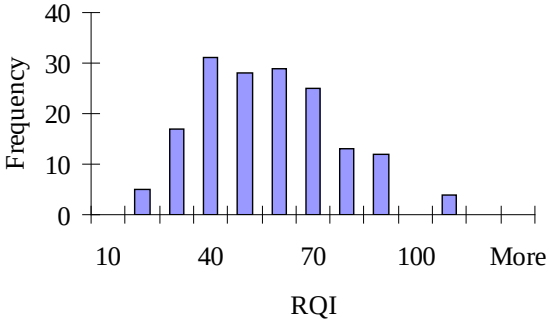

(d) Bay region

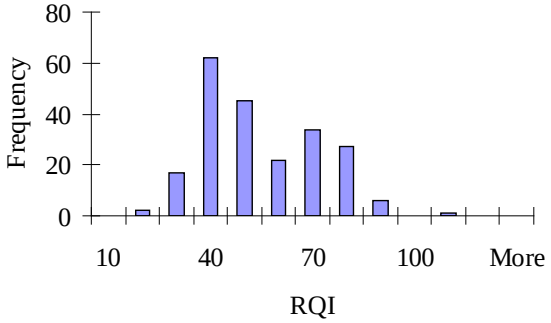

(e) Southwest region

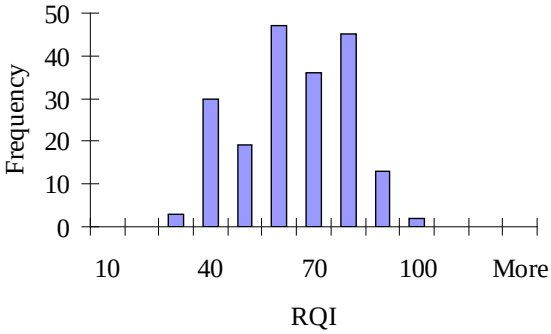

(f) University region

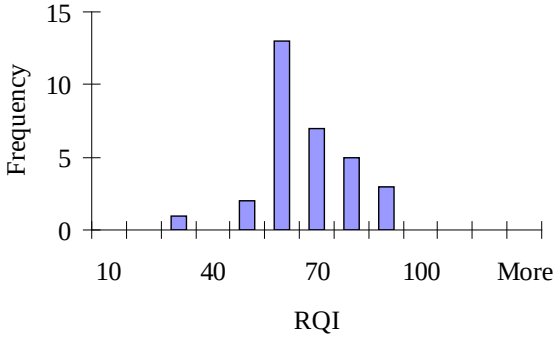

(g) Metro region

Figure C-3 Distribution of Roughness for Michigan Regions (Michigan DOT, 2001)

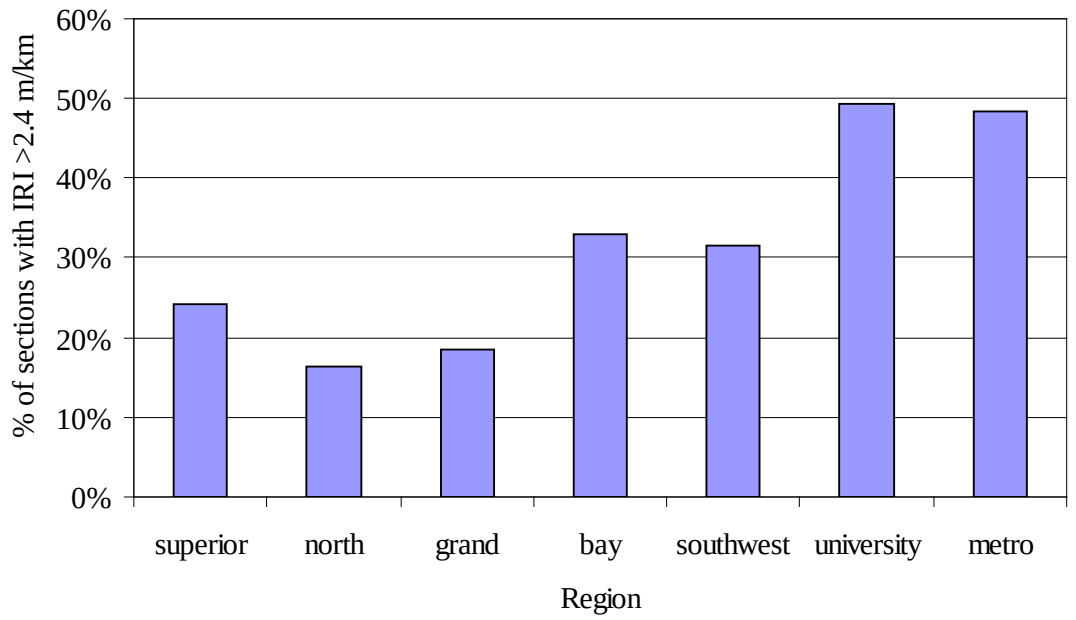

Figure C-4 Percent of Sections with IRI > 2.4 m/km

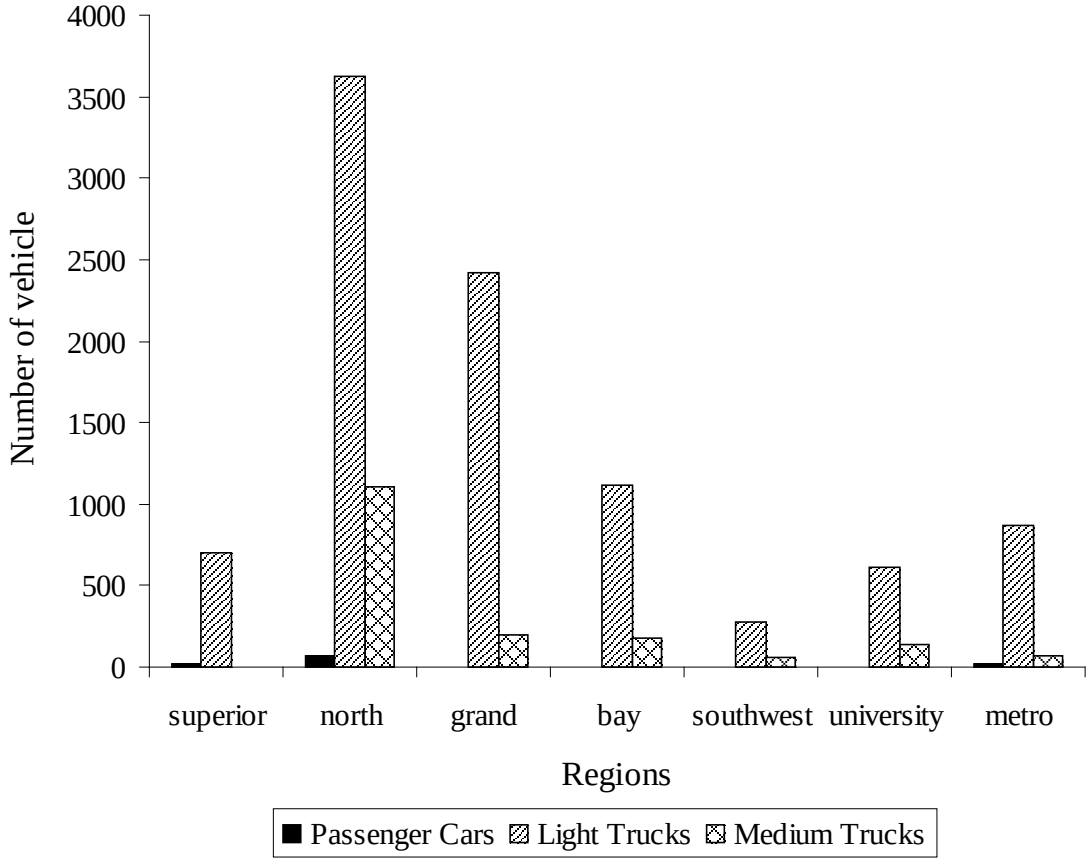

Figure C-5 Distribution of Repairs by District and Vehicle Class (Michigan DOT)

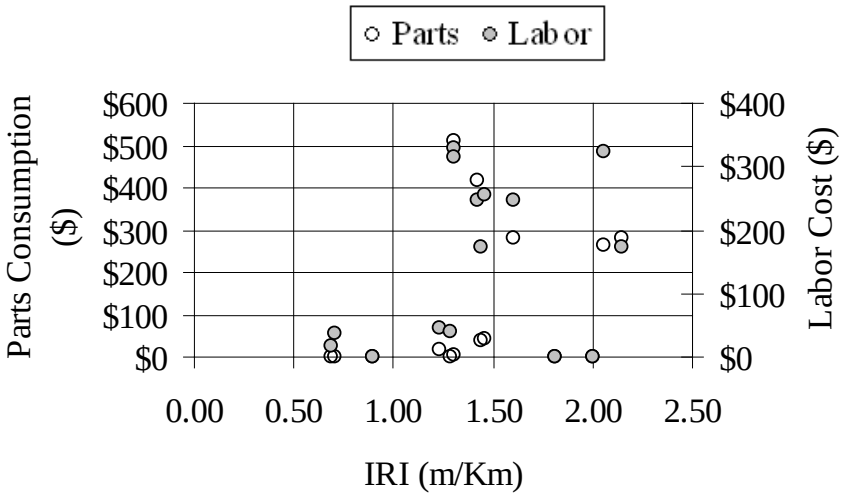

(a) Passenger cars

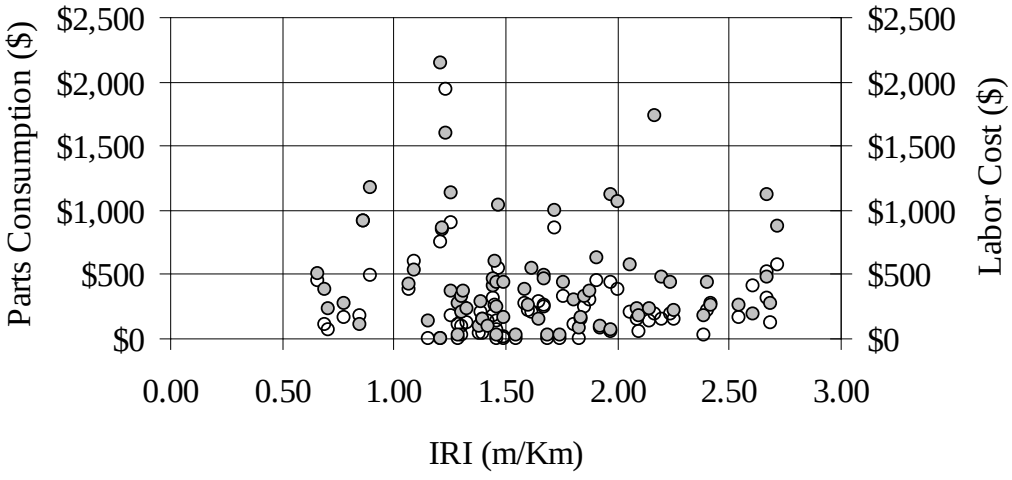

(b) Light Trucks

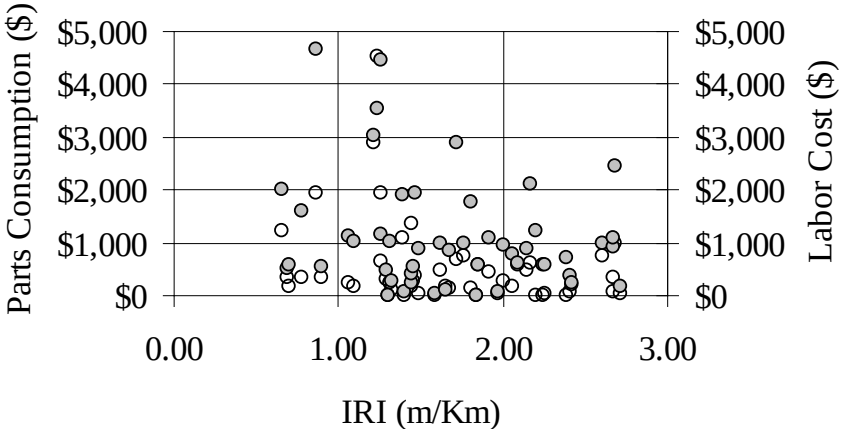

(c) Medium Trucks

Figure C-6 Summary of the Repair and Maintenance Data (Michigan DOT)

TEXAS DEPARTMENT OF TRANSPORTATION (MDOT) DATA

The state of Texas has 25 congressional districts. Figure C-7 shows a map view of Texas districts. Figure C.8 shows the average roughness measured during the financial year 2006 for each district of the state of Texas. It should be noted that there is 100% roadbed coverage that includes all state maintained road network, i.e. interstate, national and state road and farm-to-market network. Figures C.9 through C.11 show the distribution of repairs by district (Texas) for different vehicle classes. Figures C.12 and C.13 show the average labor and parts costs by district for different vehicle classes. It should be noted that the graphs present the corrected data for age and mileage. A data point in the graphs represents the median values of labor or parts costs for all the vehicles within a district for each vehicle class.

District	code	
PHARR	PHR	1
ODESSA	ODA	2
ATLANTA	ATL	3
AUSTIN	AUS	4
HOUSTON	HOU	5
LUBBOCK	LBB	6
SAN ANGELO	SJT	7
AMARILLO	AMA	8
WACO	WAC	9
CHILDRESS	CHS	10
BEAUMONT	BMT	11
FORT WORTH	FTW	12
YOAKUM	YKM	13
WICHITA FALLS	WFS	14
BROWNWOOD	BWD	15
SAN ANTONIO	SAT	16
TYLER	TYL	17
ABILENE	ABL	18
BRYAN	BRY	19
CORPUS CHRISTI	CRP	20
EL PASO	ELP	21
PARIS	PAR	22
LAREDO	LRD	23
LUFKIN	LFK	24
DALLAS	DAL	25

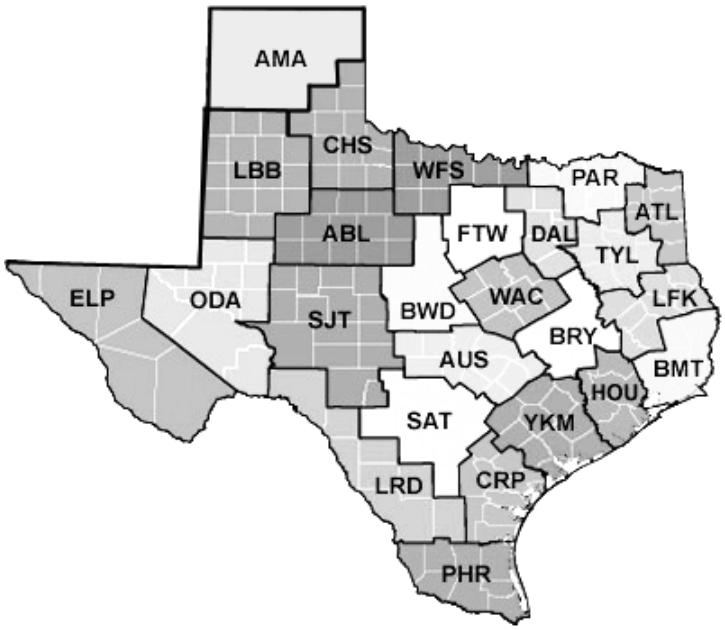

Figure C-7 Texas Districts

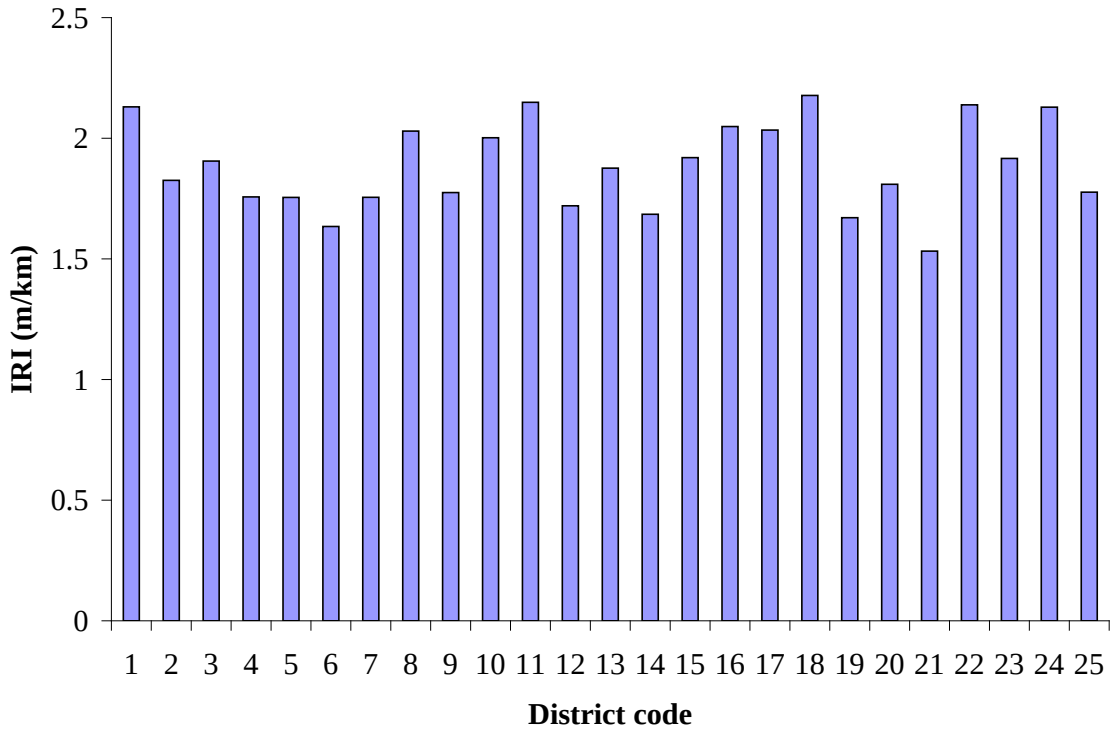

Figure C-8 Distribution of IRI by District for Texas (Texas DOT)

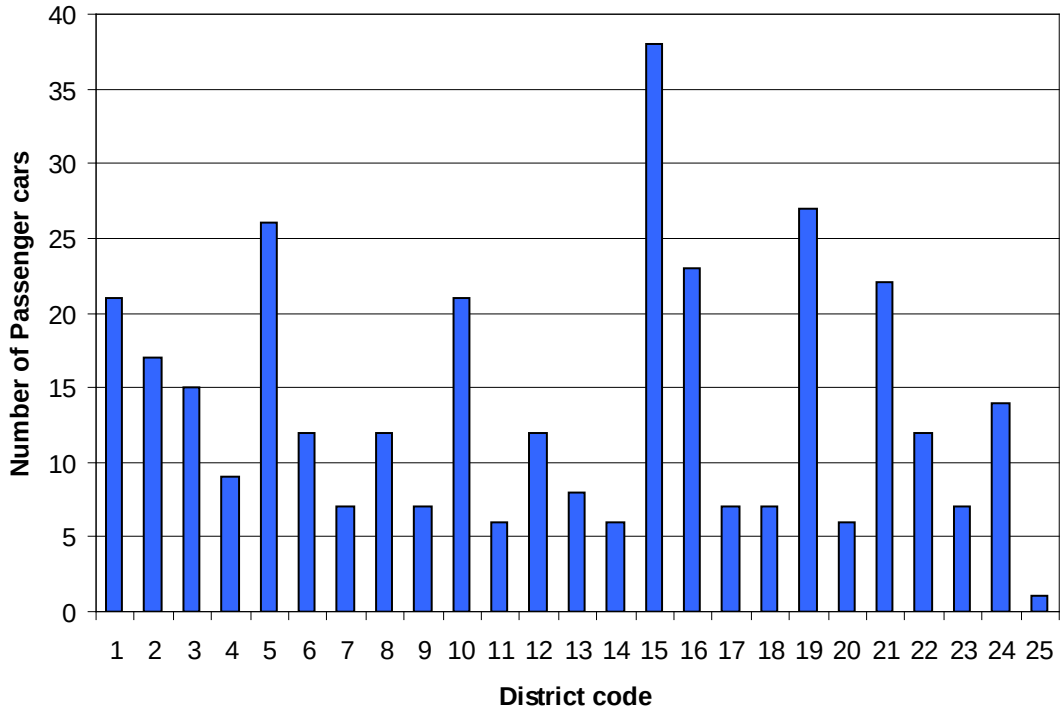

Figure C-9 Distribution of Repairs by District for Passenger Cars (Texas DOT)

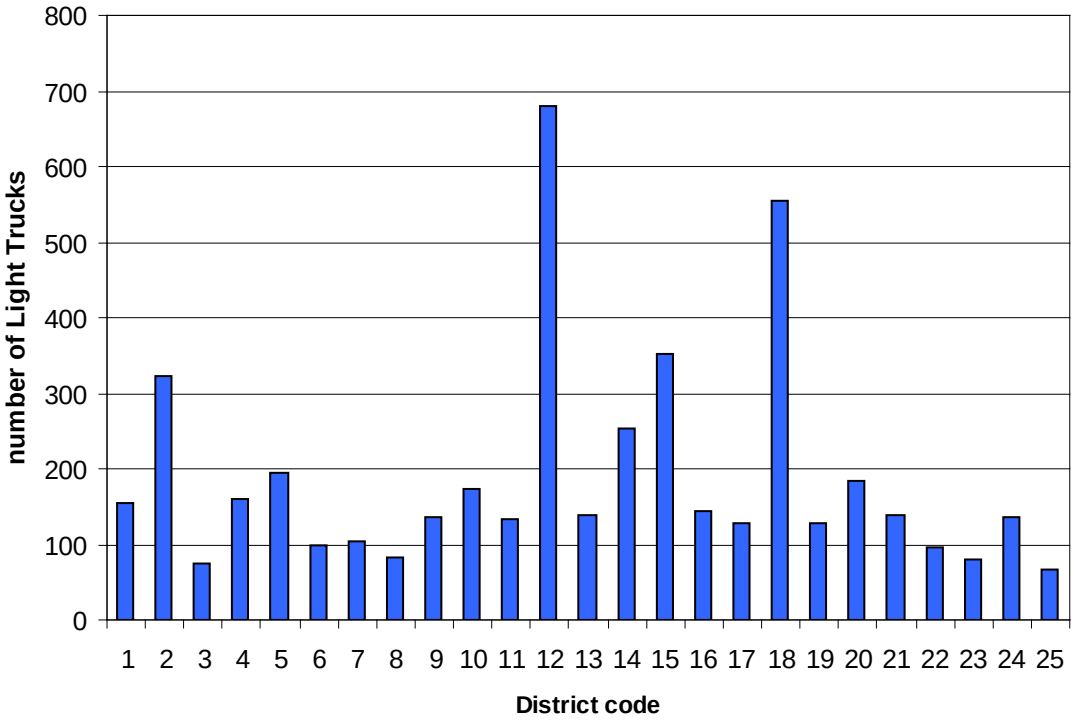

(a) Light truck

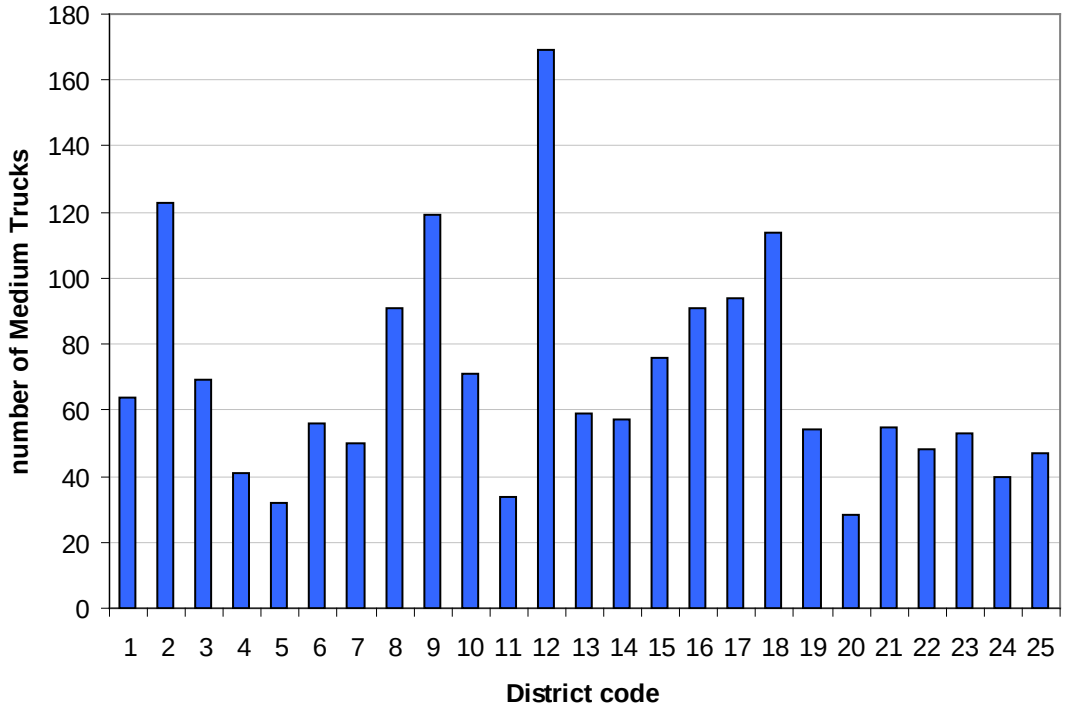

(b) Medium trucks

Figure C-10 Distribution of Repairs by District (Texas DOT)

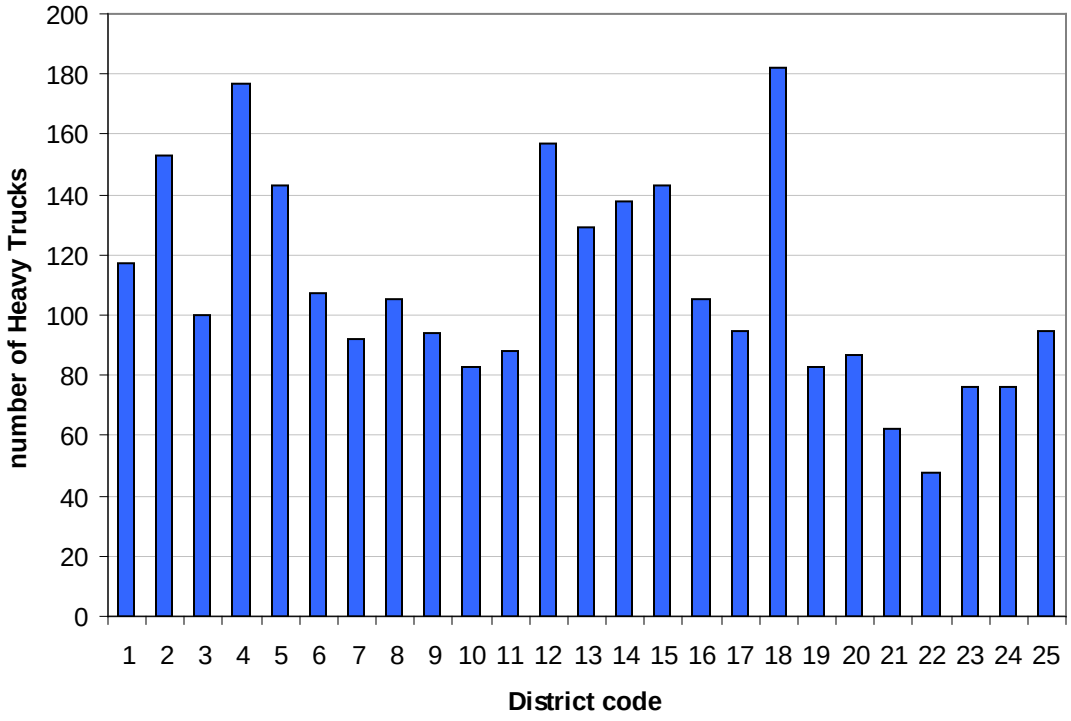

(a) Heavy truck

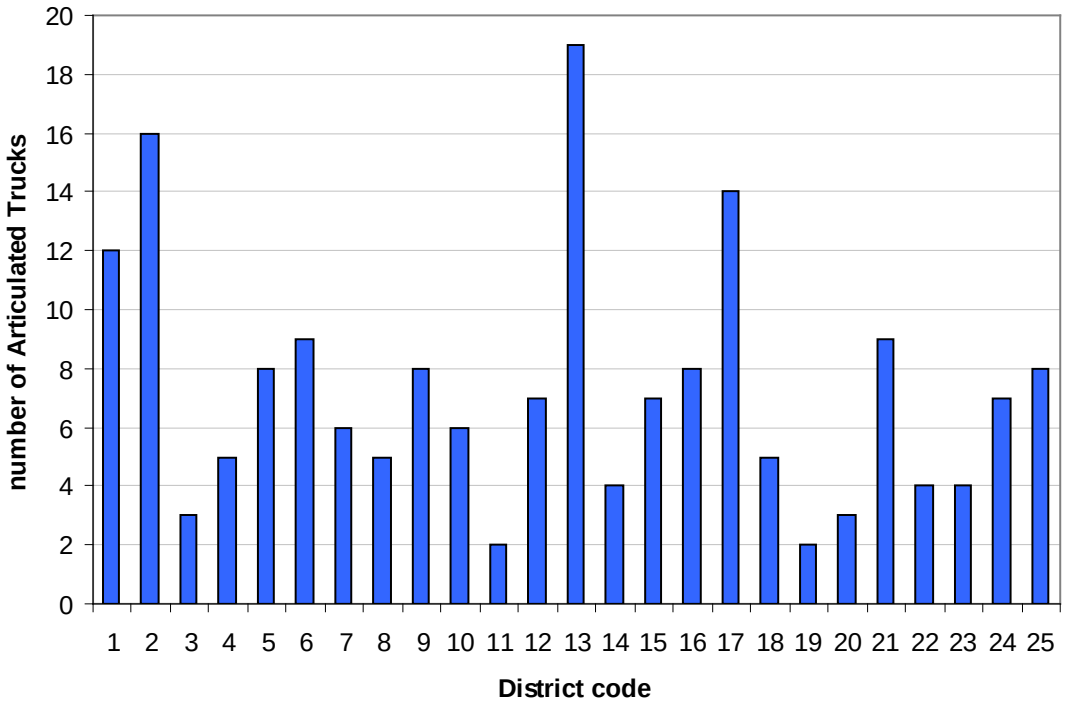

(b) Articulated truck

Figure C-11 Distribution of Repairs by District (Texas DOT)

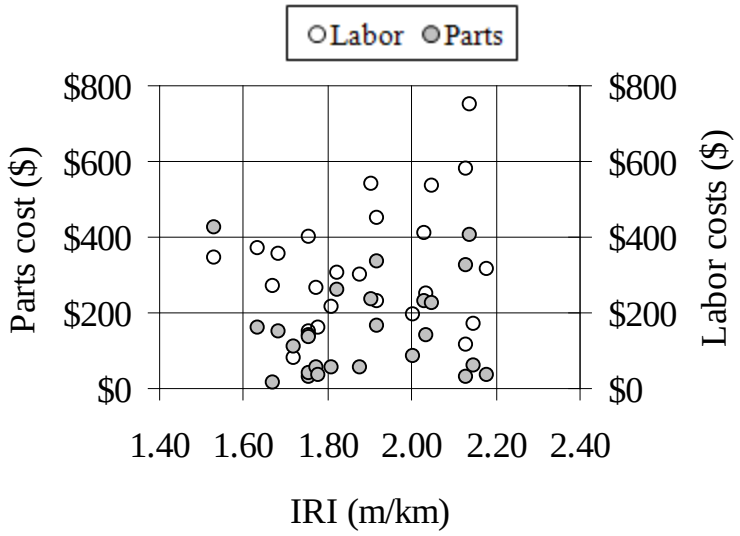

(a) Passenger Cars

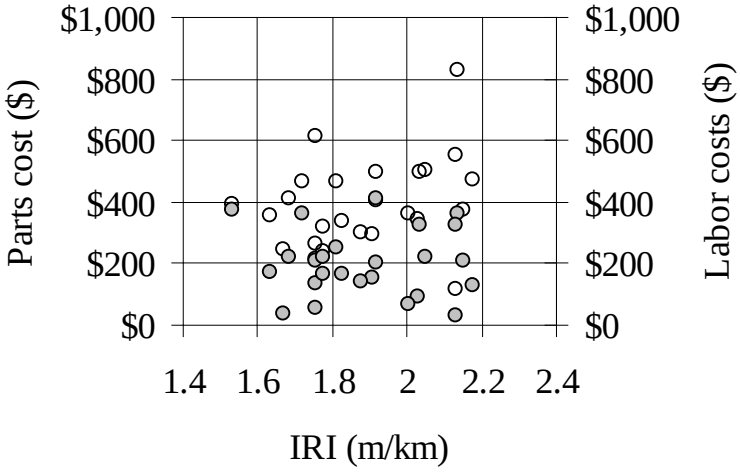

(b) Light Trucks

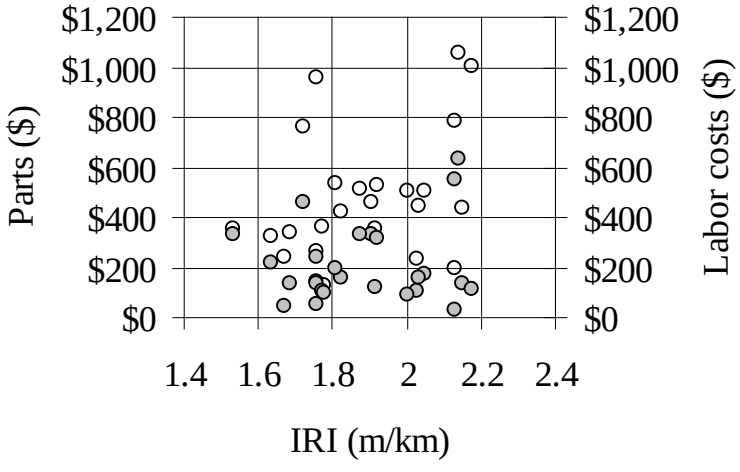

(c) Medium Trucks

Figure C-12 Summary of the Repair and Maintenance Data for Light and Medium Vehicles (Texas DOT)

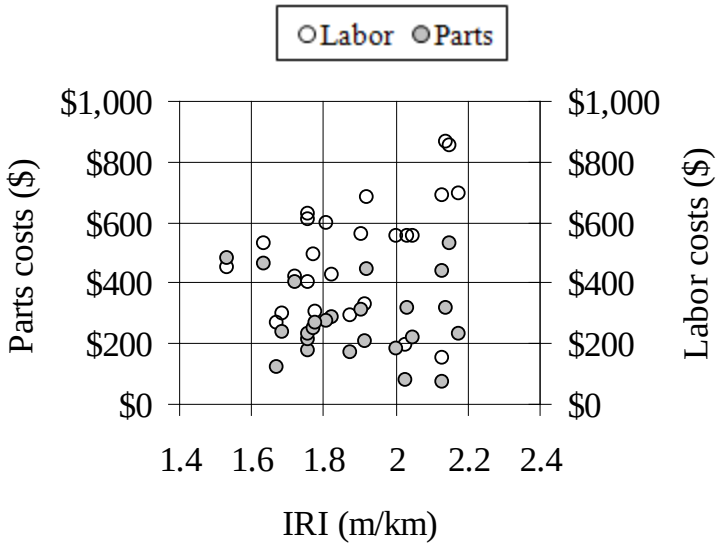

(a) Heavy Trucks

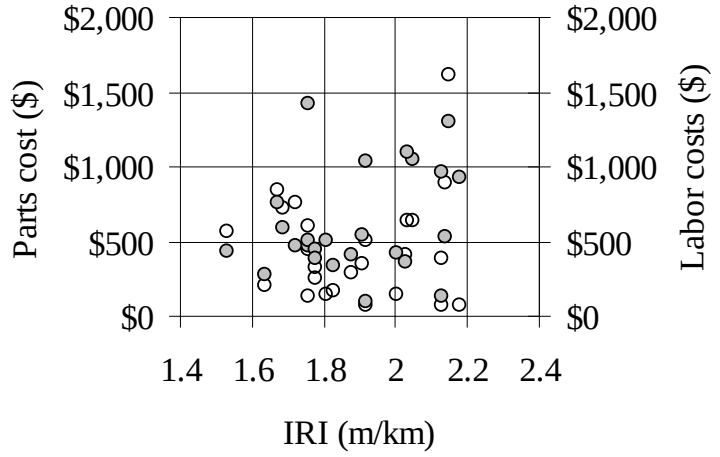

(b) Articulated Trucks

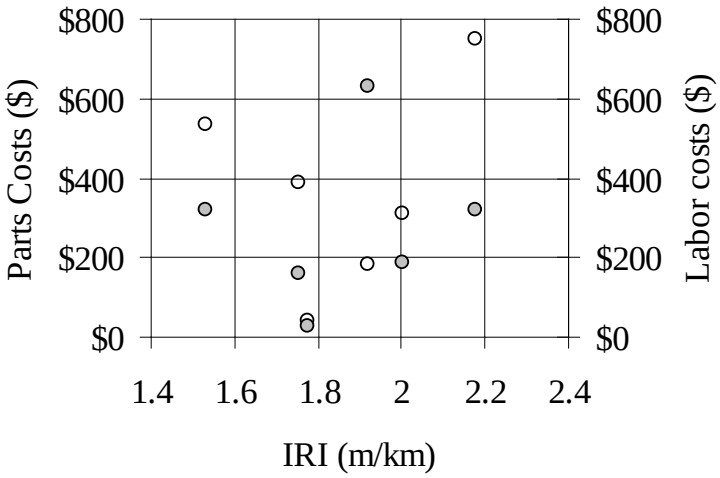

(c) Buses

Figure C-13 Summary of the Repair and Maintenance Data for Heavy Vehicles (Texas DOT)

NCHRP 1-33 DATA

Data from previous research conducted as part of NCHRP 1-33 project were also obtained. It should be noted that the data is only for heavy trucks. Figures C.14 shows the raw data and Figure C.15 show the corrected data for mileage and age.

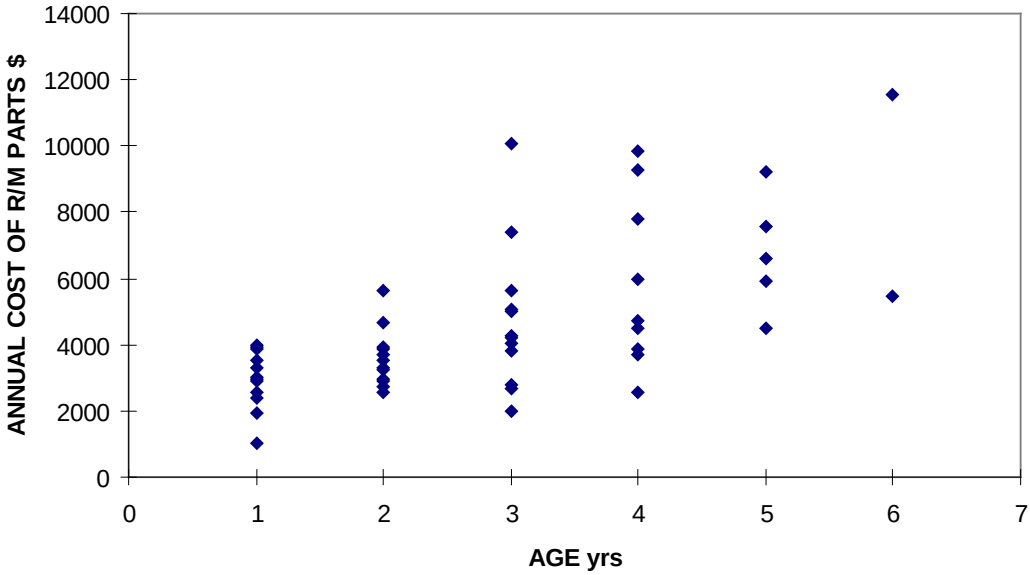

(a) Annual Parts Cost versus Age

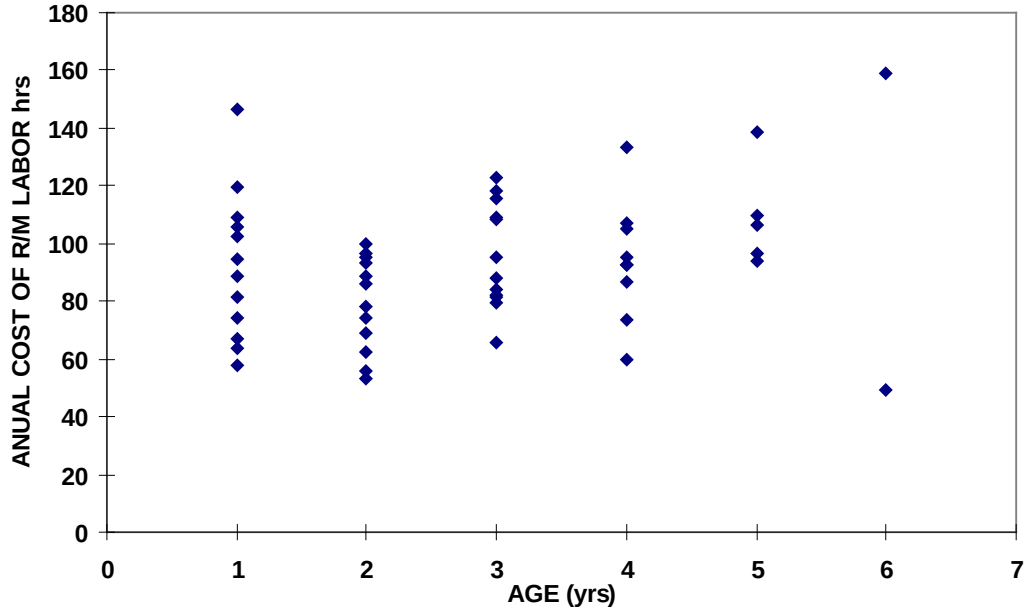

(b) Annual Labor Cost versus Age

Figure C-14 NCHRP 1-33 Raw Data (Papagiannakis, 2000)

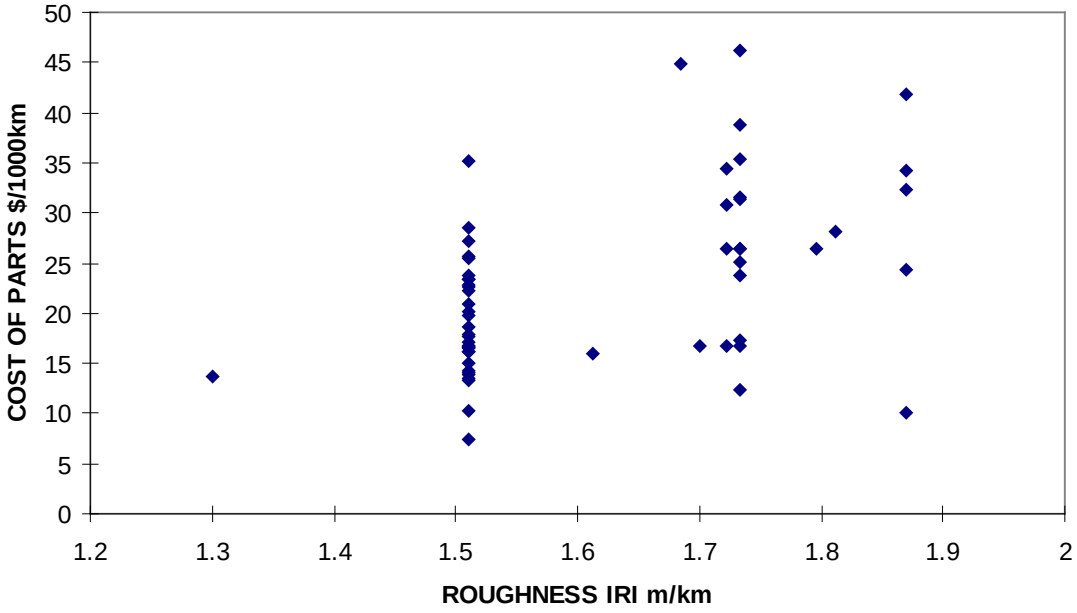

(c) Cost of Parts per 1000 km

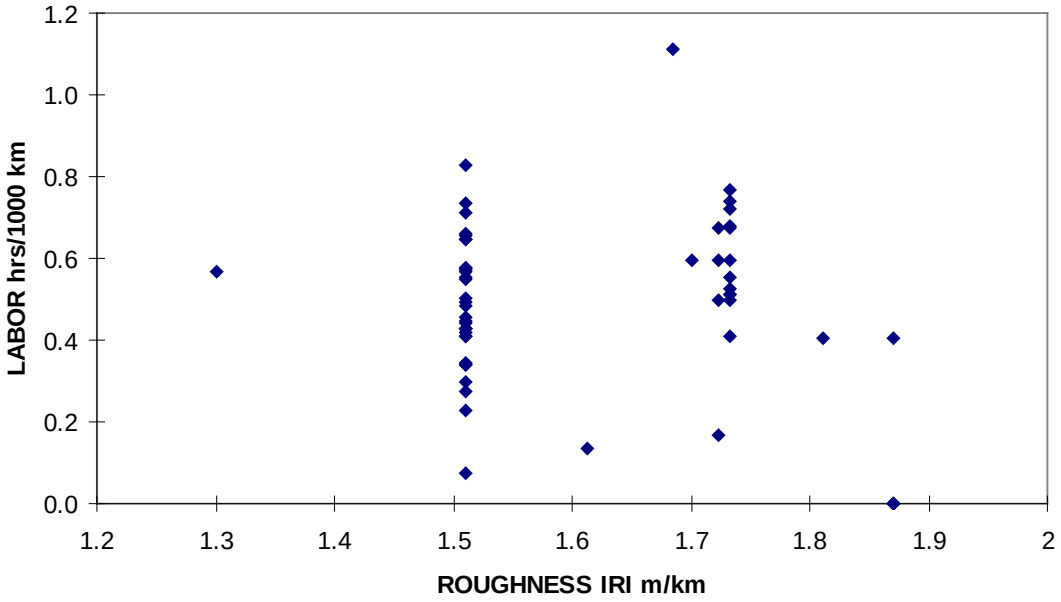

(d) Labor Hours per 1000 km

Figure C-15 NCHRP 1-33 Data Corrected for Age and Mileage (Pappagianakis, 2000)

C3 - UPDATED ZANIEWSKI ET AL TABLES

Table C-6 Updated Repair and Maintenance Costs (% avg cost/1000 km) – Small Car

Table C-7 Updated Repair and Maintenance Costs (% avg cost/1000 km) – Medium Car

Table C-8 Updated Repair and Maintenance Costs (% avg cost/1000 km) – Large Car

Table C-9 Updated Repair and Maintenance Costs (% avg cost/1000 km) – Pickup and Van

Table C-10 Updated Repair and Maintenance Costs (% avg cost/1000 km) – Light Truck

Table C-11 Updated Repair and Maintenance Costs (% avg cost/1000 km) – Medium Truck, Heavy Truck and Bus

Table C-12 Updated Repair and Maintenance Costs (% avg cost/1000 km) – Articulated Truck

Table C-6 Updated Repair and Maintenance Costs (% avg cost/1000 km) – Small Car

Grade %	Speed (km/h)													
	8	16	24	32	40	48	56	64	72	80	88	96	104	112
8	30.4	32.3	34.6	37.2	40.2	43.4	46.6	50.0	53.4	57.0	60.7	64.4	68.8	73.8
7	30.3	32.0	34.1	36.6	39.4	42.4	45.5	48.8	52.1	55.4	58.9	62.5	66.9	71.9
6	30.1	31.7	33.6	35.9	38.6	41.5	44.4	47.5	50.6	53.9	57.3	60.9	65.0	69.4
5	30.0	31.4	33.1	35.2	37.9	40.6	43.3	46.2	49.3	52.3	55.5	58.9	62.5	67.5
4	29.8	31.1	32.7	34.7	37.1	39.6	42.3	44.9	47.8	50.8	53.8	57.1	60.8	65.0
3	29.7	30.8	32.2	34.1	36.3	38.7	41.1	43.7	46.4	49.2	52.1	55.2	58.8	63.1
2	29.5	30.4	31.8	33.4	35.5	37.8	40.1	42.4	45.0	47.6	50.4	53.3	56.7	60.7
1	29.4	30.1	31.3	32.8	34.8	36.8	38.9	41.2	43.6	46.1	48.6	51.4	54.7	58.5
0	29.2	29.8	30.8	32.2	33.9	35.8	37.9	39.9	42.2	44.5	46.9	49.6	52.6	56.3
-1	29.1	29.5	30.3	31.6	33.2	34.9	36.8	38.7	40.8	42.9	45.2	47.7	50.6	54.1
-2	25.0	24.1	22.7	20.7	18.1	33.9	35.6	37.4	39.4	41.4	43.5	45.8	48.6	51.9
-3	39.8	38.9	37.4	35.4	32.9	29.6	25.6	20.8	37.9	39.8	41.8	43.9	46.5	49.8
-4	54.4	53.6	52.2	50.2	47.6	44.3	40.3	35.6	30.1	24.0	40.1	42.1	44.5	47.6
-5	69.4	68.1	66.9	65.0	62.4	59.1	55.1	50.3	44.9	38.8	31.9	24.4	42.4	45.4
-6	83.8	83.1	81.9	79.4	76.9	73.8	70.0	65.0	59.6	53.5	46.6	39.1	31.0	43.2
-7	98.8	98.1	83.8	94.4	91.9	88.8	84.4	80.0	74.4	68.1	61.4	53.8	45.8	37.2
-8	113.8	112.5	111.3	109.4	106.9	103.1	99.4	94.4	89.4	83.1	76.3	68.8	60.4	51.9

Table C-7 Updated Repair and Maintenance Costs (% avg cost/1000 km) – Medium Car

Grade %	Speed (km/h)													
	8	16	24	32	40	48	56	64	72	80	88	96	104	112
8	30.8	32.6	35.1	37.9	41.0	44.3	47.7	51.3	54.9	58.6	58.0	66.3	70.6	76.3
7	30.6	32.3	34.5	37.2	40.4	43.3	46.5	49.8	53.3	56.8	60.5	64.4	68.8	73.8
6	30.4	31.9	34.0	36.4	39.3	42.2	45.3	48.4	51.7	55.1	58.6	62.3	66.3	71.3
5	30.2	31.6	33.5	35.8	38.4	40.6	44.1	47.0	50.1	53.3	56.6	60.2	64.4	68.8
4	30.1	31.3	32.9	35.1	37.5	40.1	42.8	45.6	48.6	51.6	54.7	58.1	61.8	66.3
3	29.9	30.9	32.4	34.4	36.6	39.1	41.6	44.3	47.0	49.8	52.8	55.9	59.6	63.8
2	29.7	30.6	31.9	33.7	35.8	38.0	40.4	42.8	45.4	48.1	50.9	53.9	57.3	61.3
1	29.5	30.2	31.4	32.9	34.9	36.9	39.1	41.4	43.8	46.3	48.9	51.8	55.0	58.9
0	29.3	29.9	30.9	32.3	34.0	35.9	37.9	40.0	42.3	44.6	47.0	49.6	52.7	56.4
-1	29.2	29.5	30.3	31.6	33.1	34.8	36.7	38.6	40.7	42.8	45.1	47.6	50.4	53.9
-2	24.4	23.6	22.3	20.4	18.1	33.8	35.4	37.3	39.1	41.1	43.1	45.4	48.1	51.5
-3	39.1	38.3	36.9	35.1	32.8	29.7	26.0	21.7	37.6	39.3	41.2	43.4	45.9	49.1
-4	53.8	52.9	51.6	49.8	47.4	44.4	40.7	36.4	31.3	25.6	39.3	41.3	43.6	46.6
-5	68.1	67.5	66.3	64.4	62.1	59.1	55.4	51.0	46.0	40.3	33.9	27.1	41.3	44.1
-6	83.1	82.5	81.3	79.4	76.9	73.8	70.0	65.6	60.7	55.0	48.6	41.7	34.2	41.7
-7	97.5	96.9	95.6	93.8	91.3	88.1	85.0	80.6	75.6	69.4	63.1	56.4	49.2	41.0
-8	112.5	111.9	110.6	108.8	106.3	103.1	99.4	95.0	90.0	84.4	78.1	71.3	63.8	55.7

Table C-8 Updated Repair and Maintenance Costs (% avg cost/1000 km) – Large Car

Grade %	Speed (km/h)													
	8	16	24	32	40	48	56	64	72	80	88	96	104	112
8	31.1	33.1	35.5	38.4	41.6	44.9	48.4	52.0	55.7	59.4	63.1	67.5	71.9	76.9
7	30.9	32.8	34.9	37.6	40.7	43.9	47.1	50.6	54.1	57.6	61.4	65.0	69.4	74.4
6	30.7	32.4	34.4	36.9	39.8	42.8	45.9	49.1	52.4	55.8	59.4	63.1	67.5	70.6
5	30.5	32.0	33.9	36.2	38.9	41.7	44.6	47.7	50.8	54.1	57.4	61.0	65.0	69.4
4	30.3	31.6	33.4	35.5	38.0	40.6	43.4	46.3	49.3	52.3	55.4	58.9	62.5	66.9
3	30.1	31.3	32.8	34.8	37.1	39.6	42.1	44.8	47.6	50.4	53.5	56.7	60.3	64.4
2	30.0	30.9	32.3	34.1	36.2	38.5	40.9	43.4	46.0	48.6	51.5	54.6	58.0	62.1
1	29.8	30.6	31.8	33.4	35.3	37.4	39.6	41.9	44.4	46.9	49.5	52.4	55.7	59.6
0	29.6	30.2	31.2	32.6	34.4	36.3	38.4	40.5	42.8	45.1	47.6	50.3	53.3	57.1
-1	29.4	29.9	30.7	31.9	33.5	35.3	37.1	39.1	41.1	43.3	45.6	48.1	51.0	54.6
-2	211.6	23.4	22.3	20.8	18.8	34.2	35.8	37.6	39.6	41.5	43.6	45.9	48.7	52.1
-3	37.6	37.0	35.9	34.3	32.3	29.8	26.6	22.8	37.9	39.7	41.6	43.8	46.3	49.6
-4	51.2	50.6	49.4	47.9	45.9	43.3	40.1	36.4	32.1	27.1	39.7	41.6	44.0	47.0
-5	65.0	64.4	63.1	61.5	59.4	56.9	53.7	49.9	45.6	40.7	35.2	29.1	41.7	44.5
-6	78.1	77.5	76.9	75.0	73.1	70.6	67.5	63.8	59.2	54.3	48.8	42.8	36.3	29.4
-7	91.9	91.3	90.0	88.8	86.9	83.8	80.6	76.9	72.5	68.1	62.3	56.3	49.8	43.0
-8	105.6	105.0	103.8	102.5	100.0	97.5	94.4	90.6	86.3	81.3	75.6	70.0	63.1	56.6

Table C-9 Updated Repair and Maintenance Costs (% avg cost/1000 km) – Pickup and Van

Grade %	Speed (km/h)													
	8	16	24	32	40	48	56	64	72	80	88	96	104	112
8	30.7	33.0	35.4	38.1	41.2	44.4	47.8	51.3	54.9	58.6	62.4	66.3	70.6	75.6
7	30.9	32.7	34.8	37.4	40.2	43.4	46.6	50.0	53.4	56.9	60.6	64.4	68.8	73.8
6	30.8	32.4	34.4	36.8	39.5	42.4	45.0	48.6	51.9	55.3	58.7	62.4	66.3	71.3
5	30.6	32.0	33.9	36.1	38.7	41.4	44.3	47.3	50.4	53.6	56.9	60.4	64.4	68.8
4	30.4	31.7	33.4	35.4	37.9	40.4	43.2	46.0	48.9	51.9	55.1	58.4	62.2	66.9
3	30.3	31.4	33.0	34.8	37.0	39.5	42.0	44.7	47.4	50.3	53.3	56.4	60.1	64.4
2	30.1	31.0	32.4	34.1	36.2	38.5	40.9	43.4	45.9	48.6	51.4	54.5	57.9	62.0
1	29.9	30.7	31.9	33.4	35.4	37.5	39.7	42.0	44.4	46.9	49.6	52.5	55.8	59.7
0	29.8	30.4	31.4	32.8	34.6	36.5	38.6	40.7	43.0	45.3	47.8	50.5	53.6	57.3
-1	27.1	30.1	30.9	32.1	33.7	35.4	37.4	39.4	41.5	43.6	45.9	48.5	51.4	55.0
-2	19.6	18.8	17.4	15.6	33.1	34.5	36.1	38.1	40.0	41.9	44.1	46.5	49.3	52.7
-3	34.6	33.8	32.4	30.5	28.1	24.9	21.2	36.8	38.5	40.3	42.3	44.6	47.1	50.4
-4	49.6	48.8	46.1	45.5	43.0	39.9	36.1	31.7	26.6	38.6	40.5	42.6	44.9	48.1
-5	64.4	63.8	62.4	60.4	58.0	54.9	51.1	46.6	41.5	35.7	30.4	40.6	42.8	45.8
-6	79.4	78.8	77.5	75.6	73.1	70.0	66.3	61.6	56.5	50.6	44.1	36.9	29.3	43.4
-7	94.4	93.8	92.5	90.6	88.1	85.0	81.3	76.9	71.3	65.6	59.1	52.0	44.3	36.3
-8	109.4	108.8	107.5	105.6	103.1	100.0	96.3	91.9	86.3	80.6	74.4	66.9	59.3	51.2

Table C-10 Updated Repair and Maintenance Costs (% avg cost/1000 km) – Light Truck

Grade %	Speed (km/h)													
	8	16	24	32	40	48	56	64	72	80	88	96	104	112
8	32.2	35.3	39.4	44.3	49.8	55.8	62.2	68.8	75.6	83.1	90.6	97.5	105.0	112.5
7	31.8	34.3	38.0	42.4	47.5	53.1	59.0	65.0	71.9	78.8	85.6	91.9	98.8	105.6
6	31.3	33.4	36.6	40.6	45.3	50.3	55.8	61.6	67.5	73.8	80.6	86.9	93.1	99.4
5	30.8	32.5	35.3	38.8	42.9	47.6	52.6	57.9	63.8	69.4	75.6	81.3	87.5	93.1
4	30.4	31.6	33.9	37.0	40.7	44.9	49.4	54.3	59.5	66.3	70.6	75.6	81.3	86.9
3	29.9	30.7	32.6	35.2	38.3	42.1	46.3	50.7	55.4	60.3	65.6	70.6	75.6	80.6
2	29.4	29.8	31.2	33.4	36.1	39.4	43.1	47.1	51.3	55.8	60.3	65.0	69.4	74.4
1	29.0	28.9	29.8	31.6	33.8	36.7	39.9	43.4	47.3	51.2	55.3	59.4	63.8	67.5
0	28.6	27.9	28.4	29.8	31.6	33.9	36.7	39.8	43.2	46.7	50.3	54.0	57.7	61.4
-1	10.4	9.3	27.1	27.9	29.3	31.2	33.6	36.2	39.1	42.1	45.3	48.5	51.8	55.0
-2	20.3	19.3	18.3	17.3	14.9	15.0	13.6	12.1	35.0	37.6	40.3	43.1	45.9	48.1
-3	30.2	29.2	28.3	27.3	26.1	24.9	23.6	22.0	20.3	18.4	16.2	37.6	39.9	41.9
-4	40.1	39.1	38.1	37.1	36.1	34.8	33.5	31.9	30.3	28.3	26.1	23.8	21.0	35.6
-5	50.1	49.0	48.1	47.1	46.0	44.8	43.4	41.9	40.2	38.3	36.1	33.1	30.9	28.0
-6	60.0	58.9	58.0	57.0	55.9	54.7	53.3	51.8	50.1	48.1	46.0	43.6	40.9	37.9
-7	70.0	68.8	68.1	66.9	65.6	64.4	63.1	61.8	60.0	58.1	55.9	53.5	50.8	47.9
-8	80.0	78.8	78.1	76.9	75.6	74.4	73.1	71.9	70.0	68.1	65.6	63.1	60.8	57.8

Table C-11 Updated Repair and Maintenance Costs (% avg cost/1000 km) – MediumTruck, Heavy Truck and Bus

Grade %	Speed (km/h)													
	8	16	24	32	40	48	56	64	72	80	88	96	104	112
8	32.4	36.8	41.1	45.7	50.4	55.4	60.5	65.6	71.9	77.5	83.8	90.6	97.5	105.0
7	32.0	35.8	39.8	43.9	48.1	52.6	57.3	62.3	67.5	73.1	78.8	85.0	91.9	98.8
6	31.5	34.9	38.4	42.1	45.9	49.9	54.1	58.6	63.1	68.1	73.8	79.4	85.6	92.5
5	31.1	34.0	37.0	40.2	43.6	47.1	50.9	54.9	59.2	63.8	68.8	73.8	80.0	85.6
4	30.6	33.1	35.6	38.4	41.3	45.0	47.7	51.3	55.1	59.2	63.8	68.8	73.8	79.4
3	30.1	32.2	34.3	36.6	39.0	41.6	44.4	47.6	50.9	54.6	58.7	63.1	68.1	73.1
2	29.7	31.3	32.9	34.7	36.7	39.5	41.3	43.9	46.8	50.1	53.6	57.6	61.9	66.9
1	29.3	30.3	31.5	32.9	34.4	36.1	38.1	40.3	42.7	45.4	48.6	53.3	55.6	60.2
0	28.8	29.4	30.1	31.1	32.1	33.4	34.8	36.6	38.6	40.9	43.6	46.6	49.9	53.8
-1	10.4	9.9	9.4	29.2	29.8	30.6	31.6	32.9	34.4	36.3	38.5	41.1	44.0	47.4
-2	19.6	19.1	18.6	18.1	17.4	16.6	15.9	15.0	14.1	13.2	33.4	35.6	38.1	40.9
-3	28.8	28.3	27.8	27.2	26.6	25.8	25.0	24.2	23.3	22.4	21.4	20.4	19.5	18.5
-4	37.9	37.5	37.0	36.4	35.8	35.0	34.2	33.4	32.4	31.6	30.6	29.6	28.7	27.7
-5	47.1	46.6	46.1	45.6	44.9	44.1	43.4	42.5	41.6	40.7	39.8	38.8	37.8	36.9
-6	56.3	55.8	55.3	54.8	54.1	53.3	52.6	51.7	50.8	49.9	48.9	48.0	47.0	46.0
-7	65.6	65.0	64.4	63.8	63.1	62.5	61.7	60.9	60.0	59.1	58.1	57.1	56.2	55.2
-8	74.4	74.4	73.8	73.1	72.5	71.9	70.6	70.0	69.4	68.1	67.5	66.3	65.6	64.4

Table C-12 Updated Repair and Maintenance Costs (% avg cost/1000 km) – Articulated Truck

Grade %	Speed (km/h)													
	8	16	24	32	40	48	56	64	72	80	88	96	104	112
8	35.1	41.1	48.0	55.6	63.8	72.5	81.3	90.6	100.6	110.6	120.0	130.6	140.6	150.6
7	34.3	39.5	45.6	52.4	59.8	67.5	76.3	84.4	93.1	102.5	111.9	120.6	130.0	139.4
6	33.4	37.9	43.3	49.3	55.8	63.1	70.6	78.1	86.3	94.4	103.1	111.3	120.0	128.8
5	32.7	36.3	40.9	46.1	51.9	58.1	65.0	71.9	79.4	86.9	94.4	101.9	109.4	117.5
4	31.9	34.8	38.5	42.9	47.9	53.4	59.4	65.6	71.9	78.8	85.6	92.5	99.4	106.3
3	31.1	33.2	36.1	39.8	43.9	48.6	53.8	59.3	65.0	70.6	76.9	83.1	88.8	95.0
2	30.3	31.6	33.8	36.6	40.0	43.9	48.3	52.9	57.8	63.1	68.1	73.1	78.8	84.4
1	29.5	30.0	31.4	33.4	36.1	39.2	42.8	46.6	50.8	55.1	59.4	63.8	68.8	73.1
0	28.7	28.4	29.0	30.3	32.1	34.4	37.3	40.3	43.6	47.1	50.8	54.5	58.2	62.1
-1	10.8	10.4	10.1	9.9	9.8	29.7	31.7	34.0	36.5	39.3	42.1	45.0	47.9	51.0
-2	20.7	20.3	20.0	19.8	19.6	19.4	19.3	19.0	18.7	18.3	17.8	17.1	37.6	39.9
-3	30.6	28.9	29.9	29.7	29.5	29.3	29.1	28.9	28.6	28.2	27.6	27.0	26.3	25.4
-4	40.5	40.1	39.8	39.6	39.4	39.2	39.0	38.8	38.4	38.1	37.6	36.9	36.1	35.3
-5	50.4	49.9	49.7	49.4	49.3	49.1	48.9	48.6	48.3	47.9	47.4	46.8	46.1	45.2
-6	60.3	59.9	59.6	59.4	59.2	58.9	58.8	58.6	58.3	57.8	57.3	56.7	55.9	55.1
-7	70.0	70.0	69.4	69.4	69.4	68.8	68.8	68.1	68.1	67.5	67.5	66.9	65.6	65.0
-8	80.0	79.4	79.4	79.4	78.8	78.8	78.8	78.1	78.1	77.5	76.9	76.3	75.6	75.0

C4 - MODELS FOR GENERATION OF ARTIFICIAL ROAD PROFILES

ARTIFICIAL ROAD PROFILE GENERATION

Various types of road models have been in use for years to represent roads for analyzing vehicle ride behavior (Gillespie and Sayers, 1981). One of the first proposed stochastic models is an equation of the form:

$$Gz(v) = \frac{A}{(2\pi v)^2} \qquad \text{(C.15)}$$

Where,

Gz(v) = PSD function of elevation (z)
v =Wavenumber
A = Roughness coefficient obtained by fitting the OSD of a measured road to the above equation

As the elevation is perceived to be changing with time, it also has a velocity (proportional to slope) and acceleration (proportional to the derivative of slope), which also have PSDs for the same road section. Since velocity is the derivative of position, the velocity PSD is related to the elevation PSD by the scale factor (2πv). And, likewise, the acceleration PSD is related to the velocity PSD by the same scale factor. The concept of the road as an acceleration input to the vehicle is important to understand because its ultimate effect - vehicle ride vibration- is invariably quantified as accelerations (Gillespie and Sayers, 1981). Gillespie et al. (1993) proposed the following equation for the PSD model:

$$Gz(v) = \frac{Ga}{(2\pi v)^4} + \frac{Gs}{(2\pi v)^2} + Ge \qquad \text{(C.16)}$$

The first component, with the amplitude Ga, is a white noise acceleration that is integrated twice. The second, with amplitude Gs, is a white noise slope that is integrated once. The third, with amplitude Ge, is a white noise elevation. The model can also be written to define the PSD of profile slope by looking at the derivative of the above equation.

$$Gz'(v) = \frac{Ga}{(2\pi v)^2} + Gs + Ge(2\pi v)^2 \qquad \text{(C.17)}$$

Gillespie et al. (1993) suggested ranges of roughness parameters based on the road profiles measured in North America, England and Brazil (Table C-13). When traversed by a vehicle, the profile is perceived as an elevation that changes with time, where time and longitudinal distance are related by the speed of the vehicle. The time-varying elevation can also be characterized by a PSD that has units of elevation.

Table C-13 Roughness Parameters for the White-Noise PSD Model (Gillespie et al., 1993)

SURFACE TYPE	Gs (m/cycle× 10^{-6})	Ga (1/m cycle ×10^{-6})	Ge (m3/cycle ×10^{-6})
Asphalt (Ann Arbor)	1~300	0.0~7	0.0~8.0
Asphalt (Brazil)	4~100	0.4~4	0.0~0.5
PCC (Ann Arbor)	4~ 90	0.0~1	0.0~0.4
Surface treatment (Brazil)	8~ 50	0.0~4	0.2~1.2

Marcondes et al. (1991) developed another equation to predict PSD. Elevation profiles of federal and interstate highways near Lansing, Michigan, were measured with a profilometer and PSD were calculated. They developed the following equations to fit the above data:

$$PDpe(v) = A_1 e^{(-kvp)}, \qquad v \le v_1 \qquad \text{(C.18)}$$
$$PDpe(v) = A_2 (v - v_0), \qquad v > v_1$$

Where,

PDpe(v) = Power density value [in^3/cycle] for the pavement elevation
v_1 = Discontinuity frequency, cycles/in
v_0 = Asymptote frequency, cycles/in
A_1, A_2 = Constants
k, p, q = Constants

Marcondes (1990) reported the range of values of parameters for the equations as shown in Table C-14.

Table C-14 Ranges of Variable Values for PSD Equations (Marcondes, 1990)

Category	A_1	k	p	A_2	v_0	q
OC*	1.3~7.2	7000~ 67000	1.6~2.0	5.9E-7~ 4.2E-5	0~ 3.9E-3	-2.6~ -1.5
NC*	1.5~3.4	24000~ 83000	1.8~2.0	6.0E-7~ 6.0E-5	2.5E-3~ 4.9E-3	-2.2~ -1.1
AC*	1.8~5.7	63000~ 240000	2.0~2.2	1.4E-4~ 7.7E-4	4.6E-3~ 5.2E-3	-1.1~ -0.5

*Note: OC: old concrete pavement; NC: new concrete pavement; and AC: asphalt concrete pavement.

They investigated the relationship between RMS (Root Mean Square) elevation and IRI (International Roughness Index); the measured data showed that the correlation between them is weak (R^2 <0.7). It was found that a good correlation exists between the IRI and the PSD only for spatial frequencies between 0.002 and 0.015 cycle/in.

From the same data, Marcondes et al. (1992) found strong correlations between the IRI and the RMS vertical acceleration at the truck bed. The following models were developed for these relationships:

- For vehicle speed = 45 mph:

$$RMS = 3.794\times10^{-2} + 1.902\times10^{-3}\times IRI - 8.89\times10^{-7}\times IRI^2 \qquad R^2 = 0.937 \tag{C.19}$$

- For vehicle speed = 52mph:

$$RMS = 4.467\times10^{-2} + 2.144\times10^{-3}\times IRI - 1.819\times10^{-6}\times IRI^2 \qquad R^2 = 0.914 \tag{C.20}$$

- For vehicle speed = 60 mph:

$$RMS = 0.105 + 1.25\times10^{-3}\times IRI - 1.63\times10^{-6}\times IRI^2 \qquad R^2 = 0.866 \tag{C.21}$$

Most researchers have used generated road profiles for dynamic vehicle simulation. Road profiles, like any other random signal, can be generated using a random number algorithm. To generate random numbers, Gillespie et al. (1993) used a Gaussian distribution with a mean value of zero, and the standard deviation is:

$$s = \left(\frac{G}{2\Delta}\right)^{1/2} \tag{C.22}$$

Where,

G = White-noise amplitude for one of the three coefficients; Gs, Ge and Ga

Δ = Interval between samples used for wavenumber.

A simulated road profile that matches the target PSD is generated using the following procedures:

1) Create an independent sequence of random numbers for each of the three white-noise sources, scaled according to the above equation.
2) Integrate each sequence as needed to obtain the desired distribution over wavenumber.
3) Sum the outputs of the filters.

Thus, the sequence corresponding to the Ga term is integrated twice, the sequence corresponding to the Gs term is integrated once, while the sequence corresponding to the Ge term is not integrated. Table C-15 shows PSD coefficients and IRI values used by Gillespie et al. (1993).

Table C-15 PSD Coefficients in the Roughness Model (Gillespie et al, 1993)

Pavement Type	Surface Type	IRI (in/mi)	Gs (m/cycle×10^{-6})	Ga 1/(m×cycle×10^{-6})	Ge (m3/cycle×10^{-6})
Flexible	Smooth	75	6	0.00	0.000
	Medium	150	12	0.17	0.000
	Rough	225	20	0.20	0.003
Rigid	Smooth	80	1	0.00	0.000
	Medium	161	20	0.25	0.100
	Rough	241	35	0.30	0.100

In the case of a rigid pavement, faulting and curling/warping should be considered. The slab roughness between joints has similar characteristics to that of a flexible pavement; and, therefore, the periodic faults caused by the slab joints are superimposed on to this model. The resulting road profile over a slab length is:

$$y(x) = y_r(x) + y_{jf}(x) \quad \text{(C.23)}$$

Where,

$y_r(x)$ = The profile due to the slab roughness

$y_{jf}(x)$ = $\begin{cases} \left(\frac{h}{L}\right)x & for \quad 0 < x < L \\ 0 & for \quad x = L \end{cases}$

h = Joint fault magnitude

L = Joint spacing

Thermal and moisture gradient across the slab thickness result in significant bending moments along the edges of the slab. The curling/warping is modeled as a periodic hemispheric wave added to the above road model:

$$\left(x - \frac{L}{2}\right)^2 + \left(y_W(x) - \left(\frac{L}{2} - \delta\right)\right)^2 = R^2; \quad R^2 = \left(\frac{L}{2}\right)^2 + (R - \delta) \quad \text{(C.24)}$$

Where,

δ = Mid-slab deflection due to warping

R = Radius of curvature of slab

y_W = Vertical displacement due to warping

L = Joint spacing

The final road profile is:

$$y(x) = y_r(x) + y_{jf}(x) + y_w(x) \quad \text{(C.25)}$$

ARTIFICIAL GENERATION OF ROUGHNESS FEATURES

The identified roughness features that were proven to affect vehicle suspensions are: Faulting, breaks and curling in concrete pavements and potholes in asphalt pavements. To investigate their effect, these roughness features were artificially generated and superimposed on to the generated road surface profile. Figure C-16 presents schematic description of roughness features.

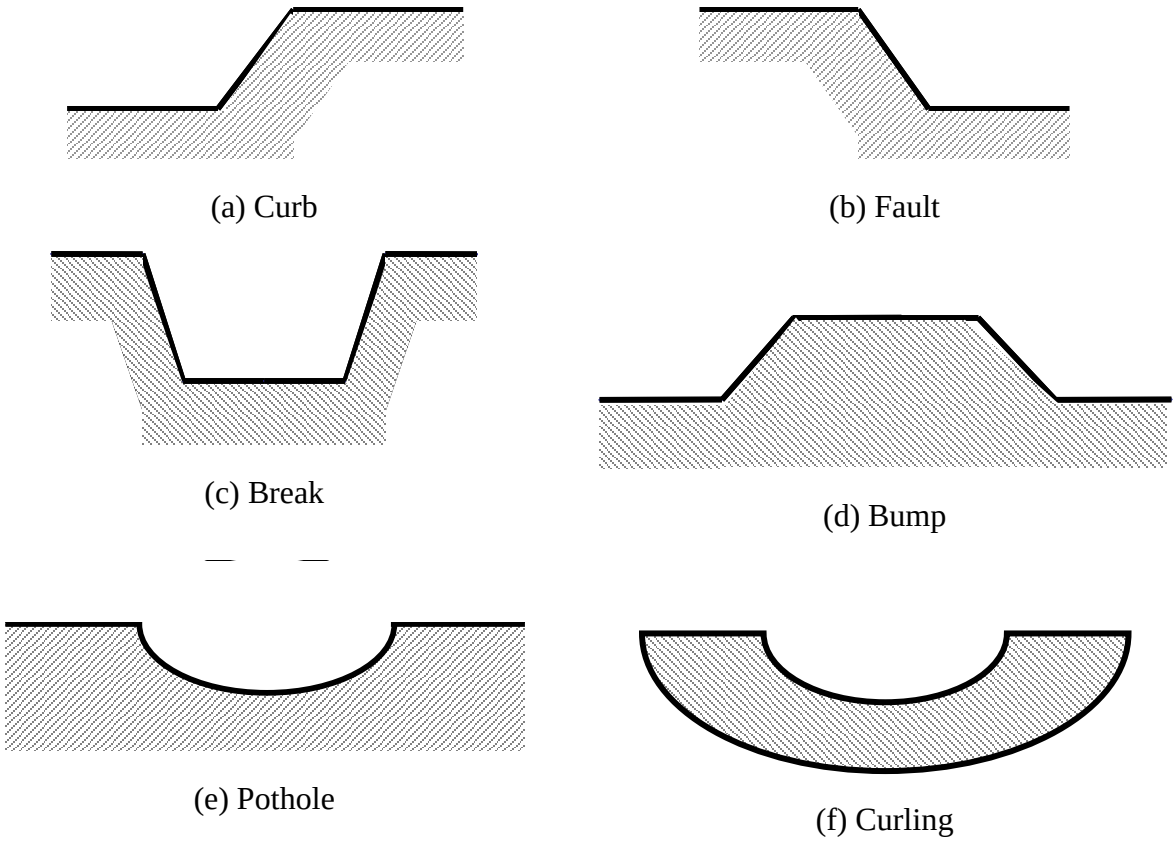

Figure C-16 Schematic Description of Roughness Features

Artificial Generation of Faults

Faulting is the difference in elevation across a joint or crack. It is determined by measuring the difference in elevation between the approach slab and the adjacent slab. In the current practice of road surface profile measurement in the US, the reporting interval for elevation is 0.025 to 0.075 m (1 to 3 inches). Based on previous study by Chatti et al. (2009), for a sampling interval of 0.019 m and a reporting interval of 0.075 m, the correct height of a fault is detectable when it is calculated as the difference in elevation between points that are 0.15 m apart. Accordingly, the width of a fault was taken as this value. The general form of a fault is given by Equation C.25. Figure C-17 shows the form used to find the mathematical description of a fault.

$$l = \frac{1600}{N_f - 1}$$

For $l \le L$:

$$u_f(x) = \begin{cases} -\dfrac{h}{0.15}x & for \quad 0 \le x \le 0.15 \\ \dfrac{h}{l-0.15}(x-l) & for \quad 0.15 \le x \le l \end{cases} \qquad \text{(C.26)}$$

For $l \ge L$:

$$u_f(x) = \begin{cases} -\dfrac{h}{0.15}x & for \quad 0 \le x \le 0.15 \\ \dfrac{h}{L-0.15}(x-L) & for \quad 0.15 \le x \le L \\ 0 & for \quad x \ge L \end{cases}$$

Where,

$uf(x)$ = Road profile due to fault

Nf = Number of faults per 1.6 km
h = Joint fault magnitude in mm
l = Distance between faults
L = Joint spacing,

$$= \begin{cases} 4.6 \text{ m} & \text{for Jointed Plain Concrete Pavement (JPCP)} \\ 12.5 \text{ m} & \text{for Jointed Reinforced Concrete Pavement (JRCP)} \end{cases}$$

0.15 = Fault width in m

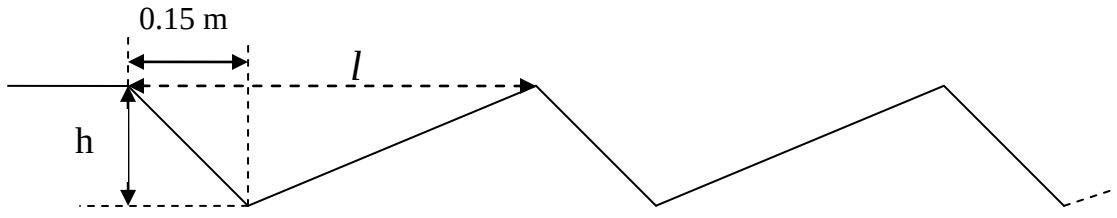

Figure C-17 Profile of a Faulted Rigid Pavement

The resulting road profile over 1.6 km is:

$$u(x) = u_r(x) + \sum_{j=0}^{N_f - 1} u_f(x - jl) \tag{C.27}$$

Where,

$u(x)$ = Road profile

$u_r(x)$ = Road profile due to roughness

$u_f(x)$ = Roughness features (Equation C.25)

N_f = Number of faults per 1.6 km

Artificial Generation of Breaks/Bumps

Break is a broken portion of the pavement section that starts with a negative fault and ends with a positive fault. The distance between the two opposite faults should not exceed 0.9 m (3ft), see (Huang, 2003). The general form of a break is given by Equation C.28. Figure C-18 shows the form used to find the mathematical description of a break. The same equation is used to generate bumps except that the magnitude is h instead of $(-h)$.

$$l = \frac{1600}{N_b - 1}$$

$$u_b(x) = \begin{cases} -\dfrac{h}{0.15}x & for \quad 0 \le x \le 0.15 \\ -h & for \quad 0.15 \le x \le 0.75 \\ \dfrac{h}{0.15}(x - 0.9) & for \quad 0.75 \le x \le 0.9 \\ 0 & for \quad 0.9 \le x \le l \end{cases} \tag{C.28}$$

Where,

$u_b(x)$ = Road profile due to break

N_b = Number of Break per 1.6 km

h = Break magnitude in mm

l = Distance between breaks in m

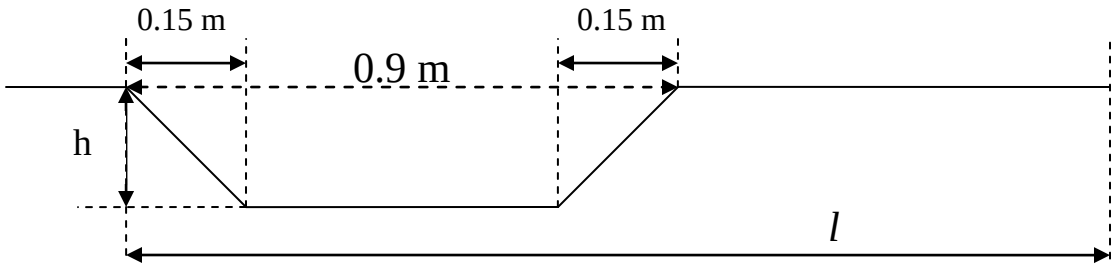

Figure C-18 Profile of a Concrete Slab with One Break

The resulting road profile over 1.6 km is:

$$u(x) = u_r(x) + \sum_{j=0}^{N_b - 1} u_b(x - jl) \qquad \text{(C.29)}$$

Where,

$u(x)$ = Road profile

$u_r(x)$ = Artificially generated road profile due to roughness

$u_b(x)$ = Roughness features (Equation C.27)

N_b = Number of breaks per 1.6 km

Artificial Generation of Curling

Curling is the distortion of a slab into a curved shape by upward or downward bending of the edges. This distortion can lift the edges of the slab from the base leaving an unsupported edge or corner which can crack when heavy loads are applied. Sometimes, curling is evident at any early age. In other cases, slabs may curl over an extended period of time. Curling is described as ellipse and its general form is given by Equation C.30. Figure C-19 shows the form used to find the mathematical description of curling.

$$u_c(x) = -h \times \sqrt{\left(1 - \frac{(2x - l)^2}{l^2}\right)} \qquad \text{(C.30)}$$

$$l = \frac{1600}{N_c - 1} \leq L$$

Where,

$u_C\ (x)$ = Road profile due to curling in mm
N_C = Number of curling per 1.6 km
h = Curling magnitude in mm
l = Curling width in m
L = Joint spacing in m

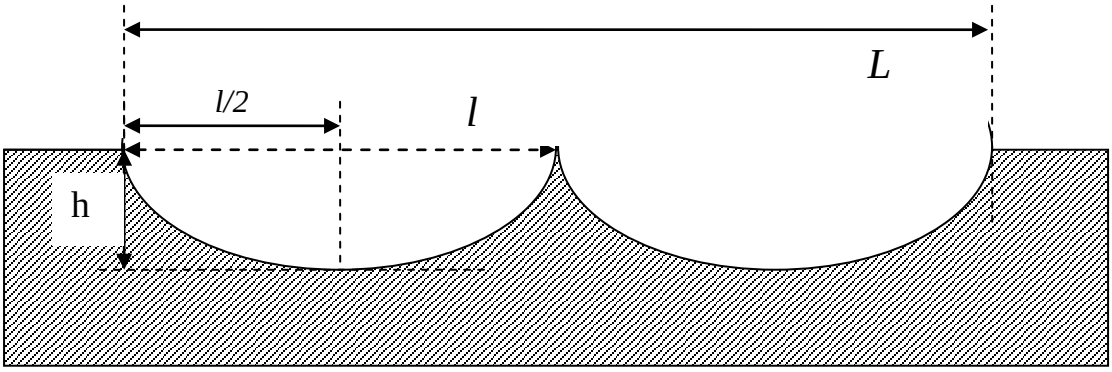

Figure C-19 Profile of a Curled Concrete Pavement

The resulting road profile over 1.6 km is:

$$u(x) = u_r(x) + \sum_{j=0}^{N_C-1} u_C(x - jl) \qquad \text{(C.31)}$$

Where,

$u(x)$ = Road profile
$u_r(x)$ = Road profile due to roughness
$u_C(x)$ = Roughness features (Equation C.29)
N_C = Number of curling per 1.6 km

Artificial Generation of Potholes

A pothole is when a portion of the road material has broken away, leaving a hole. Most potholes are formed due to fatigue of the pavement surface. As fatigue cracks develop they typically interlock in a pattern known as "alligator cracking". Then, the pavements between fatigue cracks become loose by continued wheel loads forming a pothole. The width of a pothole

was taken as 0.3 m (1ft). The general form of a pothole is similar to that for curling and it is given by Equation C.32. The only difference is the ellipse width. Figure C-20 shows the form used to find the mathematical description of a pothole.

$$l = \frac{1600}{N_p - 1}$$

$$u_p(x) = \begin{cases} -h \times \sqrt{\left(1 - \dfrac{(x-0.15)^2}{0.15^2}\right)} & for \quad 0 \le x \le 0.3 \\ 0 & for \quad 0.3 \le x \le l \end{cases} \qquad \text{(C.32)}$$

Where,

$u_p(x)$ = Road profile due to potholes
N_p = Number of Potholes per 1.6 km
h = Pothole magnitude in mm
l = Distance between potholes in m

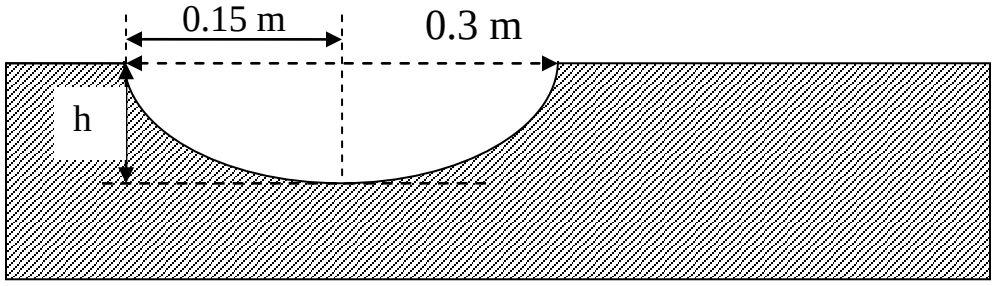

Figure C-20 Profile of Asphalt Concrete Pavement with One Pothole

The resulting road profile over 1.6 km is:

$$u(x) = u_r(x) + \sum_{j=0}^{N_p - 1} u_p(x - jl) \qquad \text{(C.33)}$$

Where,

$u(x)$ = Road profile
$u_r(x)$ = Road profile due to roughness
$u_p(x)$ = Roughness features (Equation C.31)
N_p = Number of potholes per 1.6 km

APPENDIX D

AN OVERVIEW OF EMERGING TECHNOLOGIES

INTRODUCTION

Background

In recent years, growing world population and the increase demand for road transportation (with its associated energy requirements that are primarily derived from fossil fuels) has led to the consideration, design and development of energy efficient vehicles and processes. Furthermore, to realize improvements in energy efficiency (wrt road transportation) the various engineering processes and/or technologies that have been developed range from - drag reducing vehicle designs; intelligent vehicle operating technologies, e.g., adaptive cruise control; the use of alternative energy sources, e.g., electricity; or intelligent transportation systems that facilitate wireless communication between vehicles and transport infrastructure. These and other technological interventions seek to assist in the reduction of vehicle operating costs (VOC) and fossil energy consumption as well as minimize carbon footprints. This appendix seeks to give an overview of emerging vehicle technologies that are set to play a major role in reducing automobile VOC and also have the potential to mitigate negative environmental impacts.

The highly competitive nature in the quest to develop energy efficient vehicles and/or technologies that lower VOC has created an environment where intellectual property is heavily guarded so not to precipitate a competitive disadvantage. Several unsuccessful attempts were made to contact Research and Development (R&D) units of original equipment manufacturers (OEM) to understand current and future vehicle, processes and technological developments. The emerging technologies presented in this appendix are those where information about them are publicly available, gained from published reports, slide presentations and/or online sources.

Vehicle Operating Costs

VOC are costs that arise from the direct use/operation of a vehicle and typically comprise, gas, oil, maintenance and tires (all of which directly impact the other). VOC differ from vehicle ownership costs such as insurance, licensing, registration, local taxes and financing charges. Together (i.e., expenditures wrt operation and ownership) these costs represent the total driving cost of operating and owning a vehicle. VOC can be measured in several ways, such as cost per vehicle-mile or passenger-mile. According to the American Automobile Association

(AAA) for the year 2010, VOC costs per mile (excluding ownership costs) range from 14.10 cents to 19.31 cents dependent on the size of the vehicle (see Table D-.1). The figures in Table D-1 generally indicate that as vehicle size increase so too do VOC. However, in order to accommodate the growing demand for vehicles with low VOC, several OEM in recent years have introduced innovative fuel efficient automobiles, e.g., Toyota Prius.

On average gas and oil costs account for 70 percent of VOC. Typical proportions of these two VOC contributors are presented in Table D-2. It is also known that "the fuel consumption of a vehicle is proportional to the forces acting on the vehicle. These forces are rolling resistance, gradient, inertia, curvature and aerodynamic forces," (Zaabar and Chatti, 2010) Thus, the dominance in the contribution of gasoline/fuel costs to VOC has precipitated the drive to develop and utilize alternative fuels alongside an increasing use of technology in vehicle operations.

Table D-1 2010 Vehicle Operating Costs Cents per Mile (by vehicle size)

Operating Item	Small Sedan	Medium Sedan	Large Sedan	Sport Utility Vehicle 4WD	Minivan
Gas	9.24	11.97	12.88	16.38	13.70
Maintenance	4.21	4.42	5.00	4.95	4.86
Tires	0.65	0.91	0.94	0.98	0.75
Total	14.10	17.30	18.82	22.31	19.31

Source: American Automobile Association - Your Driving Costs (2010)

Table D-2 Cost Components for Owning and/or Operating a Vehicle

Costs	Detail	Average Proportion (%) of per mile Cost*	Vehicle technologies impacting this cost component covered in this overview
Operating Costs	Gas & Oil	70.0	Yes
	Maintenance	26.0	Yes
	Tires	4.0	Yes
Ownership Costs	Insurance		No
	License & Registration		No
	Depreciation		No
	Financing		No

*see Table D-1

Vehicle Operation Energy Wastage

Table D-2 indicated that typically 70 percent of VOC is derived from gas/oil requirements to propel the vehicle. Once this fuel requirement is fulfilled approximately 15 percent of the energy generated is actually used to move the vehicle (i.e., provide power to the wheels) in urban conditions the rest is wasted. Furthermore, 67 percent of potential energy that can be derived from fuel is lost while converting heat into mechanical work at the engine (Transportation Research Board (TRB) Special Report, 2006). Figure D-1 schematically represents automobile component energy uses and losses for urban driving environments. Figure D.1 also reinforces the current trend of automobile engineering and/or technology research that focuses on minimizing engine and drive train energy losses simultaneously increasing fuel efficiency. Indeed, "there are various ways to increase vehicle fuel economy. Among them are reducing the loads that must be overcome by the vehicle and increasing the efficiency of its engine, its transmission, and other components that generate and transfer power to the axles." (TRB Special Report 286, 2006) The majority of emerging vehicle technologies reviewed in this report focus on vehicle propulsion and alternative fuels when compared to technologies reducing road surface friction (i.e., indirectly road roughness).

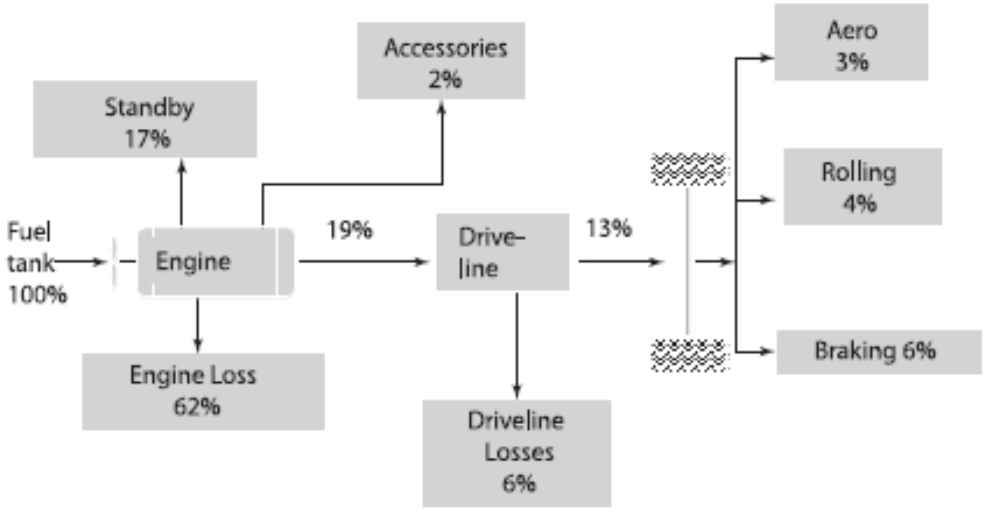

Source: TRB Special Report 286 (2006)

Figure D-1 Energy Uses and Losses for a mid-sized Passenger Car (operated in urban conditions)

Vehicle Technologies Roadmap

The drive for increased energy efficiency in an environment of finite/non-renewable resources has spurred R&D institutions explore the use of alternative regenerative fuels, materials of complex chemical makeup and/or sustainable processes to meet current and future mobility needs. As knowledge and application boundaries are breached new challenges arise necessitating continued research and development. The commercialization of vehicles using hydrogen is a case in point a development which could take place at some point in the future. Figure D-2 schematically encapsulates the current and potential development over time of vehicle propulsion technologies.

Observation of Figure D-2 indicates that as time progresses and gasoline (for vehicle propulsion) is displaced in favor of alternative fuels commercial use by automobiles using these alternative fuels will increase. The use of alternative fuels in vehicle propulsion will bring significant VOC savings but the storage and the safe integration into vehicles, fueling infrastructure and vehicle cost are challenges that still require many more years of R&D to be completely overcome. Indeed, the U.S. Energy Secretary Steven Chu stated in 2009 that "cars powered by hydrogen fuel cells will not be practical over the next 10 to 20 years." (Wald, 2009)

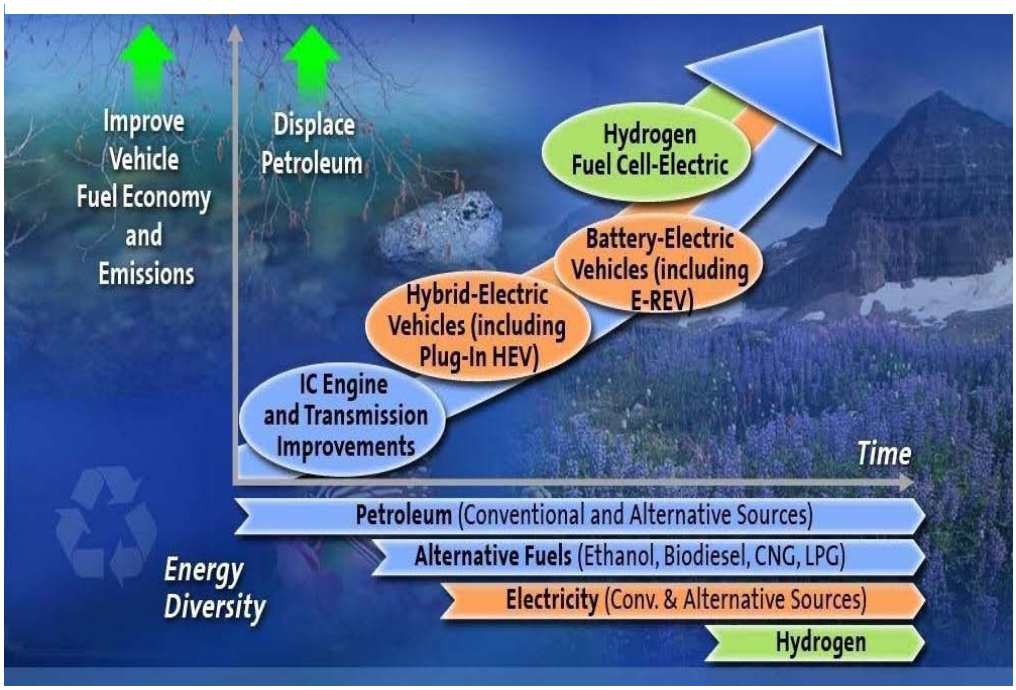

Figure D-2 Advanced Propulsion Fuels/Technologies R&D Timeline

ENGINE AND COMBUSTION TECHNOLOGIES

Sixty two percent of fuel energy lost in the propulsion of an automobile is attributable to the engine (see Figure D-1). Thus, technologies that can increase engine efficiency whilst reducing energy wastage will contribute to the overall lowering of VOC. The following section provides an overview of emerging engine and [internal] combustion technologies.

Engine Friction Reduction

Engine friction is defined as "the part of mechanical efficiency lost to friction in such engine components as bearings and rods" (National Highway Traffic Safety Administration (NHTSA), 2009). The valve train and pistons for example are among several components of the internal combustion engine (ICE) that are significant sources of engine friction and heat. Two general approaches are used in reducing engine friction; namely, 'asperity' or 'viscous.' The asperity approach seeks to reduce the roughness of surfaces that in turn reduces the amount of friction between reciprocating and rotating components in the engine. On the other hand, the viscous approach, seeks to reduce friction between two surfaces through the viscous properties of fluids (i.e., the lower the viscosity of a fluid the greater its ease of movement). This can be achieved through coating moving parts with friction reducing agents/additives. Another engine friction reducing approach involves the redesign of engine components, e.g., shortening the distance moving parts travel; roller cam followers; piston surfaces and rings, crankshaft design, etc. Computer modeling continues to play a major role in the design and testing of engine friction reduction technologies.

Gasoline Direct Injection (GDI)

GDI is a process where air is drawn into cylinder during the intake stroke and highly pressurized gasoline is injected directly into the combustion chamber during this event. Through this method the combustion process/engine load (that in turn controls engine power output) can be more tightly controlled and stabilized leading to increased engine performance, fuel efficiency and exhaust energy, in addition to lowering exhaust emissions. VOC gains are achieved through eliminating "the substantial throttling energy losses associated with load control achieved by restricting the intake air and fuel charge in current spark-ignited engines." (Basic Energy Science Workshop, 2006) Currently, Audi and Hyundai are two of several OEMs that have harnessed this

technology in the production of V6 engines. This intervention has the potential to realize an increase in engine efficiency of up to 12 percent. (fueleconomy.gov, 2010)

Engine Downsizing

Engine downsizing "involves a substitution of a naturally-aspirated engine by an engine of smaller swept volume." (Energy Technology System Analysis Program (ETSAP), 2010) In this procedure downsizing to a smaller engine may contribute to a reduction of its power output, if not corrected. Correcting this potential deficiency to maintain torque and power output can be achieved through turbocharging (i.e., boosting technology). VOC benefits of engine downsizing are realized through: 1) increased engine efficiency requiring less fuel; 2) lower engine weight contributing to a lower overall weight of the vehicle and 3) lower frictional losses as a result of the smaller components within the engine itself. Several European OEMs produce models with downsized/turbocharged engines, e.g., Audi (Audi S4) and Volkswagen (VW GTI 1.4 liter TSI). This intervention coupled with turbocharging has the potential to realize an increase in engine efficiency of up to 7.5 percent. (fueleconomy.gov, 2010)

Variable Valve Actuation (VVA)

VVA involves the alteration of the lift extent (i.e., variable value lift systems (VVL)) or the duration and/or air intake timing (i.e., variable valve timing systems (VVT)) of valves within ICEs. The control of these events significantly impacts engine performance and efficiency. "In a standard engine, the valve events are fixed, so performance at different loads and speeds is always a compromise between drivability (power and torque), fuel economy and emissions. An engine equipped with a variable valve actuation system is freed from this constraint, allowing performance to be improved over the engine operating range.' (Wikipedia, 2010) This intervention has the potential to realize an increase in engine efficiency of up to five percent. (fueleconomy.gov, 2010)

Cylinder Deactivation

Simply put, cylinder deactivation enables cylinders within the ICE to be deactivated in light load situations (i.e., low speeds or cruising). This type of intervention usually occurs in large capacity ICEs, e.g., V6, V8+. Using a V8 engine as an example, in light load situations

such an engine would use four cylinders instead of the normal eight. With respect to heavy load situations (i.e., acceleration, traveling uphill) all eight cylinders would be used. VOC benefits arising from this intervention translate into improved fuel efficiency. This intervention has the potential to realize an increase in engine efficiency of up to 7.5 percent. (fueleconomy.gov, 2010)

Variable Compression Ratio (VCR)

Compression ratios in standard gasoline ICEs are fixed - a compromise between engine demands at high or low speeds/loads. The principle of the VCR ICE permits compression ratios to vary according to the demands placed on the engine. Permitting variation in compression ratios enables an improvement in the combustion process which in turn improves fuel efficiency and reduces VOC. Further improvement in VOC benefits of VCR engines can be achieved through engine downsizing and boosting (i.e., turbocharging).

Homogeneous Charge Compression Ignition (HCCI)

In HCCI ICEs a spark (often generated through an electrical discharge) is not used to commence the combustion process, instead, compression of air within the cylinder causes the fuel mix to ignite spontaneously. Compression raises the temperature in the combustion chamber to a level where the fuel mix can ignite spontaneously. VOC benefits of the HCCI ICE can be realized through increased fuel efficiency and lower throttle losses, however, these benefits need to be offset by the difficulty of such engines to efficiently operate over a range of engine speeds and loads.

Integrated Starter/Generator Systems (ISG)

ISG automatically switch-off the engine when idling and immediately restart it once the gas pedal is pressed. This saves on the use of fuel while the engine is idling during extended stops at traffic signals or when operating in stop-go operations (i.e., often experienced in heavily congested traffic environments). VOC benefits arise from reduced fuel usage on trips where extended stops are prevalent. Several European based OEMs (e.g., BMW, Fiat and Volkswagen) have introduced this technology into a selection of their models.

Continuously Variable Transmission (CVT)

Standard transmissions use gearsets that govern the ratio between the engine and wheel speed. These gear ratios are fixed (i.e., usually, 4, 5 or 6) and to move between them gear changing, initiated by the driver, is required. In the typical automobile, the lowest gears are used for starting out, middle gears for acceleration and passing, and higher gears for fuel-efficient cruising. CVT technology uses a pair of pulleys connected by a belt or chain, instead of typical metal gears. This arrangement permits an infinite number of engine/wheel speed ratios be obtained. CVT engines are more precise in optimizing engine speed to power output in different driving conditions and this operation results in significant fuel consumption savings. Other VOC savings arise from smoother acceleration/deceleration and less "gear hunting" when the vehicle is traveling up or down hills (these latter benefits arise when compared to automatic transmission vehicles). Several U.S. based OEMs have models using CVT technology such as, Dodge Caliber, Jeep Compass, and Saturn Vue, etc. This intervention has the potential to realize an increase in engine efficiency of up to six percent. (fueleconomy.gov, 2010)

Automated Manual Transmission (AMT)

AMT ICEs engage the engineering elements of manual and automatic transmission systems. This form of transmission is also referred to as semi-automatic or clutchless manual transmission. In this system a clutch pedal is not required to change gears, instead electronic or hydraulic systems are used, initiated by the driver. Electronic or hydraulic systems allow precise gear change to optimize torque and timing, an advantage of this system over that of manual transmission. The recently introduced micro vehicle the Smart For Two employs AMT technology (see Figure D-3). Vehicles employing AMT technology have the potential to realize an increase in engine efficiency of up to seven percent. (fueleconomy.gov, 2010)

Figure D-3 The Smart for Two (an automobile that uses Automated Manual Transmission Technology

Six+ Speed Gearboxes

Gear boxes permitting 6 or more gear ratios/transmissions are available in manual or automatic automobiles. A higher number of gears (from the standard 4 or 5) permits finer tuning of the engine torque to optimal power output to the wheels required under different driving conditions. In other words, automobiles which have 6 or more gears attain a better match of engine speeds in the correct gear since there are more gears to choose from. This in turn optimizes engine efficiency contributing to VOC savings. Several OEMs offer 6+ speed automobile models, e.g., Chrysler, Ford and Toyota. Audi, BWM and Lexus also offer (or will offer in 2011) 8 speed models.

ALTERNATIVE FUELS AND Technologies

Recent years have realized a greater awareness of the finiteness of energy resources derived from fossil fuels. Alternative and sustainable energy resources are being explored and developed for powering transportation vehicles. Alternative fuels and their associated technologies are presented in this section.

Vehicles Powered by Natural Gas

Natural gas often in the form of compressed natural gas (GNG) can be used as an alternative to regular gasoline to power vehicles. Advantages of using this fuel source are its clean burning quality as well its wide availability domestically (i.e., in homes) in the U.S. However, several barriers exist in the U.S. for the widespread take-up of CNG powered vehicles, some of which are, limited traveling range, reduced trunk space and lack of refueling infrastructure. Overall, there has not been a proliferation of vehicles fueled by CNG in the U.S. Nevertheless, transit buses have applied this technology (e.g., New Flyer Manufactured buses operated by the Washington DC Metropolitan Area Transit Authority). With respect to automobiles the Honda Civic GX (shown in Figure D-4) is the only commercially CNG vehicle available but only sold in four states of the U.S., namely, California, New York, Oklahoma and Utah.

Figure D-4 The Honda Civic GX (an automobile powered by Compressed Natural Gas)

Vehicles Powered by Electricity

The electric vehicle (EV) uses one or more electric motors for propulsion working in tandem with rechargeable battery packs. Electric vehicles have been around for some time and their potential as a viable alternative to gasoline has increased in recent years due to environmental sustainability and energy security concerns. VOC benefits and disadvantages of EVs can be listed as:

Advantages

- When the vehicle is not moving, energy consumption is minimal or absent
- Quiet and smooth operation reducing wear, tear and vibration effects on vehicle

Disadvantages

- Bulk, weight and onboard storage of fuel cells
- Limited travel range, therefore, journeys require more recharge stops

Vehicles Powered by Hydrogen

Exploring the use of alternative fuels to power automobiles, hydrogen, is also seen as a potential fuel source. Propulsion using hydrogen can be achieved by storing this gas in onboard fuel cells which power electric motors or by burning hydrogen directly in an ICE. Vehicles powered by hydrogen are still in the R&D phase (i.e., demonstration fleets) and there are several challenges to overcome before the hydrogen vehicle (HV) can enter into commercial production. Potential VOC benefits and disadvantages of HVs can be listed as:

Advantages

- High levels of conversion energy are achieved (i.e., relationship between each unit of fuel consumed and the resulting energy produced)
- When the vehicle is not moving, energy consumption is minimal or absent
- Quiet and smooth operation reducing wear, tear and vibration effects on vehicle

Disadvantages

- Bulk and weight of fuel cells
- High initial cost could result in higher lifetime VOC
- Limited travel range, therefore, journeys require more refuelling stops

Vehicles Powered by Biodiesel

Biodiesel is a renewable fuel derived from vegetable oils (e.g., soybean, canola), animal fats, or recycled restaurant grease (i.e., yellow or brown). Biodiesel can only be used in diesel engines the majority of which are found in trucks and buses. Biodiesel has varied levels of purity ranging from 100 percent (i.e., pure B100), B2, B5 and B20 (i.e., 2, 5 and 20 percent Biodiesel respectively blended with regular diesel). VOC savings through the use of biodiesel are marginal, i.e., it is a performance enhancer to conventional diesel due to its higher lubricity levels. However, increases in VOC may arise from 1) retail biodiesel prices tend to be higher than regular diesel; 2) biodiesel blends higher than 5 percent may have the potential to negatively impact engine durability; and 3) a lower fuel economy and power output compared to diesel (10% lower for B100, 2% for B20) (fueleconomy.gov, 2010)

Ethanol Fueled Vehicles

Ethanol is an alcohol and can be used as an additive to regular gasoline to power automobiles. Indeed, most automobiles can use regular gasoline containing up 10 percent ethanol without any engine modification. However, vehicles using gasoline blends where the ethanol proportion is higher than 10 percent (up to 85 percent) are termed Flex Fuel Vehicles (FFV) and require a slightly modified engine. VOC savings through the use of ethanol are marginal, i.e., the retail price of ethanol in some parts of the U.S. is typically lower than gasoline. However, increases in VOC may arise from 1) low energy content of ethanol resulting in fewer miles per gallon (see Table D-3); 2) increasing internal wear of electric pumps (Wikipedia[2], 2010) and 3)

higher initial cost of FFV could result in higher lifetime VOC. The limited regional availability (in a U.S. context) of ethanol may result in FFVs not maximizing potential VOC savings. Table 3 presents miles per gallon and corresponding annual fuel costs for a selection of regular gasoline and flex fuel vehicles.

Table D-3 2010 Flex Fuel Vehicles and estimated Annual Fuel Cost*

	Model	Gasoline		FlexFuel	
		MPG (city)	Annual Fuel Cost	MPG (city)	Annual Fuel Cost
1	Chevrolet Malibu	22	$1,571	15	$2,018
2	Pontiac G6	19	$1,775	14	$2,175
3	Chevrolet Impala	18	$1,856	14	$2,134
4	Chrysler Town & Country	17	$2,146	12	$2,719
5	Ford Crown Victoria	16	$2,146	12	$2,592

Source: Fueleconomy.gov

Hybrid Vehicles

The term hybrid in an engineering context may refer to an automobile that has two components that produce the same or similar results. This type of technology has been applied to automobiles for more than 10 years. With respect to the hybrid electric vehicle (HEV) this would be the combination of a conventional gasoline ICE together with an electric motor. In HEVs both the gasoline engine and electric motor are used as energy sources for the drive train. Additionally, supplementary technologies are often used to maximize VOC savings in HEVs, e.g., rechargeable batteries, ISG systems and regenerative braking, etc. VOC savings are realized through:

- Electric motor assists gasoline ICE during peak power needs, i.e., acceleration phases, thus, a smaller fuel efficient ICE is required
- During idling, the electric motors provide power allowing the ICE to shutdown
- Batteries allow energy to be stored to be re-used to assist the ICE

Currently, more than two dozen HEVs models are produced for the U.S. automobile market. Fuel cost and miles per gallon data for a selection of these vehicles are presented in Table D-4. A derivative of the HV is the plug-in hybrid electric vehicle (PHEV) which having larger battery packs can recharge by connecting directly to domestic household electricity supply.

Table D-4 Top Five 2010 Hybrid and Gasoline Small Vehicles

Rank	Hybrid			Conventional/Gasoline		
	Model	MPG	Annual Fuel Cost (city)	Model	MPG	Annual Fuel Cost (city)
1	Toyota Prius	51	$816	Toyota Yaris (manual)	36	$1,277
2	Ford Fusion	41	$1,044	Toyota Yaris (automatic)	35	$1,318
3	Mercury Milan	41	$1,044	Honda Fit	35	$1,318
4	Honda Civic	40	$971	Hyundai Accent	34	$1,359
5	Honda Insight	40	$996	Kia Rio	34	$1,318

Source: Fueleconomy.gov

VEHICLE DESIGN & MAINTENANCE

Regenerative Braking Systems (RBS)

Regenerative braking is the process where the energy used in slowing down the vehicle (i.e., while braking) is recycled through an electric motor to further slow the vehicle down or stored in the battery. In conventional vehicles the kinetic energy created during the braking process dissipates as heat, however, with RBS this same energy is harvested through reversing the electric motors. Instead of the electric motors propelling the vehicle forward the braking energy from the wheels reverse this relationship. Thus, the torque created by this reversal counteracts forward momentum and assists in stopping the vehicle. RBS are commonly found in HVs equipped with battery packs such as the Toyota Prius.

Electric Motor Drive/Assist (EMD)

Electric motor drive/assist technology is an intervention where an electric motor assists an ICE through the provision of additional power as and when needed, e.g., during accelerating or hill climbing. This intervention allows a lower swept capacity of an ICE to be achieved (i.e., a smaller engine). Several models of HVs employ this type of technology, e.g., Honda Insight. VOC benefits are similar to engine downsizing as described earlier.

Lightweight Materials

Vehicle weight is a significant contributor to VOC, fuel consumption and vehicle performance. In fact, "75% of vehicle gas (energy) consumption directly relates to factors associated with vehicle weight." (Oak Ridge National Laboratory (ORNL), 2010) In recent years there has been continued research in the use of alternative lightweight materials in vehicle building instead of traditional steel. The use of these new materials, though lightweight, aim not to compromise material strength characteristics, environmental impact, financial viability and vehicle performance and safety, as well as occupant safety characteristics of vehicles made with materials such as steel. Lightweight materials that have shown promise are: aluminum, magnesium, titanium, advanced high-strength steels, fiber-reinforced composites, and metal matrix composites. VOC benefits arise from increased fuel efficiency and smaller powerplant requirement (e.g., ICE or fuel cell, etc.) as a result of reduced vehicle weight.

Vehicle Aerodynamics

As an object moves through air it creates a disturbance (or instability) which can be manifested as drag, wind and/or vehicle noise and unwanted lift. The extent of drag/air friction significantly impacts fuel efficiency and vehicle performance and tends to increase as vehicle surface area and/or speed increase. Thus, vehicle aerodynamics seeks through vehicle design to minimize or eradicate aerodynamic instability of a vehicle as it travels. Smother vehicle shapes can significantly contribute to drag reduction. The drag coefficient (C_d) is a measure of a vehicle's aerodynamic smoothness and it was projected that C_d typically ranges from 0.25 to 0.35. In the U.S. this vehicle characteristic has generally fallen in the current decade as vehicles have become smaller and more fuel efficient due to the increased fuel efficiency requirements of new vehicle designs and a growing retail market for smaller vehicles. For example, in 2003 a C_d = 0.57 was associated with the Hummer H2 compared to a C_d = 0.25 for the 2009 Toyota Prius (model ZVW30) (see Figure D-5). Automobile designers can improve aerodynamic characteristics vehicles by:

- rounding the edges of the front end
- adjusting the grille and fascia openings
- installing small spoilers in front of the tires to reduce turbulence
- adjusting the size and shape of the outside mirrors and their attachment arms
- adding side skirts

- installing a rear spoiler
- adjusting the angle of the rear window
- tucking up the exhaust system
- installing underbody panels that cover components and smooth airflow

VOC benefits arising from improved aerodynamics can significantly increase fuel efficiency and vehicle performance.

Figure D-5 The Hummer H2 (2003) and Toyota Prius ZVW30

Intelligent Transportation Systems (ITS)

ITS involve the application of information and communication technology to transportation infrastructure or vehicles. With respect to lowering VOC, in-vehicle ITS technologies can take the form of:

- Cruise Control Systems (CCS) are systems that maintain a selected cruising speed without the need to constantly depress the gas pedal
- Adaptive Cruise Control Systems (ACC) that maintain a minimum lead distance between the lead and following vehicle
- Global Positioning Systems (GPS) or mapping systems that can identify the shortest distance between two points or indicate the slowest, fastest or congested route enabling a driver to make informed choices as to route choice
- Fuel Efficiency Gauge that allows the real-time monitoring of mpg while traveling
- Maintenance Required Gauge that alerts the driver when a preventative maintenance check is due

TIRE TECHNOLOGIES

Research has shown that tires through their rolling resistance are directly responsible for approximately four percent of energy losses in the typical automobile (see Figure D-1). It is also known that underinflated tires contribute to lower fuel economy as do vehicle load and erratic vehicle handling. Ongoing research efforts continue to develop tire technologies that primarily address tire inflation (and indirectly rolling resistance) as described below.

Tire Pressure Monitors Systems (TPMS)

Air pressure in tires needs to be continually monitored as pressure decreases over time and use precipitating changes in VOC. In fact, "under normal driving conditions, air-filled tires can lose from 1 to 2 psi per month as air permeates through the tires." (Government Accountability Office (GAO), 2007) TPMS monitor the air pressure of pneumatic tires and report this information back to the driver by way of an indicator on the vehicle dashboard. TPMS generally are of two types; direct and indirect. Direct TPMS monitor pressure directly from inside the tire compared to indirect TPMS which monitor differentials between individual rotational wheel speeds (i.e., rotational wheel speed is influenced by the air pressure inside the wheel). If the pressure in any individual wheel falls below a government regulated minimum threshold or an OEM specified level a warning signal is sent to the driver to take corrective action, i.e., inflate the tire to its OEM recommended pressure. Recently, NHTSA has required that all new automobile models from 2008 are equipped with TPMS. Maintaining tires at their correct pressure optimal mpg can be achieved.

Tire Innerliners

A tire innerliner is a sheet of rubber that is used to line the inside of a tire casing. This sheet typically is made from varying blends of synthetic rubber and other chemical additives with the purpose of reducing the potential of air escaping through the tire structure. Different chemical additives, e.g., bromobutyl have been shown to improve the air retention characteristics and durability of a tire casing. Other tire innerliner technologies have sought to reduce the weight of the tire casing through the use of innovative tire innerliner materials, e.g., . Exxcore™ DVA of the ExxonMobil corporation. As air leakage through the casing wall is reduced tires are able

to maintain their correct pressure for longer assisting in minimization of engine-wheel energy losses.

Nitrogen

Recently, the use of nitrogen has been promoted as an alternative gas for filling tires especially with respect to truck tires. Slower permeation of rubber (i.e., the tire casing) than regular air is the primary benefit of using nitrogen in tires. In such a case, nitrogen filled tires should maintain tire air pressure and durability for longer periods of time. VOC benefits are similar to those achieved from tire innerliners.

Low Rolling Resistance Tires

Low rolling resistance tires seek to reduce the energy wasted as heat as the tire rolls over a surface (i.e., energy is lost due to tire deformation as it passes over a surface or is underinflated). “It is estimated that 5%-15% of light-duty fuel consumption is used to overcome rolling resistance for passenger cars.” (U.S. Department of Energy (DOE), 2010) By conserving the energy wasted from tire rotation less energy is required to move the tires and so VOC benefits can be realized. A lower rolling resistance in tires may be achieved by correct air pressure and/or a stiffer tire casing. Typically, HVs are equipped with low rolling resistance tires that contribute to their high fuel efficiency. However, such tires are usually more inflated than regular tires and stiffer.

In order to maintain the VOC savings of low rolling resistance tires (which often come with new vehicles) consumers require detailed information about the fuel saving properties of aftermarket tires. Currently, this information is difficult to find as the provision of this tire statistic is not a government mandated requirement with respect to aftermarket retail sales. However, the California Energy Commission continues to undertake extensive research of the rolling resistance properties of tires and codifying results into a format that will enable consumers to make informed choices when purchasing aftermarket tires.

CONCLUSION

The continued push for fuel efficient vehicles coupled with growing demand for them has accelerated the R&D efforts to meet this need. This development has prompted the harnessing of

alternative fuels in vehicle propulsion, redesign and reevaluation of combustion and propulsion processes and a reassessment of how vehicles interact with their immediate environment in terms of their environmental impact, aerodynamic/pavement friction efficiency, congestion impacts, etc. All of the technologies presented in this report have the potential to lower VOC. Nevertheless, the majority of current R&D efforts focus on engine and combustion technologies (including alternative fuels) which have the potential to significantly reduce energy loss of vehicle operation. Moving into the future, the cost of retrofitting existing fleets and the take up and affordability of new vehicles with these technologies will determine the extent, sustainability and reality of predicted VOC savings to individual motorists and society.

This appendix presented the results of the literature review and summarized the collected information regarding the emerging technologies that lower VOCs. To summarize, the new technologies that were proven to affect vehicle operating costs are: the engine and combustion technologies, alternative fuels and technologies, vehicle design & maintenance, and tire technologies. The last two emerging technologies will affect the effect of pavement conditions on VOCs.